Heat & Electricity Storage Annual Report 2016

Storage
Swiss Competence Center
for Energy Research

In Zusammenarbeit mit der KTI

Förderprogramm Energie
Swiss Competence Centers for Energy Research

Schweizerische Eidgenossenschaft
Confédération suisse
Confederazione Svizzera
Confederaziun svizra

Kommission für Technologie und Innovation KTI

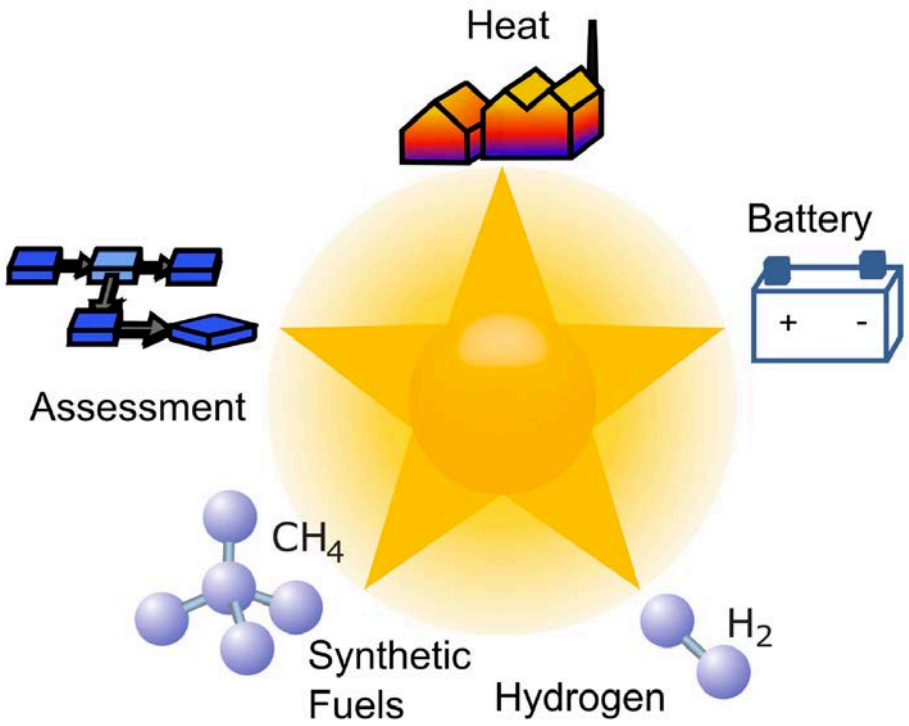

Annual Report 2016

Imprint

SCCER HaE-Storage – Annual Activity Report 2016

Published by

Swiss Competence Center for Energy Research – Heat and Electricity Storage

Concept by

Thomas J. Schmidt

Technical Review

Thomas J. Schmidt, Jörg Roth

Editorial work, design and layout by

Peter Lutz, lutzdocu.ch, Uster
Ursula Ludgate

Printed by

Paul Scherrer Institut, Villigen

Available from

Swiss Competence Center for Energy Research
Heat and Electricity Storage (SCCER HaE-Storage)
c/o Paul Scherrer Institute
5232 Villigen PSI, Switzerland

Phone: +41 56 310 5396
E-Mail: info@sccer-hae.ch
Internet: www.sccer-hae.ch

DOI: 10.3929/ethz-a-010687042

Table of Contents

Editorial

Heat – Thermal Energy Storage

Batteries – Advanced Batteries and Battery Materials

Hydrogen – Production and Storage

Synthetic Fuels – Development of Advanced Catalysts

Table of Contents

Assessment – Interactions of Storage Systems

Appendix

SCCER Networked Research – One-stop Shop for New Developments in Energy Storage

The Swiss Competence Center for Energy Research (SCCER) Heat and Electricity Storage successfully finished its third year of operation in 2016, which in turn also means, the first phase since its implementation in 2014 finally came to its end. Last year, therefore, was dictated by two important aspects, viz. the efforts to demonstrate scientific and technical progress in the final year of the first SCCER funding period and the preparation and submission of the proposal for the second funding period 2017–2020. The latter we successfully submitted and it was finally accepted for funding by the Commission for Technology and Innovation Switzerland (CTI) which enables us now to continue our research and development (R&D) on energy storage until 2020 under the roof of the SCCER Heat&Electricity Storage.

Within the SCCER Heat&Electricity Storage the 23 participating groups from Cantonal Universities, Universities of Applied Sciences and ETH domain institutions are working on different technologies for energy storage ranging from power and heat storage to the storage of energy in gases and synthetic fuels. Through our networked R&D within Switzerland, the SCCER H&E understands itself as a one-stop shop for new developments in energy storage.

This annual report 2016 summarizes all progress achieved by SCCER Heat&Electricity Storage over the last year. Besides lots of remarkable achievements on the more fundamental level of understanding materials and processes, the great progress in building different demonstration platforms should be emphasized at this point.

For instance, the SCCER Heat&Electricity Storage contributed to the construction and operation of the world's first Advanced Adiabatic Compressed Air Energy Storage (AA-CAES) plant built near Biasca in Switzerland. This plant demonstrated a storage efficiency of > 70 % which is in line with values typically seen for pumped-hydro energy storage plants therefore offering potential for better flexibility in grid-scale energy storage.

As a second example, Switzerland's first Power-to-Methane plant in Rapperswil was operated and characterized further within the last year, enabling important insights into practical operation and applications of the technology as well as in-depth understanding with respect to different operational aspects, e.g., CO_2 source or the use of the product gas for grid-injection or mobility applications.

These are only two examples of our demonstrators built within the framework of the SCCER with many equally important ones described in this Annual Report. With this I would like to invite you dive into the world of energy storage while reading our 2016 achievements in the following pages.

Prof. Dr. Thomas J. Schmidt
Head SCCER Heat and Electricity Storage

List of abbreviations

CTI	Commission for Technology and Innovation Switzerland
R&D	Research and Development
SCCER	Swiss Competence Center for Energy Research

Heat

Thermal Energy Storage

Work Package "Heat Storage" at a Glance

In Switzerland, nearly 50 % of the total energy is consumed in the form of heat. The consump-tion can be classified into 60 % for space heating, 27 % for process heat, and 13 % for warm water.
Several projects are ongoing within this work package to tackle materials and systems develop-ment for low-temperature seasonal heat storage for building applications and high temperature heat storage for industrial applications.

Low-temperature storage

A central goal of the low-temperature storage activities is the development of a compact, retrofittable seasonal-storage unit for building applications. The solution being investigated by the Institute for Solar Technology at the University of Applied Sciences Rapperswil is a closed sorption heat storage based on water vapour absorption in an aqueous sodium hydroxide solution ($NaOH$-H_2O) or other aqueous solutions. The key advantage of sorption storage is the significantly higher volumetric energy density compared to sensible hot water storage systems. As part of the EU-financed COMTES project, a $NaOH$-H_2O prototype with 10 kW output power was designed, built, and operated. For the discharging (absorption) process, however, the measured exchanged power is lower than expected. This has been traced to the poor wetting of the stainless steel tube bundle in the adsorption/desorption unit of the storage and the short residence time of NaOH in the water vapour. Surface modifications and the use of surfactants are being investigated in a dedicated 1 kW test rig in an effort to improve the discharging performance.

At the University of Applied Sciences Lucerne, the interaction of power and heat in combination with thermal energy storage is being investigated through the Dual Energy Storage and Converter (DESC) concept. Their storage system is based on the combination of a heat pump, a heat engine, and two thermal storage units and can be operated either as pure electricity storage or as a combination of heat, cold, and electricity storage. The primary focus is on latent heat storage because of higher energy densities compared to sensible heat storage and because the constant temperatures during phase changes simplify the storage integration. New phase-change materials were identified for temperatures of 93 °C and 12 °C, allowing efficient coupling with heat pumps and chillers. Laboratory setups were designed to test and evaluate the application potential of these technologies under realistic conditions.

High-temperature storage

For high temperature applications, the efforts have focused on two applications and involved researchers from ETH, EPFL, and SUPSI. The first application is advanced adiabatic compressed air energy storage (AA-CAES). For AA-CAES plants, thermal storage at temperatures of about 550–600 °C is the key to raising the cycle efficiency from about 40–50 % for diabatic CAES to about 70–75 %. These efficiencies are close to those observed in practice for pumped hydro storage, which is one reason why AA-CAES is often viewed as an attractive technology for the bulk storage of surplus electrical energy. The efforts on AA-CAES include simulations and experiments. The simulations, in turn, encompassed 1d, 2d, and 3d simulations of the thermal storage itself as well as simulations of entire AA-CAES plants that include a 1d model of the thermal storage. These simulations were instrumental in the design and operation of the world's first AA-CAES pilot plant near Biasca, Switzerland, in a close collaboration with Airlight Energy SA/ALACAES SA. Pilot-scale experiments were carried out using both a sensible-only storage based on a packed bed of rocks as well as a combined sensible-latent storage in which the packed bed of rocks was supplemented with a separate latent storage using a metallic phase-change material encapsulated in steel tubes.

The second high temperature application is the development of heat exchangers based on silicon carbide for temperatures up to 1600 °C.

Illustration: Atropat / iStock

Sensible and Combined Sensible / Latent-Heat Thermal Energy Storage for Advanced Adiabatic Comressed Air Energy Storage

Scope of project

The growing share of fluctuating renewable energy sources like wind and solar requires short- and long-term energy storage to guarantee the power supply. Pumped hydro storage is at present the main option for large-scale storage. However, its economic viability is threatened and alternative large-scale storage technologies must be being investigated. One promising alternative to pumped hydro storage is advanced adiabatic compressed air energy storage (AA-CAES). In contrast to the diabatic form of CAES, which has been proven for several decades at the industrial scale with the plants in Huntorf (Germany) and McIntosh (USA), AA-CAES stores the heat generated during air compression in a thermal energy storage (TES). During expansion, the heat is recovered from the TES by the air, leading to an increase of potential round-trip efficiencies from around 45–50 % to more than 70 %. Compared to diabatic CAES, AA-CAES has the additional advantage of not requiring the burning of fossil fuels; during operations, AA-CAES does not emit CO_2.

Status of project and main scientific results of workgroups

In collaboration with industrial partner ALACAES and SUPSI, an AA-CAES pilot plant has been designed and constructed in an unused tunnel near Pollegio (Switzerland). The 10 MWh sensible-heat thermocline TES is placed inside the cavern to prevent large pressure differentials acting on the TES walls, thereby simplifying its design considerably. Multiple charging-discharging cycles were performed with the pilot plant. During charging, compressed air of about 550 °C flows through the TES, releases its heat to a packed bed of rocks, and the cooled air is then stored in the cavern. During discharging, the cold air flows through the TES and leaves the cavern as hot air. To our knowledge, the cycling experiments with the pilot plant represent the first time an AA-CAES pilot plant has been operated worldwide.

To design the experimental schedule for the pilot plant and to predict the performance of large-scale plants, a quasi-one-dimensional heat transfer model [1] was used. This model was extended to include the temperature and pressure evolution inside the cavern [2]. The comparison of the simulated temperature profile inside the TES and the experimental results shows good agreement, see Figure 1. In addition to the sensible-heat storage, a separate latent-heat storage with a capacity of 500 kWh was constructed and tested, see Figure 2. The latent-heat storage contains 296 steel tubes filled with the metallic phase-change material (PCM) $Al_{68.5}Cu_{26.5}Si_5$ (melting temperature of 518 °C). The goal of this storage was to stabilize the discharging outflow temperature of the sensible storage near the melting temperature of the PCM and thus enable higher AA-CAES plant efficiencies.

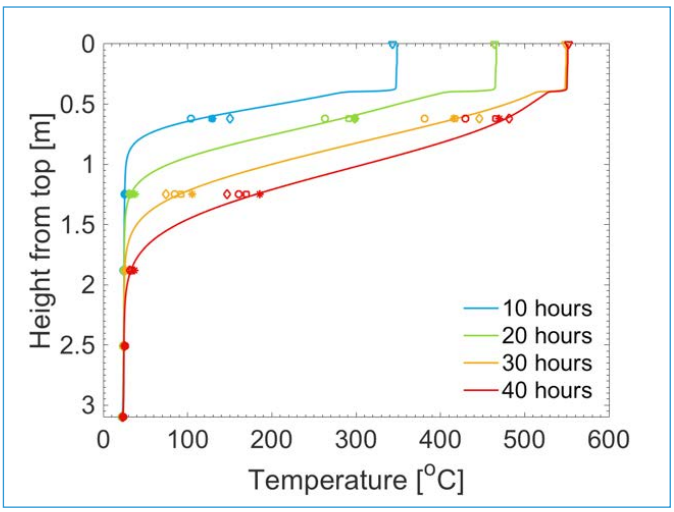

List of abbreviations

AA-CAES	Advanced Adiabatic Compressed Air Energy Storage
HTF	Heat Transfer Fluid
PCM	Phase Change Material
TCC	Thermocline Control
TES	Thermal Energy Storage

Figure 1 (left):

Comparison of temperature distribution inside the sensible-heat TES in Pollegio between 1D model (solid lines) and experiment (symbols) during 40 h of charging.

Figure 2 (right):

Latent–heat TES inside the tunnel in Pollegio.

Authors

Geissbühler[1],
V. Becattini[1],
G. Zanganeh[2],
A. Haselbacher[1],
A. Steinfeld[1]

[1] ETH Zurich,
[2] ALACAES SA, Biasca

Sensible and Combined Sensible / Latent-Heat Thermal Energy Storage for Advanced Adiabatic Comressed Air Energy Storage

Figure 3:

Experimental outflow temperature during discharging of the combined sensible/latent-heat TES in Pollegio.

In Figure 3, the measured air temperature at the outflow of the latent storage during discharging is presented. The results of the experimental campaign with the sensible and combined sensible-latent storage units are currently being investigated in detail.

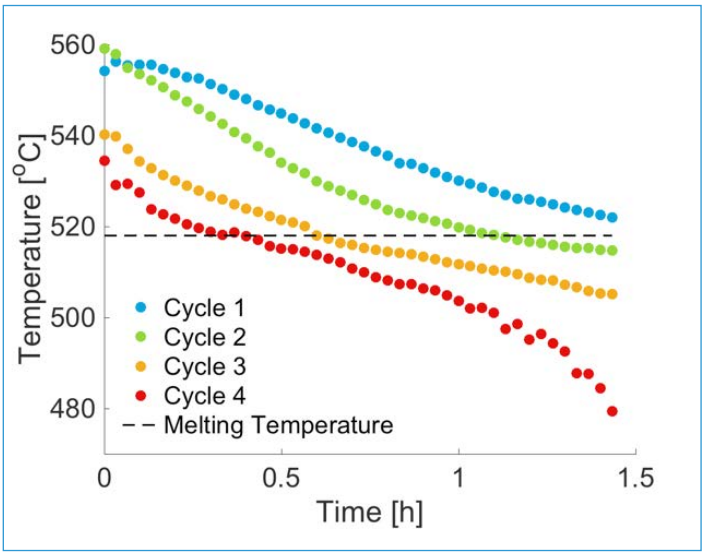

The temperature drop during discharging in a sensible-heat TES is a consequence of thermocline degradation. Reasons for thermocline degradation are axial heat conduction, radiation, and poor convective heat transfer. These mechanisms are influenced by the storage geometry, storage material, and the manner in which the TES is operated. Adding PCMs, either on top of the packed bed or in a separate latent heat TES unit (as in the AA-CAES pilot plant), allows the impact of thermocline degradation on the air outflow temperature to be reduced.

An alternative to PCMs is to actively increase the thermocline steepness inside the tank. This approach, referred to as thermocline control (TCC), has two main benefits:

- Higher utilization factor: Storage size and hence material costs can be reduced.
- Lower temperature drop during discharging: More efficient plant operation.

Amongst several TCC strategies, previous work proposed extracting and returning Heat Transer Fluid (HTF) at certain positions of the thermocline [3]. Simulations with the quasi-one-dimensional heat-transfer model [1] confirmed that this can indeed steepen the thermocline and lead to higher storage utilization, as illustrated in Figure 4. The results shown in the figure were obtained for a packed bed of rocks with air as HTF. The fully charged capacity is 440 MWh. Without TCC, the discharged energy per cycle is only 143 MWh (indicated by the green-shaded area in Figure 4, left), giving a utilization factor of 0.33. With TCC, the discharged energy per cycle increases to 210 MWh (indicated by the green-shaded area in Figure 4, right), resulting in a utilization factor of 0.48, or an improvement of 45 % relative to the case without TCC.

Figure 4:

Experimental outflow temperature during discharging of the combined sensible/latent-heat TES in Pollegio.

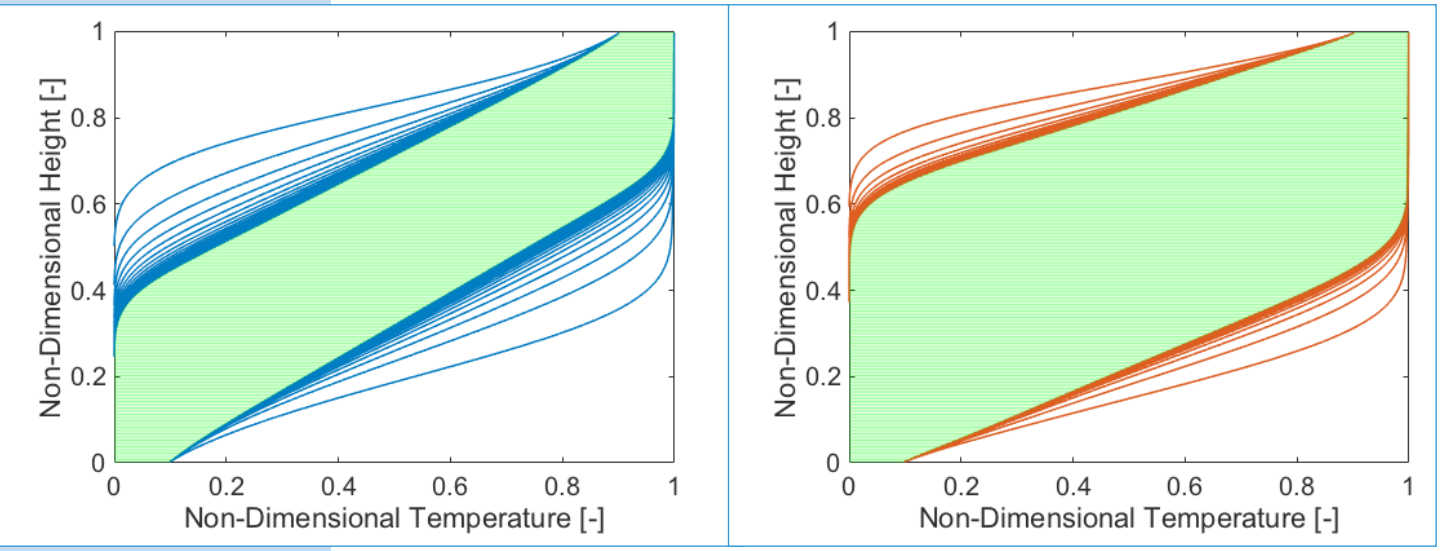

References

[1] L. Geissbühler, M. Kolman, G. Zanganeh, A. Haselbacher, and A. Steinfeld, Analysis of industrial-scale high temperature combined sensible/latent thermal energy storage. Appl. Therm. Eng., 101, 657–668 (2016).

[2] P. Zaugg, Centrales à accumulation pneumatique, 11th international congress in combustion engines (1975).

[3] A.K. Mathur and R.B. Kasetty in Thermal Energy Storage System Comprising Optimal Thermocline Management, U.S. Patent No. 8554377, 2012.

CFD Modeling of the Pollegio AA-CAES Pilot Plant TES System

Scope of project

The present study aims at modelling, by means of a computational fluid dynamics (CFD) approach, the thermo-fluid dynamics behaviour of the thermal energy storage (TES) system equipped in the first advanced adiabatic compressed air energy storage (AA-CAES) pilot-plant built in Pollegio. The sensible-heat storage system is based on a packed bed of natural rocks. Due to the unusual geometry proposed for the TES under investigation, a detailed 3D computational domain was exploited and time-dependent CFD simulations were performed. According to the CFD simulation results obtained, none relevant three-dimensional effects on the temperature distribution into the packed bed were observed.

Status of project and main scientific results of workgroups

Advanced adiabatic compressed air energy storage (AA-CAES)

Pumped hydro storage (PHS) can be considered as the most exploited solution, at global level, for large-scale electric energy storage (EES) applications [1]. However, its applicability limited to suitable sites and its relatively low energy density are among the major limitations of this EES solution.

A valuable alternative to PHS can be represented by compressed air energy storage (CAES). CAES plants operate on a «decoupled» Brayton cycle in which, depending on the grid availability/request of electric energy, compression and expansion occur at different times. In current CAES plants, during the compression stage a large amount of thermal energy is produced and removed (wasted) from the compressed-air. On the other hand, during the electricity generation stage, an extensive supply of thermal energy is required, currently provided by burning natural gas. This inadequate heat management strategy is among the main factors limiting the overall efficiency of this technology.

To overcome this limitation of conventional CAES plants, the concept of advanced adiabatic compressed air energy storage (AA-CAES) has been proposed: a thermal energy storage (TES) is exploited to store the thermal energy produced during compression to be recovered prior to expansion.

Although the AA-CAES concept is still in the research and development stage [2], the expected round-trip efficiency is in the order of 70% [3] comparable to PHS. Other advantages of AA-CAES such as limited environmental impact and lower estimated capital costs make this technology attractive as a potential alternative to PHS for achieving the long-term energy policy developed by the Swiss Federal Council (Energy strategy 2050).

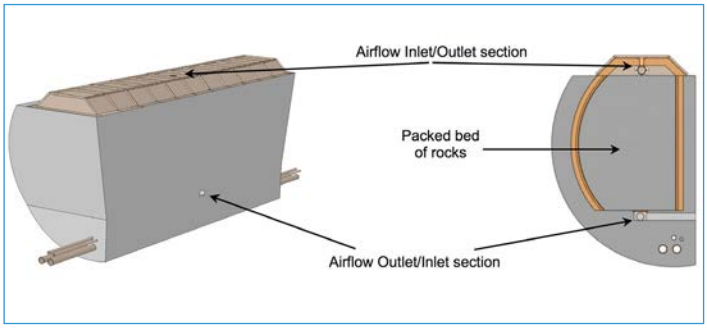

Pollegio AA-CAES pilot plant

To evaluate the feasibility and applicability of the AA-CAES concept, a pilot plant was built in Pollegio, in the framework of a project sponsored by BFE and involving, among others, ALACAES and ETHZ.

A 120 m long section of a tunnel of the Alptransit project not in use anymore was exploited as air reservoir. A thermocline TES system with a packed bed of natural rocks was selected as suitable solution for storing the thermal energy produced during compression. A schematic of the TES system under investigation is reported in Figure 1.

The volume of the packed bed is equal to about 44 m^3 with average particles diameter and void-fraction of 20 mm and 0.342 respectively. The Pollegio AA-CAES prototype is designed to operate with charge

List of abbreviations

AA-CAES	Advanced Adiabatic Compressed Air Energy Storage
CFD	Computational Fluid Dynamics
EES	Electric Energy Storage
HTF	Heat Transfer Fluid
PHS	Pumped Hydro Storage
TES	Thermal Energy Storage

Figure 1:
Schematic of the TES under investigation with cross-section on the symmetry plane.

Authors

S. Zavattoni[1]
M. Barbato[1]
L. Geissbühler[2]
A. Haselbacher[2]
G. Zanganeh[3]
A. Steinfeld[2]

[1] SUPSI
[2] ETHZ
[3] ALACAES SA

CFD Modeling of the Pollegio AA-CAES Pilot Plant TES System

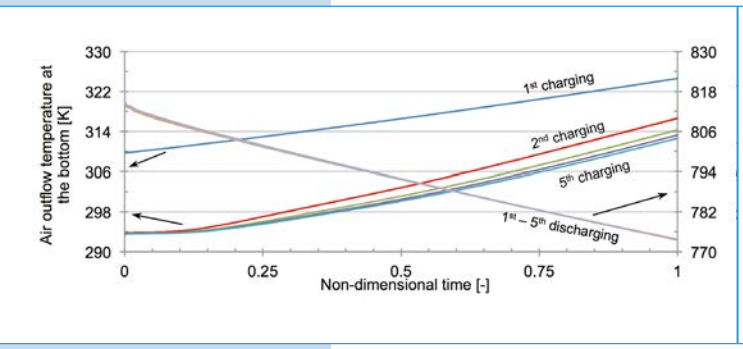

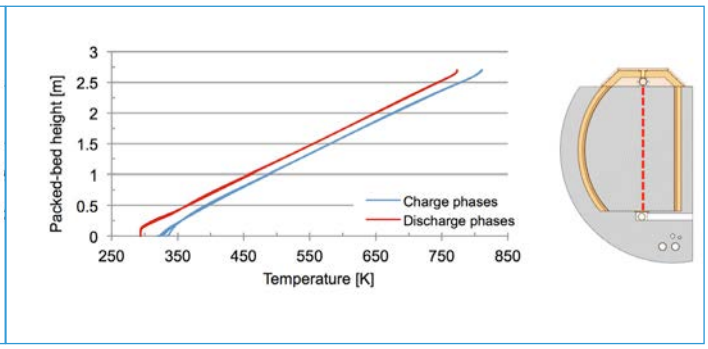

Figure 2 (left):

Air outflow temperature during charge and discharge phases.

Figure 3 (right):

Temperature distribution into the packed bed, as a function of the height, for the five cycles analysed.

References

[1] REN21, Renewables 2016 – Global status report, 2016.
[2] ADELE – adiabatic compressed-air energy storage for electricity supply. https://www.rwe.com/web/cms/mediablob/en/391748/data/364260/1/rwe-power-ag/innovations/Brochure-ADELE.pdf (accessed Sept. 2016).
[3] S. Zunft, Adiabatic CAES: The ADELE-ING project. SCCER HaE Storage Symposium, 2015.
[4] D.A. Nield, A. Bejan, Convection in Porous Media, Springer, 2006.

and discharge cycles of 2.75 h each, with a pressure variation of the reservoir between 31.5 bars and 33 bars. Since the compressors train exploited in the pilot-plant is equipped with intercoolers, to replicate the effect of air temperature increment during compression, a 260 kW electric heater is installed between compressors train and TES system to heat up the air up to 823 K.

CFD simulation results and conclusions

Since the TES system is a key component of AA-CAES technology, an extensive CFD analysis was performed with the twofold aim of evaluating its thermo-fluid dynamics behaviour and characterizing its performance. The CFD simulation, performed with ANSYS Fluent 15.0, was mimicking a 38 h thermal pre-charging, intended to rapidly reach steady working conditions, followed by five consecutive charge/discharge cycles. The packed bed was modelled exploiting the porous media approach [4] assuming local thermal equilibrium between solid and fluid phases.

Figure 2 shows the air outflow temperature at the bottom of the TES during charging and on top during discharging. According to the results obtained, the air outflow temperature at the end of discharging decreases by about 50 °C with respect to the reference charging temperature, following the same temporal evolution for all the five cycles analysed. Conversely, the air outflow temperature at the end of charging (bottom of the TES) reduces with consecutive cycles reaching 40 °C at the end of the 5th charge phase.

Figure 3 shows the temperature distribution into the packed bed as a function of the height, monitored on a line lying between the airflow inlet and outlet regions on the symmetry plane (see r.h.s. of Figure 3). The temperature into the packed bed at the end of charging and discharging is almost the same for all the five cycles indicating that the TES, thanks to the pre-charging, is operating in a repeatable working condition.

From a graphical standpoint, Figure 4 shows the contours of static temperature of the TES system at the end of the first charging.

Another interesting result obtained is, that despite the unusual shape of the TES under investigation no relevant three-dimensional effects on the temperature distribution into the packed bed should be expected. Therefore, the TES system can be accurately analysed with a simplified 2D approach reducing substantially the computational time.

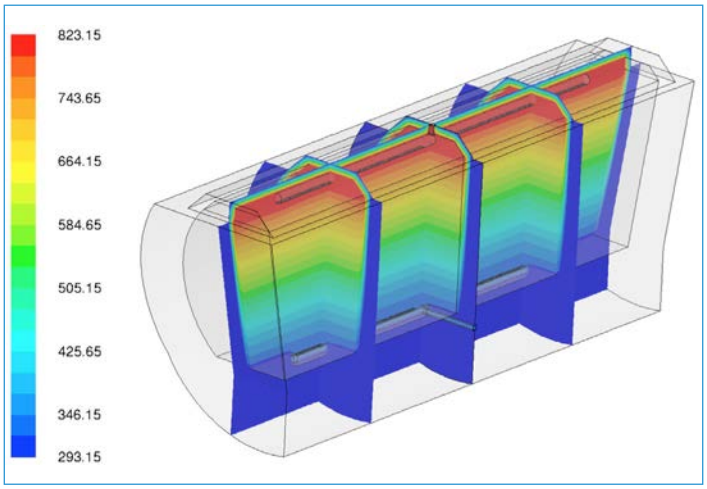

Figure 4:

Contours of static temperature on different planes.

Temperature values are [K].

Performance Evaluation of a Packed Bed TES System Exploited in Compressed Air Energy Storage Technology

Scope of project

In the field of large-scale electric energy storage, advanced adiabatic compressed air energy storage (AA-CAES) technology can be considered as valuable alternative to the most exploited solution of pumped hydroelectric energy storage. In this technology, a thermal energy storage (TES) is exploited to store the thermal energy produced during air compression stage to be recovered prior to expansion. The TES is therefore a key component for a successful exploitation of AA-CAES technology. In this work a thermocline TES, based on a packed bed of rocks, was proposed as suitable and reliable TES solution. A CFD-based approach was then followed to characterize the thermo-fluid dynamics behaviour of the TES system demonstrating the potential feasibility and reliability of its implementation in a real-scale AA-CAES plant working under realistic grid load conditions.

List of abbreviations

AA-CAES	Adiabatic Compressed Air Energy Storage
CFD	Computational Fluid Dynamics
TES	Thermal Energy Storage

Status of project and main scientific results of workgroups

Reference CAES plant and TES characteristics

The TES system was designed according to the operating condition of the 321 MW Huntorf plant [1] assumed as reference CAES plant for the purpose of this study. This plant is designed for a peak power generation of 2 h at full load of the turbines while the compressors train is dimensioned to charge the air reservoirs in 8 h. During normal plant operations, the pressure range of the air reservoirs is between 46 bars and 66 bars. The nominal air mass flow rate during charging and discharging is equal to 108 kg/s and 417 kg/s, respectively. In order to maximize the storage capacity of the reservoirs and to avoid environmental issues, compressed air is stored at a maximum temperature of 50 °C. After the compression stage, the high-pressure air reaches a temperature of about 500 °C. Calculations showed that, based upon the aforementioned Huntorf CAES plant operating conditions, a total of about 3500 m^3 of rocks are required to store the thermal energy produced during air compression stage, i.e. charging phase. A truncated cone shape of the tank, 22 m high, 18 m and 10 m for the upper and the lower diameters respectively, was exploited to prevent thermal ratcheting, i.e. plastic deformation of the tank due to different thermal expansion coefficients.

CFD simulations results and conclusions

A 2D axisymmetric slice of the TES packed bed was selected as computational domain, so to minimize computational costs of the numerous «time accurate» simulations required. Mass, momentum and energy conservation equations were solved using ANSYS Fluent 16.2. Due to the large packed bed volume, a division of the total storage volume in different tanks connected in parallel (2-tanks and 4-tanks) was proposed. The packed bed was modelled exploiting the porous media approach [2] and local thermal equilibrium between solid and fluid phases was assumed. Variable pressure conditions of the TES, according to the pressure level in the air reservoirs during charging and discharging, were also accounted for.

Figure 1 shows the CFD simulation results, of the 20 consecutive charge/discharge cycles analysed, in terms of air outflow temperature from the bottom during charging (l.h.s) and from top during discharging (r.h.s.) for the three different tank arrangements proposed. According to the results obtained, dividing the overall storage volume in different tanks has a minor influence on the TES performance. Concerning the charging, a maximum air outflow temperature of 150 °C was found after a stable thermal stratification into the packed bed was

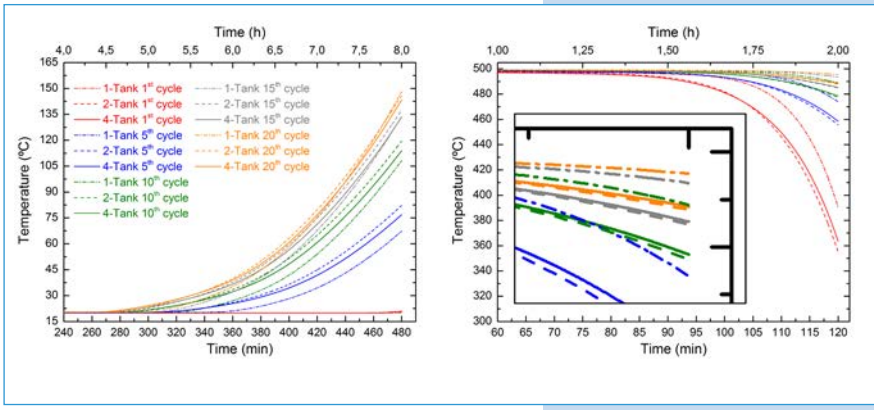

Figure 1:
Air outflow temperature for the 1-tank, 2-tanks and 4-tanks configurations during of some charging (l.h.s.) and discharging (r.h.s.).

Authors

I. Ortega-Fernández[1]
S. Zavattoni[2]
J. Rodríguez-Aseguinolaza[1]
M. Barbato[2]
B. D'Aguanno[1]

[1] CIC Energigune, Miñano (Álava), Spain
[2] SUPSI

Performance Evaluation of a Packed Bed TES System Exploited in Compressed Air Energy Storage Technology

References

[1] BBC Brown Boveri, Huntorf air storage gas turbine power plant.

[2] D.A. Nield, A. Bejan, Convection in Porous Media, Springer, 2006.

attained around the 20th cycle. On the other hand, during discharging, despite the large air outflow temperature reduction, after almost 10 cycles the air temperature was found matching the requirements of the power block during the whole discharge phase.

The TES behaviour was also analysed assuming realistic operating conditions of the CAES plant according to likely real grid load conditions. Therefore, starting from a completely charged TES at the beginning of the day (6:00), two partial charge (7:30–12:30 and 13:50–20:00) and discharge (6:00–7:30 and 12:30–13:50) stages are considered. Then, the stored energy is released in a full discharge run (20:00–22:00), followed by a complete charge process until the next morning (22:00–6:00). A total of 31 consecutive cycles were simulated and the results obtained, in terms of air outflow temperature during charging and discharging, are reported in Figure 2.

Looking at the curves of the 8 h charging overnight (Figure 2a), it can be observed that in the first day the air outflow temperature, at the bottom of the TES, increases up to 415 °C. This undesirable temperature increase is due to the 6 h pre-charging considered which leads to a TES overcharging. In particular, after 6–7 days a stable thermal stratification into the packed bed is attained with a maximum air outflow temperature that does not exceed a thermal threshold of 185 °C. On the other hand, in the two partial charge periods of 5 h (Figure 2b) and 6.2 h (Figure 2c) lower air outflow temperatures are obtained. Focusing on the air outflow temperature during the three discharging periods, in all these cases it is above 480 °C, matching the requirements of the power block from the first discharging. A detailed analysis of the two partial discharge periods (Figure 2d and 2e) reveals that almost no air outlet temperature decrease occurs. The obtained thermal behaviour in both charging and discharging periods allow to conclude that the proposed TES tank is valid not only for a continuous complete charge and discharge operation, but also for a partial charge and discharge cycling condition. Furthermore, the performed analysis has demonstrated that the TES behaviour during charging and discharging is only slightly dependent on the particular operation strategy.

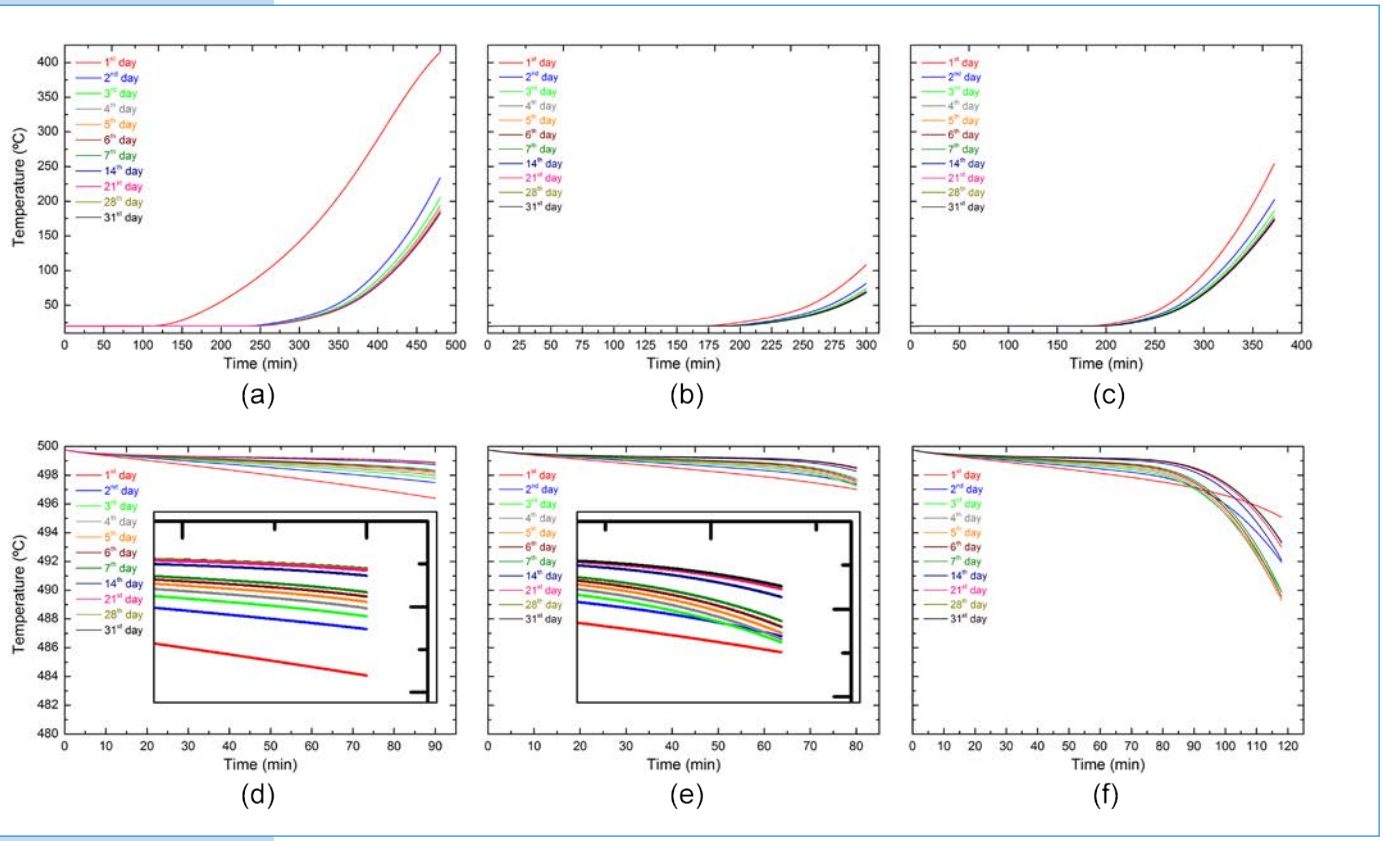

Figure 2:

Air outflow temperature during charging:
a) 22:00 – 6:00;
b) 7:30 – 12:30;
c) 13:50 – 20:00;

and during discharging:
d) 6:00 – 7:30;
e) 12:30 – 13:50;
f) 20:00 – 22:00.

Phase Change Material Systems for High Temperature Heat Storage

Scope of project

The development of technologies for high temperature energy storage has been intensified in recent years driven by the disparity between energy availability and demand. Latent heat storage by means of phase change materials (PCMs) has proven to be an attractive heat storage technology. Such a heat storage system consists of an encapsulation, a phase change medium contained in the encapsulation and the heat transfer fluid (HTF). Here, we focus on high temperature heat storage (above 300 °C) and on metal PCMs due to their advantage in terms of heat transport characteristics, energy density, and high temperature application. The development of an advanced, reliable computational model of a high temperature heat storage system and its coupling to various industrial techno-economic process models is crucial for the design of tailored high temperature heat storage systems and for the assessment of the performance and economic benefit of high temperature heat storage in industrial processes.

List of abbreviations

PCM	Phase Change Material
HTF	Heat Transfer Fluid
LHS	Latent Heat Storage
OPEX	Operational Expenditure
SHS	Sensible Heat Storage

Status of project and main scientific results of workgroups

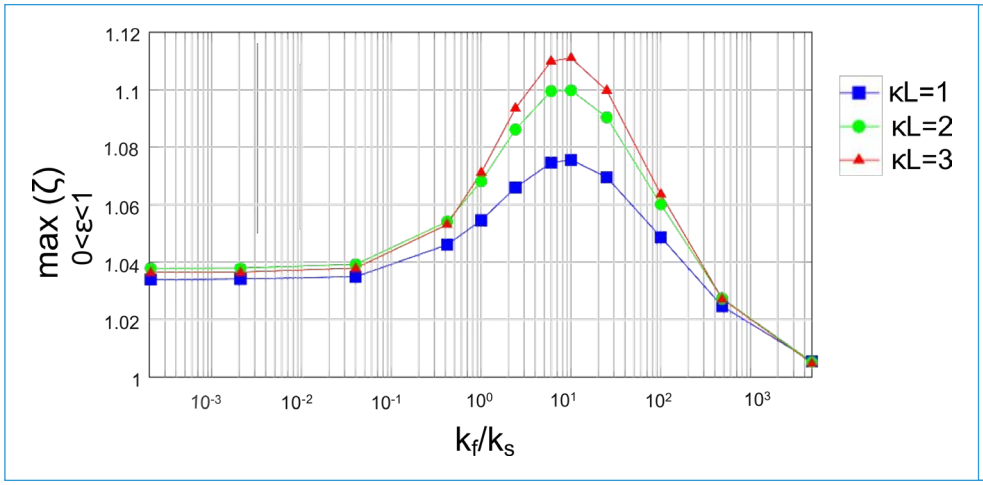

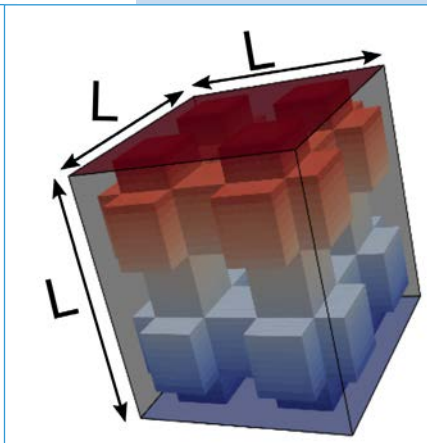

Figure 1:
Maximum coupling effect (ζ) observed for any ratio of conductive to radiative flux (ξ) for the geometry shown (right), for different optical thicknesses and varying conductivity ratios.

High-temperature heat storage model: Coupled conductive-radiative heat transfer

We focused on the understanding of the coupling between radiative and conductive heat transfer in our porous heat storage media in order to provide guidance on when coupling effects can be neglected.

At high temperatures, radiative heat transfer can dominate the heat transfer. However, the extent of domination highly depends on the material characteristics of the contributing bulk phases (their conductivity, extinction and absorption coefficients). The multiple scales present in porous media used as heat storage system further contribute to the challenge of assessing such systems (micro scale of the porous media and macro scale for the heat storage system). We used our direct pore-level simulation framework to assess the coupling effects between conductive and radiative heat transfer modes. The term «coupling effects» is used to highlight the naturally occurring interaction between the modes. We quantified the coupling effect for an example porous geometry consisting of two phases (stagnant HTF and PCM). We varied their bulk material properties in order to provide material-independent guidance on when to neglect coupling effects. We identified that coupling effects, assessed as being the ratio between the sum of the radiative and conductive heat fluxes of the uncoupled and the coupled case (ζ), can reach up to 15 % (Figure 1). The ratio of the thermal conductivities, kf/ks, and the optical thickness, κL, were identified as key parameters contributing to the importance of the coupling. Coupling effects in the range of 4 % are expected for specific HTFs and PCMs considered in our heat storage solutions (air and aluminum alloys). The model de-

Authors

David Perraudin[1]
Sophia Haussener[1]

[1] EPFL

Phase Change Material Systems for High Temperature Heat Storage

velopment and the results of this study have been submitted for publication to an international journal.

High-temperature process modeling: Techno-economic model of aluminum production

Aluminum is produced more than any other non-ferrous metal at present. There are two ways to produce aluminum: primary aluminum smelting and secondary aluminum melting.

According to the International Aluminum Institute, the primary aluminum smelting energy consumption is 690'170 GWh p.a. in Europe in 2014 [1]. Typical aluminum melting temperatures are around 650 °C to 700 °C and offer a high potential to reduce the energy consumption when operating in batch by utilizing high temperature heat storage. An optimization study of such a batch process (Figure 2, top) showed that the cost of aluminum production in terms of operational expenditure (OPEX) can significantly be reduced (in the best case by almost a factor of two) when introducing high temperature heat storage solutions (Figure 2, bottom).

The competition between sensible (SHS) and latent heat storage (LHS) in terms of cost and performance points to the optimal solution: combining both. If combined optimally, sensible and latent heat storage can preserve the advantages of both technologies: high storage capacity and discharge at constant temperature for latent options and low cost for sensible options.

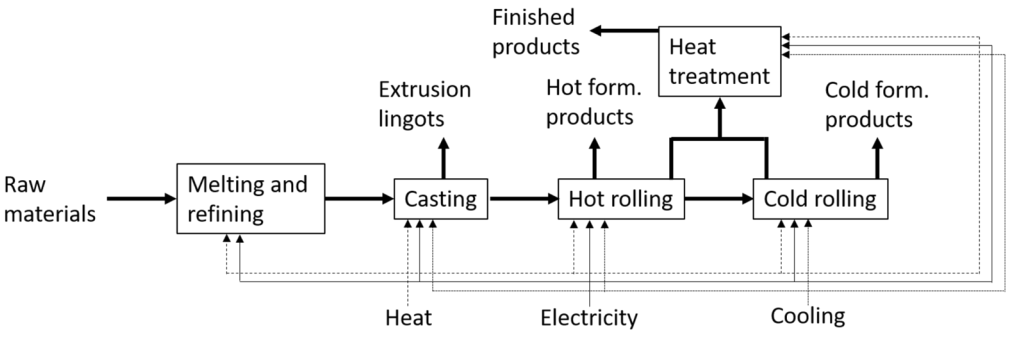

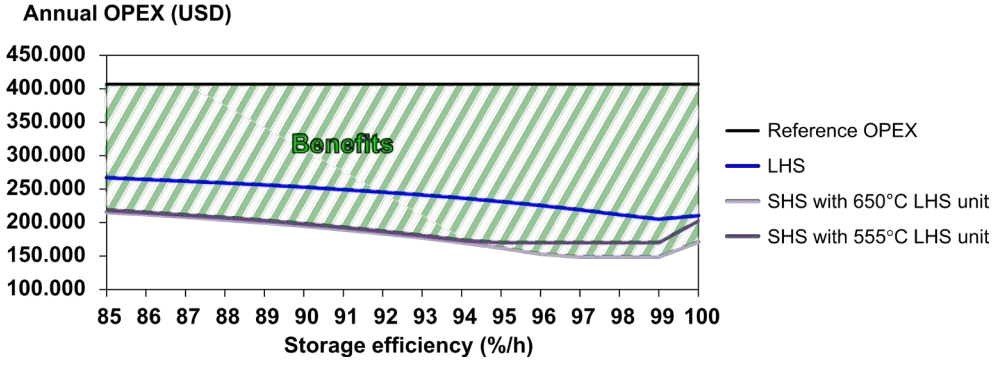

Figure 2:

Batch mode processing route of aluminum (top) and comparisons of OPEX cost using sensible and latent heat storage for varying storage efficiency (bottom).

High-temperature process modeling: Performance model of direct steam generation

The need for storage in direct steam generation is dictated by the intermittent nature of the provided heat. This intermittency can result from the utilization of renewable energy sources or variation in the process operation. Short scale intermittencies (timescale of sub-seconds) are usually compensated by an active control system activating injections at different locations. Medium scale intermittencies (timescale of minutes) can be compensated for with large heat storage units. For example, phase change materials have a potential to act as a passive control system and reduce the cost and complexity of direct steam generation power plants.

We developed a transient, one-dimensional model of the direct steam generation unit in order to get a preliminary understanding of the benefit of the usage of heat storage units in direct steam generation applications. Our model incorporates multi-model heat transfer (conduction, convection and radiation). The model reveals that there is a significant potential in terms of performance when heat storage options via PCMs are integrated in the steam generation process.

For example for an assumed input energy of 5500 W/m (per

Phase Change Material Systems for High Temperature Heat Storage

length of the tube), the steam generation operates at an efficiency (ratio of useful energy and input energy) of 78 % for the case without storage and of 73 % for the case with storage, both at steady state.

The lower efficiency of the storage-case results from the fact that part of the input energy is required to charge the storage.

Once the transients are introduced (for example: 10 seconds operation at 20 % of initial heat flux followed by 10 seconds of full heat flux, continued over 3 minutes), the useful energy drops below 36 % for a significant amount of the 3 minutes for the case without storage, while the storage case can maintain the useful energy above 67 % for the 3-minute intermittency duration. The exact behavior of the direct steam generation unit depends on the amount of incorporated storage, the charging/discharging state of the storage, and the operating conditions.

Conclusions and future work

The transient, multi-dimensional and multi-model heat transfer model of the heat storage unit was reduced and used to assess and quantify coupling effects of radiative and conductive heat transfer. The introduced error for a variety of HTF and PCM material combinations was quantified and, consequently, guidance on the validity and accuracy of simplified conduction-radiation models was provided. The heat storage unit model was mathematically reduced and incorporated into two high temperature industrial process models:

- aluminum processing, and
- direct steam generation.

The aluminum processing model was coupled to an economic model and predicted that operational cost could be reduced by almost a factor of 2 when storage was incorporated. The direct steam generation model focused on the ability of high temperature heat storage to damp and counteract intermittent heat inputs. It predicted that heat storage can maintain the useful energy at a level insignificantly below the steady state case when exposed to intermittent input energy.

Both process models contribute to the notion that heat storage integration in industrial processes can significantly benefit their performance and cost.

In a next step, we will optimize the industrial processes (in terms of cost and performance) by utilizing tailored high-temperature heat storage units (designed with our advanced heat storage unit model) with desired energy and power densities and storage temperatures.

Acknowledgement

The financial support of CTI Swiss Competence Centers for Energy Research (SCCER Heat and Electricity Storage) is kindly acknowledged.

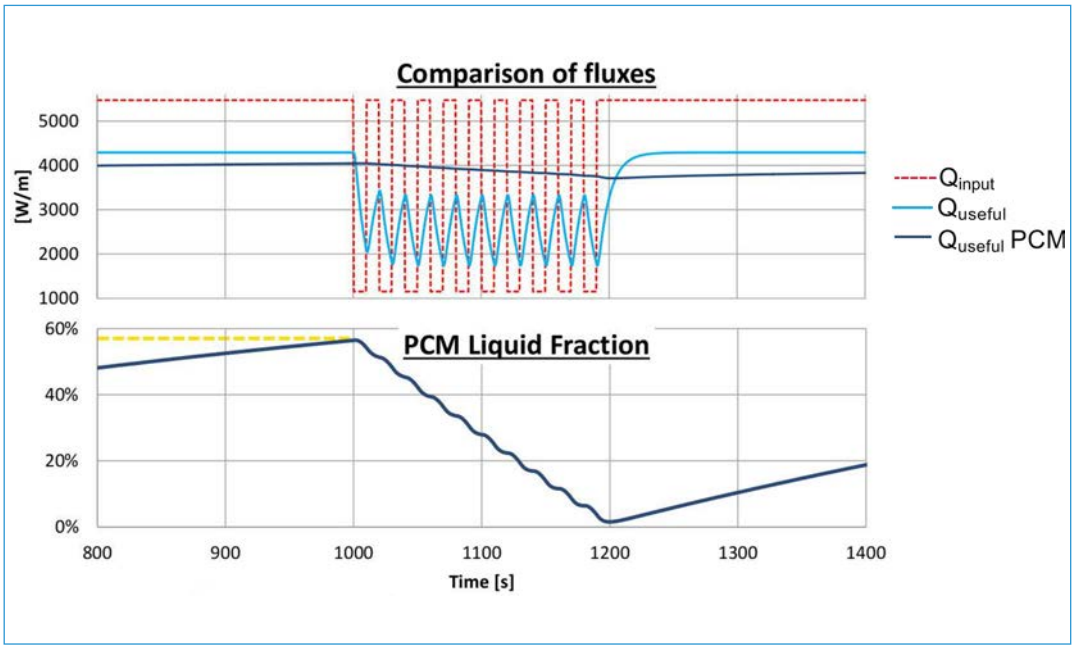

Figure 3:

Comparisons of useful heat per unit length of steam generation tube exposed to intermittent incident fluxes (10 intervals of 80 % reduction of incident heat).

References

[1] The International Aluminum Institute, «Primary aluminium smelting energy intensity», http://www.world-aluminium.org/statistics/primary-aluminium-smelting-energy-intensity/#map, accessed 2016-04-21.

Tubular SiSiC Structures for High Temperature Applications

List of abbreviations

LTNE	Local Thermal Non-Equilibrium
SiC	Silicon Carbide
SiSiC	Silicon infiltrated Silicon Carbide

Scope of project

Silicon infiltrated Silicon Carbide (SiSiC) is a prevalent ceramic material for applications in harsh environments such as burners, recuperators and heat storage systems. It has wide industrial applications due to its high mechanical and chemical stability at elevated temperatures and its excellent thermal shock resistance. SiSiC is also particularly suitable for near-net-shape production of complex components such as porous structures via melt infiltration of silicon. At temperatures above 1000 °C, three main factors may limit the performance of SiSiC: bead formation due to melting of silicon, severe oxidation especially in presence of water vapor, and high thermally induced stresses. We investigated the first two factors earlier for various SiSiC lattices [1] and here focus on the thermal behavior of SiSiC lattices. This work builds the foundation for future analysis of their thermal stress resistance.

Status of project and main scientific results of workgroups

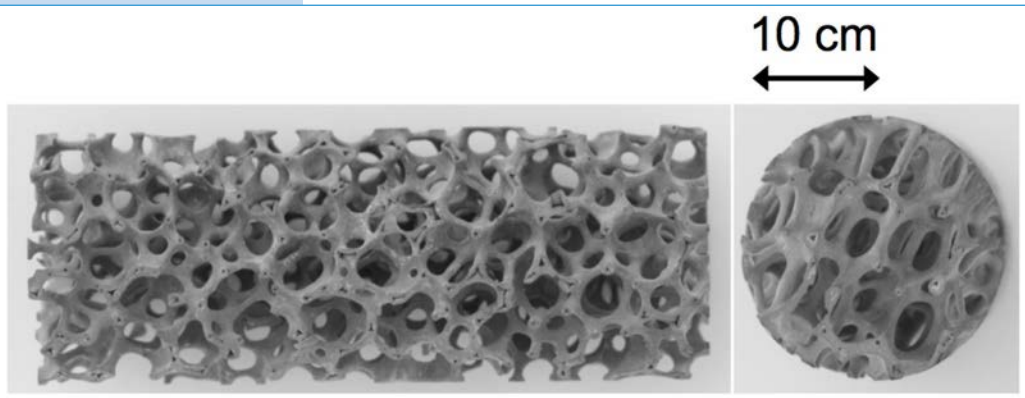

Figure 1:
As received SiSiC random foam sample side view (left) and top view (right).

Experiments

The experimental test rig consists of a SiSiC tube, which can be loaded with porous samples such as the one shown in Figure 1. The tube is considerably longer than the samples in order to ensure developed inlet and outlet flow conditions.

SiSiC tubes were manufactured from alpha-SiC powders bound within silicon, which was melt-infiltrated at high temperature (EngiCer).

The test rig (Figure 2) was designed and assembled to reach high temperatures (max. 1600 °C) in order to measure heat exchange capabilities of the porous media. A custom-made furnace able to provide high thermal power (up to 3000 W) in a well-defined cylindrical area (of 3 cm in diameter and 10 cm in length) was commissioned from Xerion (Freiberg, D). An expansion

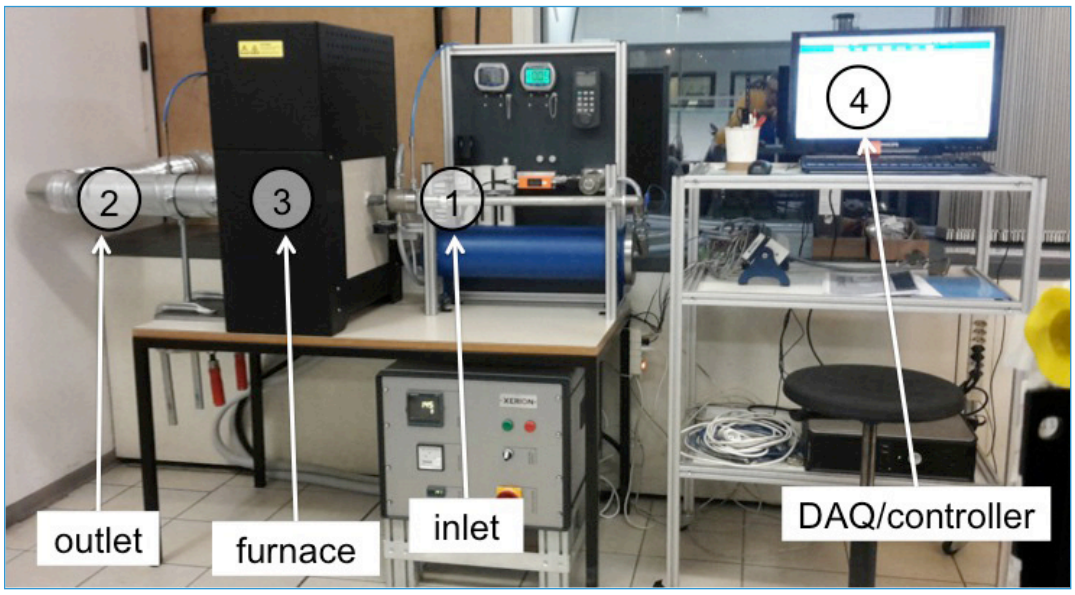

Figure 2:
High temperature measurement apparatus.

Authors

Ehsan Rezaei[1,2]
Maurizio Barbato[1]
Sandro Gianella[3]
Sophia Haussener[2]
Alberto Ortona[1]

[1] SUPSI
[2] EPFL
[3] EngiCer SA, Balerna, Switzerland

Tubular SiSiC Structures for High Temperature Applications

chamber was coupled to the extended tube in order to ensure laminar flow at the inlet. Preliminary tests at a temperature of 1280 °C were successfully performed on empty tubes and tubes filled with random foams with air flowing at 13.2 m/s. Namely, we measured the temperature and pressure of air inside the tube at the inlet and outlet. The temperature of the furnace was controlled with a thermocouple embedded inside the furnace between the two heating elements. The temperature on the outer surface of the tube was as well measured using three thermocouples placed on the tube in the middle part (the heating zone).

Numerical model

An axisymmetric LTNE (local thermal non-equilibrium) steady-state model was developed and solved using a commercial numerical solver (COMSOL Multiphysics). Similar to the experiments, the tube is filled with a porous medium, modeled by a homogenized medium with effective properties taken from Haussener et al. [2] obtained by direct pore-level simulations.

Results

During the preliminary tests neither the tube nor the porous foam showed any remarkable signs of degradation.

The results provide evidence that the heat transfer capabilities of the tube filled with a porous medium are more than two times larger than that of an empty tube (overall thermal efficiency of the empty tube was 33 % while 78 % for porous).

As depicted in Figure 3, samples with smaller cell size show to be more effective in removing heat from the tube (decreasing the nominal pore diameter by an order of magnitude increases the overall heat transfer coefficient by about 20 %). However small pore diameters lead to higher temperature variations in the solid foam (Figure 3, right), which is expected to cause higher thermally induced stresses.

Conclusions and future work

A high temperature test rig, designed to operate up to temperatures of 1600 °C, was designed to measure heat transfer effectiveness of ceramic porous media.

Preliminary experiments were successfully performed on empty tubes and tubes filled with porous ceramics made of random foam structures, indicating that the heat exchange efficiency can be almost doubled when introducing the porous media The experiments are complemented with an advanced LTNE computational model of the system.

The model was used to predict the performance of the porous ceramics and to optimize their structure for best performance. For this purpose, several random lattice structures and dimensions were modeled to verify the effectiveness of these systems and compare with the empty tubes as a benchmark.

Different structures will be designed and manufactured. These samples will be used in the developed test rig and the results will be further used to validate the numerical model and provide guidance for structural engineering for best performance.

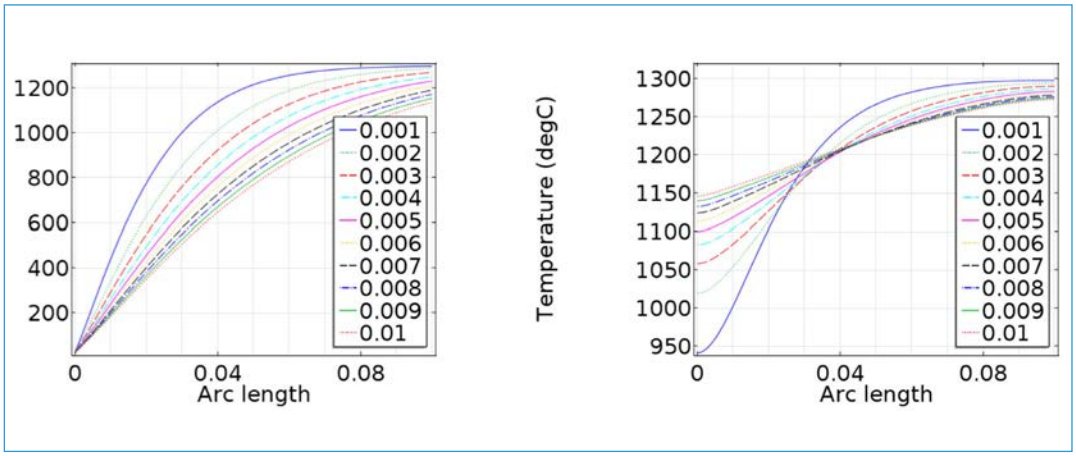

Figure 3:

Solid (right) and fluid (left) phase temperatures in the centerline of the porous medium for media with different nominal pore diameters.

References

[1] E. Rezaei, S. Haussener, S. Gianella, A. Ortona, «Early-stage oxidation behavior at high temperatures of SiSiC cellular architectures in a porous burner». Ceram. Int., 42(14), 16255–16261, (2016).

[2] S. Haussener, P. Coray, W. Lipinski, P. Wyss, A. Steinfeld, «Tomography based heat and mass transfer characterization of reticulate porous ceramics for high temperature processing». J. Heat Transfer, 132(2), 023305, (2010).

Thermal Absorption Energy Storage

Scope of project

Closed sorption heat storage, for residential applications, based on water vapor absorption in aqueous sodium hydroxide solution ($NaOH-H_2O$) or other aqueous solutions like LiCl, LiBr, KOH theoretically achieves a significantly higher volumetric energy density compared to sensible hot water storage systems [1].

Status of project and main scientific results of workgroups

Asessment of heat and masstransfer unit

In the frame of the EU FP7 project «Combined development of compact thermal energy storage technologies – COMTES», a $NaOH-H_2O$ prototype with 10 kW output power was designed and built. Operation was carried out in both process modes – absorption and desorption – in steady state boundary conditions [2]. The heat and mass exchanger assessment and the comparison with the results of the initial numerical model used to design the heat and mass exchanger was done.

For the absorption process, it appears that the dilution of the sodium hydroxide (water vapor absorption in the liquid) occurs to a limited extent. For the desorption mode, a full comparison of the experimental and modelling results was carried out [3]. For water vapor desorption from a sodium hydroxide solution over a horizontal tube bundle with smooth tubes, a proposition of a correlation for the Nusselt number is given [4]. Within 25 % of relative uncertainty, numerical and experimental results have a similar order of magnitude for the desorption process. However, for the absorption process, the measured exchanged power is much lower than expected.

Surface wetting of absorbers

The low absorption power can be explained by the poor wetting of the stainless steel (AISI 316L) tube bundle from the absoption/desorption unit [2] and the short residence time of the sodium hydroxide in the water vapor.

As wettability is depending on the solid surface properties (e.g. roughness, surface oxygen content and the polar component) and on the fluid properties [5], different surface modifications (structuring, annealing) and fluid tuning (use of surfactants to reduce the surface tension) were investigated [6].

Higher surface area is obtained by mechanical texturing; by developing structured surfaces, an enhancement of the heat transfer coefficient is aimed as well as a size reduction of the absorber unit. Moreover, annealing in air increases the surface metal oxide content; a better wetting in terms of low wetting times was obtained for all the annealed samples. This can be explained by physical bonding between polar groups from the testing fluid and the surface metal oxide.

The influence of different surface texturing on the wetting with concentrated sodium hydroxide, without/or with surfactant addition was assessed. Compared to the reference case, the surfactant addition leads to a better wetting, decreasing the wetting time. The influence of two main parameters was analyzed:

- the residence time of the sorbent (sodium hydroxide solution) in the water vapor (sorbate) and
- the surface wetting behavior of the heat transfer fluid on the exchanged power.

A 1 kW absorption/desorption unit using the falling film working principle, concentrated sodium hydroxide (aqueous solutions) and water vapor as sorbent/sorbate pair was designed. Optimized tubes and sorbent will be used for the absorber/desorber tube bundle in order to quantify the impact of these technologies on the heat and mass exchanges.

References

[1] Y. Ding, S.B. Riffat, «Thermochemical energy storage technologies for building applications: a state-of-the-art review». Int. J. Low-Carbon Technol., vol. 0, 1–11, Feb. 2012.

[2] X. Daguenet-Frick, P. Gantenbein, E. Frank, B. Fumey, R. Weber, K. Goonesekera, «Seasonal thermal energy storage with aqueous sodium hydroxide – experimental assessments of the heat and mass exchanger unit». Presented at the International Conference on Solar Heating and Cooling for Buildings and Industry, Istanbul, Turkey, 2015.

[3] X. Daguenet-Frick, P. Gantenbein, E. Frank, B. Fumey, R. Weber, T. Williamson, «Seasonal Thermal Energy Storage with Aqueous Sodium Hydroxide – Reaction Zone Development, Manufacturing and First Experimental Assessments». In EuroSun 2014, Aix-les-bains, France, 2014.

[4] X. Daguenet-Frick, P. Gantenbein, J. Müller, B. Fumey, R. Weber, «Seasonal thermochemical energy storage: comparison of the experimental results with the modelling of the falling film tube bundle heat and mass exchanger unit». Renew. Energy, accepted.

[5] D. Brutin, «Droplet Wetting and Evaporation: From Pure to Complex Fluids». Academic Press, 2015.

[6] M. Dudita, X. Daguenet-Frick, P. Gantenbein, «Seasonal Thermal Energy Storage with Aqueous Sodium Hydroxide – Experimental Methods for Increasing the Heat and Mass Transfer by Improving Surface Wetting». Presented at the 11th ISES EuroSun Conference – International Conference on Solar Energy for Buildings and Industry, Palma (Mallorca), 2016.

Authors

Xavier Daguenet-Frick[1]
Mihaela Dudita[1]
Paul Gantenbein[1]
Matthias Rommel[1]
Andreas Häberle[1]

[1] HSR (University of Applied Sciences Rapperswil

Storages for Flexibility of Power and Heat

Scope of project

The aim is the advancement of novel storage technologies used at the intersection of power-to-heat(-to-power) in the framework of the project Dual Energy Storage & Converter (DESC). In this context, various models of thermal storages as well as their combination with heat pumps for both domestic and industrial applications have been further developed and verified within 2016. The models were used to evaluate and optimize existing systems as well as to design new ones. New phase change materials were identified and implemented in novel thermal storage technologies at key temperatures to be efficiently combined with heat pumps and chillers. Laboratory setups were designed to test and evaluate the application potential of these technologies under realistic conditions.

Status of project and main scientific results of workgroups

All the defined milestones for phase I were successfully reached. This report summarizes the work conducted by the Thermal Energy Storage (TES) group at Lucerne University of Applied Sciences (HSLU) during the year 2016.

Simulation and experimental characterization of high-power, latent heat storage

In 2015, a computational model of a latent heat storage based on tube bundle heat exchangers was successfully developed and verified by HSLU within the framework of SCCER HaE [1]. Due to the low heat conductivity of phase change materials (PCM), finned heat exchangers (HEX) are often utilized as alternative to tube bundle heat exchangers.

In an extension of previous modelling work, the solidification in a commercial Sunamp Heat Battery using a finned HEX was modelled and experimentally characterized [2]. The enthalpy based method was used as the most suitable approach to predict the heat transfer rate between the PCM and the heat transfer medium. A comparison between the heat flow of the storage as a function of time and the model predicted values are presented in Figure 1. The model can be used to optimize the HEX design regarding production costs and heat transfer rate.

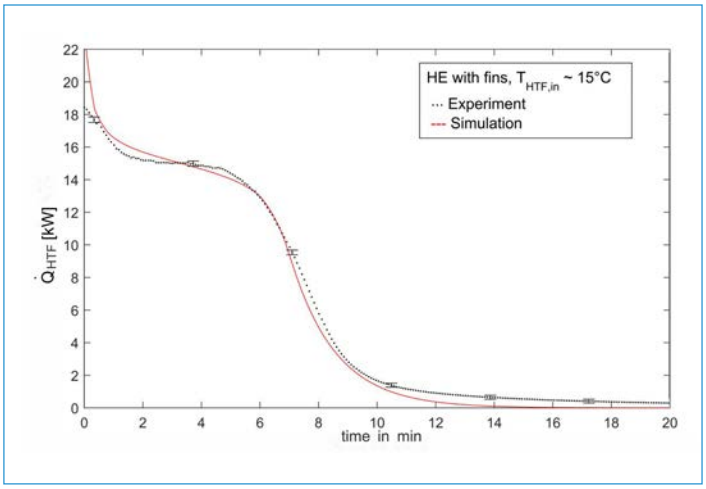

Figure 1:
Comparison between the overall heat flow of the Sunamp Heat Battery model as it was measured in the laboratories of HSLU and predicted from the developed model.

Simulation of thermal storage for residential heating systems with heat pump to increase flexibility in smart grids

Integrating large shares of variable renewable energies requires high flexibility from the major consumers to balance energy consumption and production. Ideal candidates for this balance are heat pumps due to their high efficiency and the energy demand for space heating.

To decouple heat production and consumption for residential heating, the impact of additional thermal storage systems as well as the building inertia was investigated (see Figure 2). The impact of different heat pump capacities, thermal storage systems and building types was studied with Matlab/Simulink simulations based on detailed and experimentally verified models for the individual components [3].

The integration of thermal storages enables an increase of the flexibility (fraction of the day with blocked heat pump activity) at the expenses of a lower efficiency. In particular,

List of abbreviations

DESC	Dual Energy Storage & Converter
HEX	Heat Exchangers
HTF	Heat Transfer Fluid
PCM	Phase Change Material

Authors

A. Stamatiou[1]
A. Ammann[1]
A. Abdon[1]
S. Maranda[1]
D. Gwerder[1]
F. Eckl[1]
R. Waser[1]
P.Schuetz[1]
L. Fischer[1]
J. Worlitschek[1]

[1] HSLU (Lucerne University of Applied Sciences & Arts)

Storages for Flexibility of Power and Heat

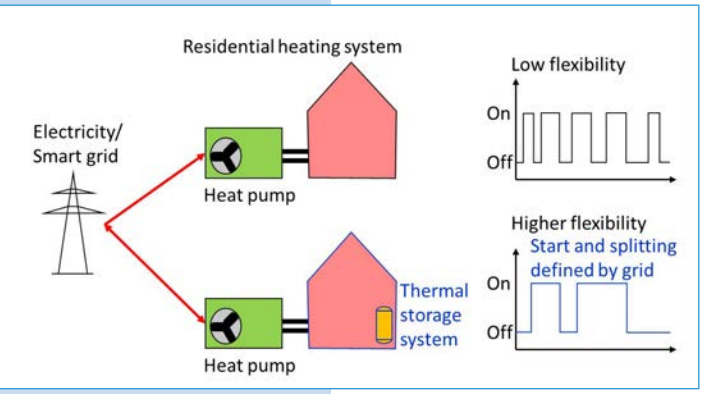

Figure 2:

Overview of modelled components and motivation for enabling flexibility by increased exploitation of thermal storages and building inertia.

References

[1] A. Stamatiou, S. Maranda, F. Eckl, P. Schuetz, L. Fischer, J. Worlitschek. Submitted.

[2] S. Maranda, R. Waser, A. Stamatiou, M. Zaglio, J. Worlitschek. In 4th SCCER Symposium Heat & Electricity Storage, 2016.

[3] P. Schuetz, D. Gwerder, L. Gasser, L. Fischer, B. Wellig, J. Worlitschek. In 10th International conference of renewable energy storage, Düsseldorf, 2016.

[4] P. Schuetz, D. Gwerder, L. Gasser, B. Wellig, J. Worlitschek. In 4th SCCER Symposium Heat & Electricity Storage, 2016.

[5] P. Schuetz, D. Gwerder, L. Gasser, L.J. Fischer, B. Wellig, J. Worlitschek. In Proceedings of the 12th IEA Heat Pump Conference, Rotterdam, 2017.

[6] A. Stamatiou, D. Leemann, A. Abdon, L. Fischer, J. Worlitschek. In 4th SCCER Symposium Heat & Electricity Storage, 2016.

[7] A. Ammann, «Aufbau, Inbetriebnahme und Messungen an einem Latentwärmespeicher mit Direktkontakt-Wärmeübertragung». Lucerne University of Applied Sciences and Arts, 2017.

[8] A. Stamatiou, M. Obermeyer, L.J. Fischer, P. Schuetz, J. Worlitschek. Renew. Energy, in review.

for the retrofitted old building, a substantial increase can be achieved. The integration of a storage element is vital to compensate the efficiency losses acquired by enabling flexibility [4, 5].

Development of novel PCM storage technologies

Concept based on PCM slurries

In this concept, similarly to ice-slurries, only a part of the phase change material changes phase during charging/discharging of the storage, enabling pumping of the storage medium. Such systems promise higher energy densities both as refrigerants and as storage media while presenting better heat transfer characteristics than conventional latent heat storage technologies. This technology is expected to deliver high thermal power and high temperature stability in a compact design that can operate with conventional components (heat exchangers, pumps, etc) [6].

An examination of the important processes in the Swiss industry revealed that the highest potential for the implementation of PCM slurries lies in the temperature range of 80 ± 20 °C. A combination of measured and literature based thermo-physical properties was gathered and aluminum ammonium sulfate dodecahydrate ($NH_4Al(SO_4)_2 \cdot 12\,H_2O$) was selected as the main PCM candidate. A proof-of-concept setup has been designed and built in HSLU and a first feasibility study is taking place.

Concept based on direct contact heat exchange

In this project, a novel latent heat storage system based on a direct contact between the heat transfer fluid (HTF) and the PCM was developed, to drastically increase heat transfer in latent storage systems. These systems preserve the high energy density associated with latent heat storage while avoiding complicated and cost-intensive heat exchangers. Additionally, the ability to generate large heat exchange surface area at the interface of the HTF bubbles and the PCM can result in high thermal power output. A proof of concept test-rig has been built and evaluated in HSLU (see Figure 3). The first results show that such a system can achieve a heating power up to 25 kWm^{-3} at a logarithmic temperature mean of 2.5 K, while the power output can be controlled directly via the mass flow. [7]

Novel PCM research – esters

In this work, unbranched, saturated carboxylic esters were evaluated with respect to their suitability to be used as storage media for latent heat storage applications. Therefore, important thermophysical properties were gathered both by means of literature research as well as by experimental measurements. Additionally esters were critically evaluated against other common phase change materials in terms of their environmental impact and their economic potential. The experimental investigations were performed for eleven selected ester samples with a focus on the determination of their melting temperature and their enthalpy of fusion using differential scanning calorimetry. Both experimental results and literature data revealed that the highest potential of esters against other phase change materials lies in low temperature applications where the main alternative is using salt hydrates [8].

Figure 3:

Laboratory test-rig for the investigation of direct contact heat exchange concept.

Batteries

Advanced Batteries and Battery Materials

Work Package "Batteries and Battery Materials" at a Glance

Batteries offer the unique opportunity to directly store and when needed to release electric power with high overall roundtrip efficiencies of > 90 %, therefore offering high potential for decentralized storage of excess renewable energy from the kilowatt to the megawatt range. The main topics of research in this work package are centered around the development and testing of materials and components for next generations of alkali-ion batteries, i.e., high energy and power Li- and Na-ion batteries.

One of the options to store electrical energy is the use of batteries. This direction was investigated within this work package of this SCCER.

Along the rather exploratory phase I, the main efforts were dedicated to gaining basic knowledge on prospective battery systems, with the goal to identify the most promising ones for the development of future technologies.

Three main directions were pursued for material related activities, and all partners were involved in the different topics. Under the lead of Maksym Kovalenko from ETHZ and Empa the search for high-energy negative electrodes for lithium-ion batteries was going on in phase I, in order to outperform current commercial battery systems. Strong efforts were also made on alternative realistic systems, more specifically on sodium-ion batteries, an activity under the lead of Claire Villevieille from PSI. Also, under the lead of Katharina Fromm from the University of Fribourg, there was a search for alternative energy storage concepts being possibly important in the far future, like the lithium-air and lithium-water chemistries. The main focus was however on both Li-ion and Na-ion research where all three groups provided their core expertise and demonstrated collaboration in research, and applied for joint projects.

Of course, the production processes for the new materials as well as the electrodes thereof needed to be understood. Challenges expected during the production of real sized battery cells under real economic conditions needed to be identified and feedback given to the material developers. The underlining question is how to produce batteries in a cost effective way. These activities are under the lead of Axel Fuerst from Berner Fachhochschule (BFH) Biel.

Also, the activities at Empa formerly under the lead of Urs Sennhauser (retired) and now under the lead of Corsin Battaglia are currently being integrated into this work package dealing with all aspects of batteries.

Li-ion batteries

The research activities focusing on Li-ion batteries included highly exploratory search for novel materials as well as very practical tasks raised by the Swiss industry (Belenos Clean Power Holding). The leitmotif was the development of anode materials (nanoscale materials composed of Sn, Sb, SnSb alloys, and metal phosphides). Initially these nanomaterials were synthesized using new, often costly but precise methods. The preparation of selected materials, such as antimony, was then further followed, yielding low-cost synthesis that had been scaled-up with the help of Belenos to 100 g scale. The materials were then tested at the premises of the industrial partner Belenos. The first results from Li-ion and also Na-ion full-cell laboratory experiments, using $LiCoO_2$ and $Na_{1.5}VPO_{4.8}F_{0.7}$ as cathodes, indicate stable cycling performance of SnSb nanocrystals with respective lithium- and sodium-ion anodic specific charge of 600 mAh/g (up to 3.0 V) and 400 mAh/g (up to 2.7 V). The voltage in parentheses is the average one during cell discharge.

Within both Li-ion and Na-ion batteries research domains, experimental studies were supported with a computational structure prediction work.

Sodium based batteries

Due to the low abundance of lithium and thus projected increasing cost, cheaper alternatives based on other alkali metals were investigated.

The main focus was on sodium which is a bigger and heavier cation compared to lithium, thus the specific energy of a sodium-based battery is lower. This drawback can be compensated by higher voltage cathodes and higher specific charge anodes. For the latter, the alloy/conversion reaction of Sn as a model element was investigated but the volume change close to 400 % resulted in particle fractures and strong capacity fading.

Illustration: tolokonov / iStock

Thus, we switched to stabilized Sn-based materials ($MnSn_2$, $FeSn_2$, and $CoSn_2$) as the inactive transition metal combined to an active element mitigates the volume changes. With an appropriate engineering of the electrode, > 400 mAh/g was obtained for $MnSn_2$ during 100 cycles. However, in a full-cell, too much Na was consumed for solid-electrolyte interphase (SEI) formation.

Thus, the activities were re-focused on the development of low cost, bio-waste based negative electrodes. Nut shells from almonds were identified as a source of promising carbonaceous material and a specific charge of 270 mAh/g was demonstrated during more than 200 cycles. Regarding the positive electrode, the layered oxide P2-$Na_{0.67}(Mn_{0.6}Fe_{0.25}Co_{0.15})O_2$ was investigated, where a part of the Co has been substituted by Al. The Al-based materials demonstrated a specific charge of > 130 mAh/g. Now, the next step will be to combine the bio-waste negative electrode material with a low cost positive electrode material.

In the frame of material research activities in the long run, a concept of SnO_2@C-Nanorattles was tested, in which the active material can expand and shrink inside a conductive shell material. Also, heterometallic single source precursors were synthesized with different equivalents of sodium alkoxides, to get after combustion the phase $Na_{0.67}CoO_2$, a prospective material for sodium-ion batteries. Electrolytes based on different types of imidazolium- as well as pyrrolidinium-based ionic liquids were synthesized and their inflammability, thermal and electrochemical stabilities were examined. Pyrrolidinium-based ionic liquids based on a benzo-15-crown-5 core showed one-dimensional channel in the solid state, promising excellent Li-ion transport properties.

Further, for possible future battery chemistries, a buffer of an aqueous electrolyte for a dual-electrolyte Li-air battery was optimized. A full cell assembly of a Li-air battery system was tested.

Battery production

In parallel, steps towards a production line for small series of battery cells were taken. A technology screening was finalized and a test plant to optimize the critical system parameters for slitting and welding processes is in place. Demonstration of prototype production of battery electrodes on newly developed processing machinery is working, tested as proof-of-concept with nanosized $LiCoO_2$ cathodes.

For the battery production work a new research group was founded at BFH, focusing on the development of innovative and cost-effective production technologies and process optimization.

The aim is to support Swiss battery industry and battery production equipment suppliers from Swiss machine industry, as well as suppliers of electrode materials. The purpose is to share machine and process knowledge from a holistic approach to offer support with deeper process knowledge and to identify potential for process optimization.

Further, BFH aims to connect Swiss excellence in electrochemical research with the production at the shop floors, inter alia, due to a pilot line for testing and demonstration (cf. Figure 1).

Battery testing

Finally, a unique 500 kW battery testing facility was built at Empa, equipped with temperature, gas, and flame sensors, enabling aging experiments and stress cycling of cells and batteries. Worst case scenarios such as fire and explosion are contained by a sand extinguisher and pressure relief panels. Failure mechanisms of commercial batteries were investigated and identified using electron microscopy and focused ion beam techniques and, to facilitate the interpretation of data, a theoretical statistical model for electrochemical impedance spectra of batteries was developed.

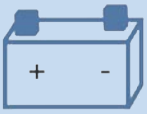

Development of Nanostructured Electrode Materials for Li- and Na-Ion Batteries

List of abbreviations

LIB	Lithium-Ion Battery
NC	Nanocrystals
SIB	Sodium-Ion Battery

Scope of project

Lithium-ion batteries (LIBs) with higher energy and power densities are actively sought to increase the competitiveness and widespread deployment of electric cars and stationary energy storage units, and for enabling new portable electronic devices. Great hopes have been extended to conceptually similar sodium-ion batteries (SIBs) due to the much greater natural abundance of Na and the possibility of replacing copper anode current collectors with aluminum foils. The eventual success of SIBs will require this technology to have the same energy density as LIBs.

Status of project and main scientific results of workgroups

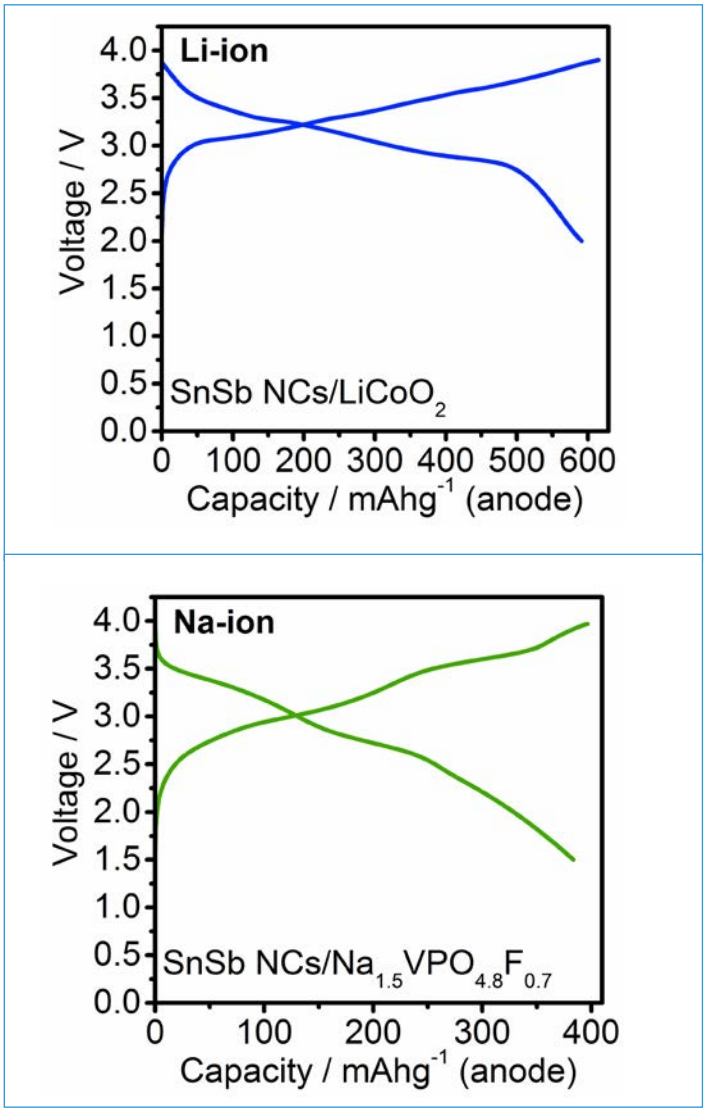

Figure 1:

Electrochemical performance of SnSb NCs in lithium-ion and sodium ion full-cells using $LiCoO_2$ (top, at a current of 400 mAg^{-1}) and $Na_{1.5}VPO_{4.8}F_{0.7}$ (bottom, at 200 mAg^{-1}) as the cathode material, respectively. Galvanostatic charge/discharge curves are shown for 30th cycle. Displayed specific capacities and currents correspond to the mass of SnSb NCs. Capacity retention for SnSb NCs at a current of 400 mAg^{-1} in Li-ion and at 200 mAg^{-1} in Na-ion full cells.

Anode materials – tin-antimony alloys

We have developed a simple and inexpensive colloidal synthesis of SnSb nanocrystals (NCs) and demonstrate their utility as lithium- and sodium-ion anode materials [1], see Figure 1.

In particular, SnSb NC Li-ion anodes deliver capacities of ~890 $mAhg^{-1}$ for 100 cycles at a current density of 200 mAg^{-1} and show excellent rate capability, reaching 90% and 80% of the theoretical capacity at current densities of 1000 and 5000 mAg^{-1}, respectively.

Similarly, SnSb NCs show also outstanding Na-ion storage properties with only ~5% capacity loss over 100 cycles at a rate of 5000 mAg^{-1}.

Full-cells can be constructed with SnSb anodes and state-of-the-art cathodes, achieving anodic capacities of 600 and 400 $mAhg^{-1}$ with an average discharge voltage of 3.0 and 2.7 V for lithium- and sodium-ions, respectively.

Authors

Maksym V. Kovalenko[1]

[1] ETHZ and Empa

Development of Nanostructured Electrode Materials for Li- and Na-Ion Batteries

Cathode materials – iron(III) fluoride

With the demands placed on batteries constantly increasing, new positive electrode materials are desired with

- higher energy density,
- satisfactory power density,
- long-term cycling capabilities,
- composed of highly abundant low-cost elements.

One such low-cost cathodic material is iron(III) fluoride – FeF_3. Its theoretical capacity for single-electron reduction, accompanied with the insertion of Li^+ ions, is 237 $mAh\,g^{-1}$. Herein we have developed a new synthesis for nanocrystalline FeF_3 using inexpensive iron trifluoroacetate as a molecular single-source precursor [2], see Figure 2.

We also extended this simple chemistry to several transition metal difluorides (M = Fe, Co, Mn).

With FeF_3, high capacities of 220 $mAh\,g^{-1}$ were attained at moderate current densities of 100 $mA\,g^{-1}$ (~ 0.5 C). In addition to high capacity, we find a strong evidence for high rate capability. Capacities of up to 155 $mAh\,g^{-1}$ were observed with 1 minute (10 $A\,g^{-1}$) charge-discharge ramps, and at least 88 % of this capacity was retained after 100 cycles. When tested as a sodium cathode, FeF_3 exhibits capacities of up to 160 $mAh\,g^{-1}$ at a current rate of 200 $mAh\,g^{-1}$.

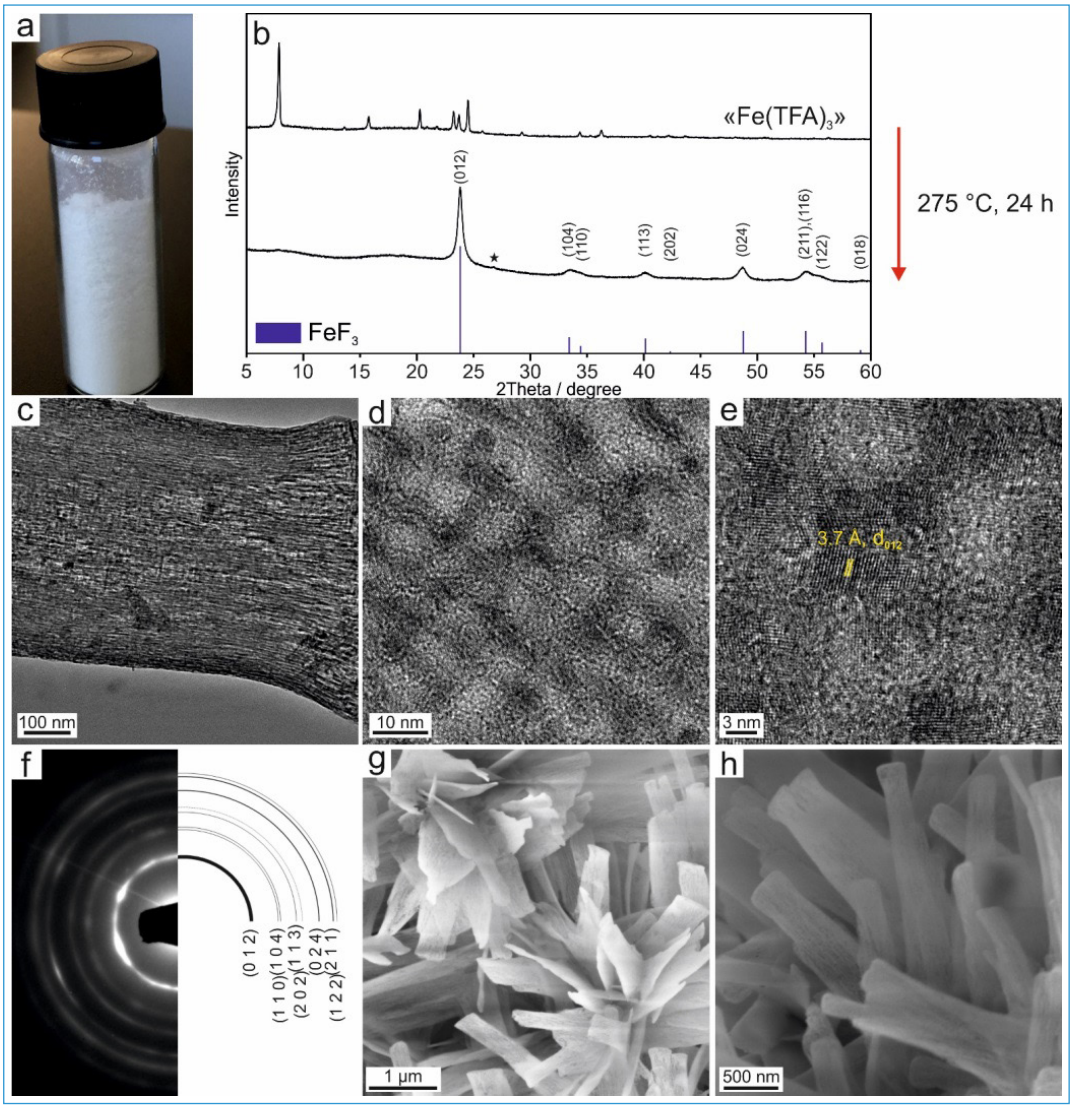

Figure 2:

(a) Photograph of a vial containing iron(III) trifluoroacetate («$Fe(TFA)_3$»);

(b) Powder XRD pattern of «$Fe(TFA)_3$» before and after decomposition to FeF_3 (PDF 033-0647) with an asterisk indicating a minor impurity of small FeF_2 (its (110) reflection (PDF 045-1062));

(c) TEM images of FeF_3;

(d),(e) HRTEM images of FeF_3;

(f) Selected-area electron diffraction (SAED) indexed with ReO_3-structure of FeF_3;

(g),(h) SEM images of FeF_3.

References

[1] M. Walter, S. Doswald, M.V. Kovalenko. J. Mater. Chem. A, 4, 7053–7059, 2016.

[2] C. Guntlin, T. Zünd, K.V. Kravchyk, M. Wörle, M.I. Bodnarchuk, M.V. Kovalenko. Submitted.

Development of Low Cost Na-Ion Batteries

List of abbreviations

CMC	Carboxymethyl Cellulose
PVDF	Polyvinylidene Difluoride
SEM	Scanning Electron Microscopy
XRD	X-ray Diffraction

Scope of project

Due to the abundance of sodium in the Earth's crust, Na-ion batteries could be a more economical alternative to lithium-ion batteries. However, one has to consider the lower energy density of this technology and thus, Na-ion batteries could be applicable for stationary energy storage. While there's a wide array of choice for cathode materials, the choice for a stable anode material is limited to disordered carbons [1] as graphite is not suitable to the sodium-ion system. Disordered carbon materials are generally synthesized out of industrial products such as sucrose and polyacrylonitrile [2]. These compounds, however, can be replaced by biowaste materials which present the advantage of further decreasing the cost of the electrode materials. In this study, shells from almonds were used as a source of carbonaceous materials and used as negative electrode for sodium-ion batteries. Various atmosphere were used for the synthesis and the impact on the carbon properties was investigated by means of galvanostatic cycling, X-ray diffraction (XRD), scanning electron microscopy (SEM). Based on this material, a full cell with layered oxide P2-$Na_{0.67}(Mn_{0.6}Fe_{0.25}Co_{0.15})O_2$,where a part of the Co had been substituted by Al, on the positive electrode was investigated.

Status of project and main scientific results of workgroups

After establishing a careful guideline to optimize the electrode engineering in conversion based materials (Sn, $MnSn_2$, $FeSn_2$, $CoSn_2$, Figure 1) [3] and the electrolyte formulation both of which strongly influence electrochemical cycling performance, we developed new materials (negative and positive electrodes) for cheap Na-ion batteries.

For the former, the most common binder used in Li-ion batteries, polyvinylidene difluoride, was found to be unsuitable for Na-ion batteries due to its decomposing to form NaF [4]. Additionally, a systematic investigation of particle size, binder and conductive additive ultimately led to an optimized electrode composition consisting of 70 %wt micron-sized active material, 18 %wt carbon black and 12 %wt sodium carboxymethyl cellulose (Na-CMC) binder [5] (Figure 1).

For the latter, we have developed a new research direction to drastically reduce the cost of the Na-ion batteries by making carbonaceous materials (negative electrodes) based on biowaste.

Experimental

Almond shells were first ground using mortar and pestle and then soaked in 10 % H_2SO_4 solution for 24 h. Removal of the acid was subsequently done by washing with deionized water until reaching neutral pH. The shells were dried at 80 °C for 12 h prior to size reduction using ball milling. Carbonization was then operated in a tubular oven at 1000 °C under different atmospheres [Ar, N_2, Ar + 5 % H_2 (AW5)]. Finally, the resulting carbonaceous samples were named as Ar, N_2, and AW5. Galvanostatic cycling was performed in

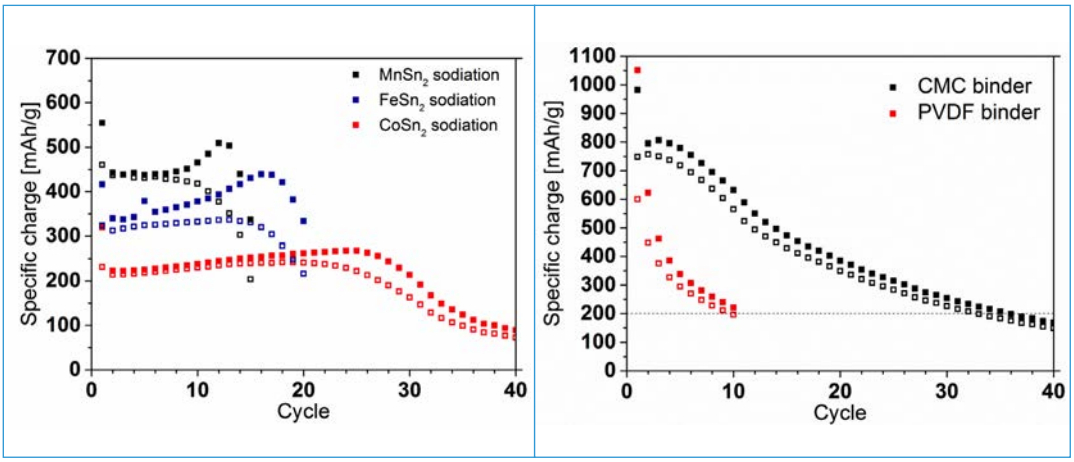

Figure 1:

Left: Cycling stability of $MnSn_2$, $FeSn_2$ and $CoSn_2$.

Right: Cycling stability of Sn electrodes using PVDF binder or Na-CMC binder.

Authors

Joel Cabañero[1]
Cyril Marino[1]
Claire Villevieille[1]

[1] PSI

Development of Low Cost Na-Ion Batteries

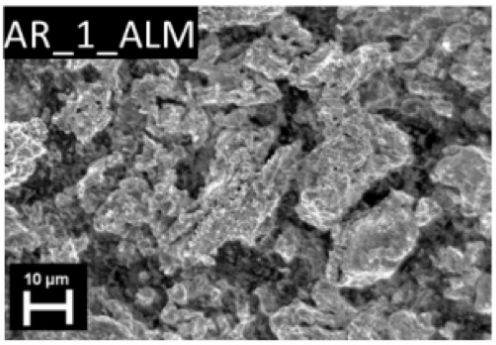

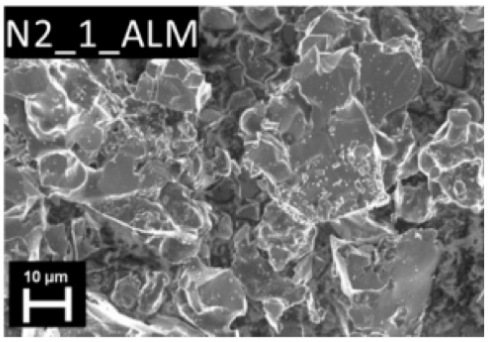

Figure 2:

SEM images of the carbonaceous samples. Left: Ar sample. Right: N_2. sample.

a half-cell with sodium metal as counter electrode and 1 M $NaClO_4$ in propylene carbonate used as the electrolyte. The electrode was composed as such 85 : 5 : 10 (active material: Super C65 : CMC).

Results

The SEM images (Figure 2) reveal similar morphological features among the carbonaceous samples whatever the atmospheres used. The primary particles are very small below the micrometre range even if some of them can be very large with several microns as can be seen in the case of the N_2 sample. As expected from the ball milling procedure, the particle size distribution is also very broad. We noticed that the particles tend to form big agglomerates of several tens of micrometres.

The XRD patterns of the carbonized samples reveal characteristic broad peaks at 2θ values ca. 22° and 44° corresponding to the (002) and (100) planes, respectively. A minor impurity (CaS) was detected at 32° and 45° in the patterns of the carbonaceous materials and originated most probably from the calcination of $CaSO_4$ present in the almond shell.

The cycling performance of the different materials is shown in Figure 3. Initially, both Ar and N_2 have specific charge values at ca. 325 mAh/g with a Coulombic efficiency of ca. 70 % for the first cycle. The sample AW5 exhibits the lowest specific charge at ca. 200 mAh/g for the first cycle and the lowest Coulombic efficiency ca. 50 %.

On succeeding cycles, the samples synthesized under Ar and N_2 present stable specific charge values at ca. 265 mAh/g whereas the one synthesized under AW5 delivers only 100 mAh/g. The relative low electrochemical performance obtained for AW5 could be linked to the higher level of graphitization obtained from Raman spectroscopy analysis.

Surprisingly, the specific charge of the N_2 sample increases accompanied by a decrease in Coulombic efficiency. This may be attributed to the electrolyte decomposition upon cycling. Further optimizations are ongoing to verify the electrochemical performance.

Full Cell Testing

The new anode material was tested in combination with the also developed new cathode materials based on the 20 most abundant elements in Earth crust [6].

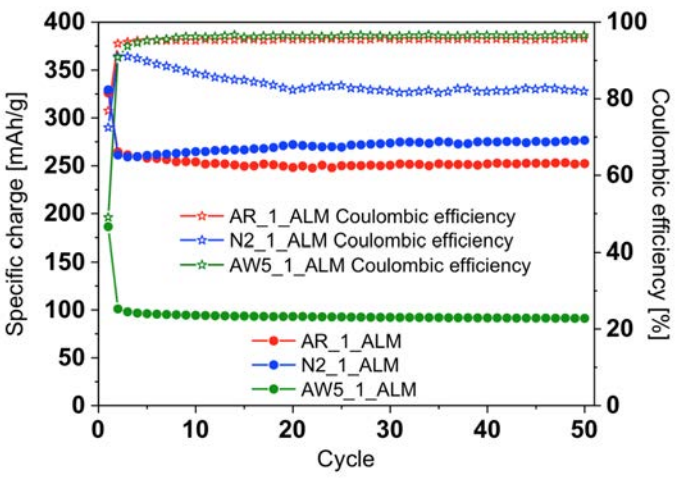

Figure 3:

Electrochemical performance of the carbonaceous samples cycled at C/10 rate.

Development of Low Cost Na-Ion Batteries

On the positive electrode we investigated the layered oxide P2-$Na_{0.67}(Mn_{0.6}Fe_{0.25}Co_{0.15})O_2$, where a part of the Co had been substituted by Al, combined with the negative electrode based on the carbonaceous biowaste material described above. The electrochemical performance of the materials is presented in Figure 4 (left) at different cycling rates. The Al-based materials demonstrated higher specific charge at ca. 140 mAh/g at 1.6C, compared to 115 mAh/g for the reference material NaMFC. After 50 cycles, a specific charge higher than 130 mAh/g is still provided for the Al-based compounds whereas only 80 mAh/g is reached in the case of NaMFC.

Conclusion

Disordered carbons have been successfully synthesized using biowaste materials i.e. almond shells.

The inert atmosphere used during synthesis has a significant impact on the physical and electrochemical performance of the disordered carbons.

Carbons synthesized out of Ar and N_2 have similar specific surface area, pore size distribution and electrochemical performance despite a probable different surface composition. Thanks to this approach, we obtained a specific charge of 259 mAh/g.

Meanwhile, carbons synthesized under a reducing atmosphere (AW5) resulted to poorer electrochemical performance compared to the ones synthesized under an inert atmosphere.

Finally, the target is to generate full-cell Na-ion batteries combining bio-waste negative electrode materials with low cost positive electrode materials.

As indicated in Figure 2 (right) some issues still need improvement to maintain the stable specific charge and this will be the challenge of the next SCCER period for the Na-ion batteries.

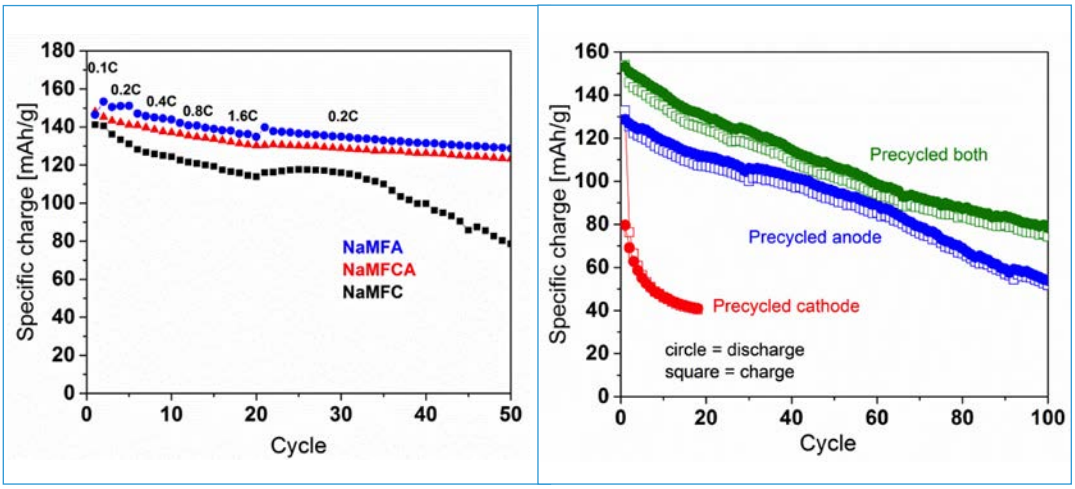

Figure :

Left: Cycling stability of $MnSn_2$, $FeSn_2$ and $CoSn_2$.

Right: Cycling stability combining carbonaceous negative electrode and NaMFA positive electrode materials.

References

[1] E. Irisarri, A. Ponrouch, M.R. Palacin, J. Elect. Soc., 162 (14), A2476–A2482, (2015).

[2] D.A. Stevens, J.R. Dahn, J. Elect. Soc., 147, 1271–1273, (2000).

[3] L. Vogt, C. Villevieille, JES 163, A1306, 2016; L- Vogt, C. Villevieille, Journal Mat. Chem. A 4, 19116, 2016.

[4] L. Vogt, M. El Kazzi, E. Berg, S. Pérez-Villar, P. Novak, C. Villevieille, Chemistry of Materials 27 (4), 1210, 2015.

[5] L. Vogt, C. Marino, C. Villevieille, Chimia, 69, 729, 2015.

[6] C. Marino, C. Villevieille, submitted, 2016; C. Marino, S. Park, C. Villevieille, submitted, 2016.

Development of Anodes, Cathodes and Electrolytes for Alkali Metal Ion Batteries and Li-Air Batteries

Scope of project

Electricity storage is an important contribution to the plans in energy turnaround. Stand-alone devices are expected to store electricity overproduction within short times of charging and releasing it when needed. This requires higher energy densities, less toxic and more abundant materials, better electrolytes and improved electrodes. Together with the teams of Maksym Kovalenko and Claire Villevieille, we contribute to the development of new cathode and anode materials, new electrolytes and test them in coin cells.

Status of project and main scientific results of workgroups

Development of ionic liquids as an electrolyte for rechargeable alkali metal ion batteries

Different types of imidazolium- as well as pyrrolidinium-based ionic liquids were synthesized with crown ether based moieties. Their inflammability, thermal and electrochemical stabilities were examined.

The imidazolium ionic liquids with benzo-15-crown-5 showed the best thermal stability up to 400 °C, while the others are stable until 320 °C. The electrochemically most stabile ionic liquids were the ones with a butyl-substituted imidazole ring (Figure 1). Pyrrolidinium-based ionic liquids based on a benzo-15-crown-5 core showed one-dimensional channel in the solid state, promising excellent Li-ion transport properties. The purification and upscaling are ongoing and first ionic liquids are under testing for sodium ion batteries at PSI (collaboration C. Villevieille).

Development of anode materials for rechargeable alkali metal ion batteries

While providing higher capacities than commercial graphite, alkali metal alloys undergo large volume changes during insertion/extraction of alkali metal ions, causing cracks in the electrode and capacity drops.

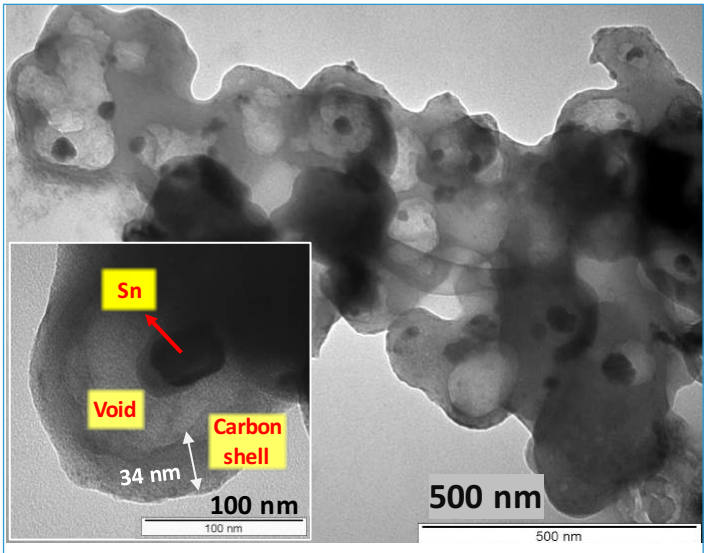

Figure 2:
Nano-rattle structure of Sn@C.

Nanorattles, in which the active material can expand and shrink inside a conductive shell material, have been designed to prevent these drawbacks. Core-shell particles of Sn@SiO_2 are formed by the reverse micelle microemulsion method. They are coated by carbon and chemically etched to form Sn@C. After this process, tin was found inside and outside of the shells (Figure 2) and the electrochemical tests of this material with lithium showed a rate capability of 590 mAh/g at C/10 after 10 cycles. We will further optimize the carbon shell size, the shell shape and the loading of Sn by slight synthesis modifications.

Development of cathode nanomaterials

Using the precursor method, we have prepared nanoscale $LiCoO_2$ of different particle and crystallite sizes, which are currently being tested in half and full cell systems. These materials can be obtained in multi-gram scale. In analogy, $NaCoO_2$ was made from similar precursors. While for the lithi-

References

[1] N.H. Kwon, H. Yin, T. Vavrova, J.H-W. Lim, U. Steiner, B. Grobéty, K.M. Fromm, «Nanoparticle shapes of $LiMnPO_4$, Li^+ diffusion orientation and diffusion coefficients for high volumetric energy Li^+ ion cathodes». J. Power Sources, 342, 231–240, 2017.

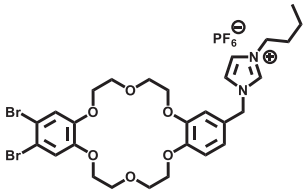

Figure 1:
Imidazolium ionic liquids with crown-6 moiety.

Authors

Benoît Baichette[1]
Nelly Hérault[1]
Nam Hee Kwon[1]
Sivarajakumar Maharajan[1]
Hervé Yao[1]
Katharina M. Fromm[1]

University of Fribourg[1]

Development of Anodes, Cathodes and Electrolytes for Alkali Metal Ion Batteries and Li-Air Batteries

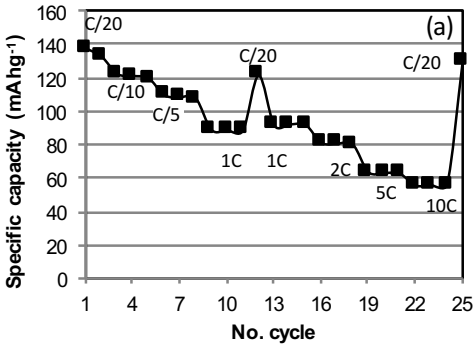

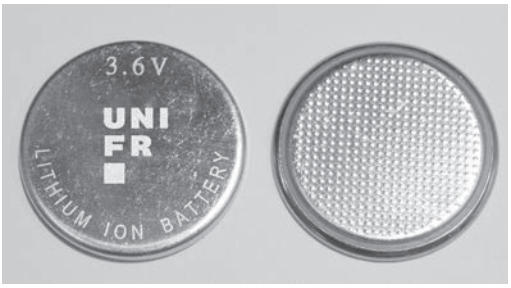

Figure 3 (top):

Left: The C-rate capability of $LiMnPO_4$ electrode prepared by rod-shaped $LiMnPO_4$.

Right: Coin cells made by UniFr.

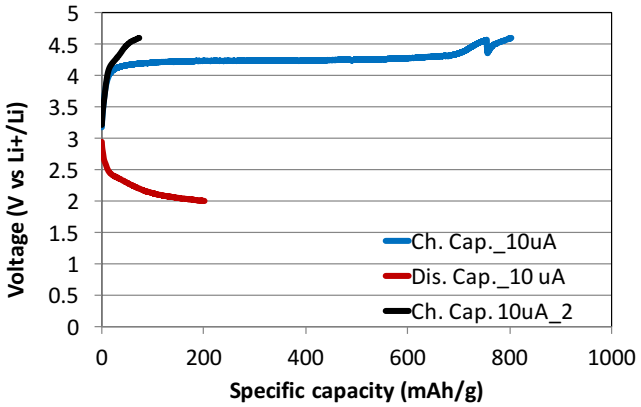

Figure 4:

The charge and discharge curves of dual-electrolyte Li-O_2 battery.

Figure 5 (bottom):

TEM and SEM pictures of (A) TiO_2-NC, (B) TiO_2-NS, (C) Ag/TiO_2-NC and (D) Ag/TiO_2-NS.

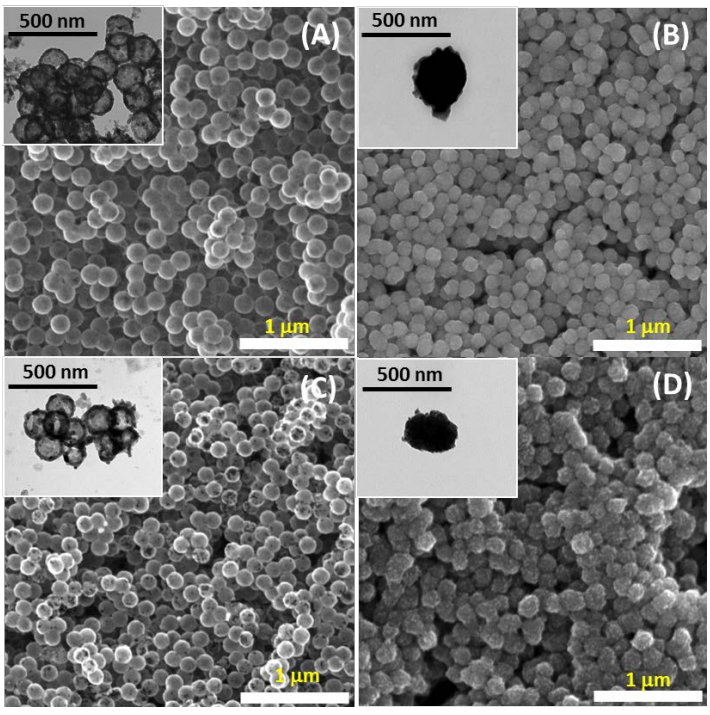

um compounds, the structures of the precursors have been mostly identified, they remain unknown for the sodium precursors.

For the olivine $LiMnPO_4$, several crystallite sizes and shapes at the nanoscale were synthesized, their preferred Li-ion diffusion pathways identified [1] and the samples are now being tested in full cells (Figure 3).

Development of Li-air batteries with dual electrolytes system

The aim of dual-electrolyte Li-air battery is to obtain reversible electrochemical reactions with high capacity. We found that a buffer solution in aqueous electrolyte increased the O_2-solubility and lowered its alkalinity.

The challenge of the full cell assembly was to seal the lithium metal tightly and to exclude CO_2 entering the cell from outside. After managing the sealing and optimizing the aqueous electrolyte, new MoS_2-electrodes from Prof. H.G. Park, ETHZ (collaboration within an NRP-70 project) were tested in full cell setups.

The cyclic voltammograms showed reversible redox reactions at the scan rate between 0.1 and 1 mV/s. While the first charge capacity provided promising 800 mAh/g at 10 µA, the capacity dropped rapidly to 70 and 20 mAh/g (Figure 4). We will investigate in-depth electrochemical analysis and characterization to understand the electrochemical behavior and to improve the capacities.

Development of TiO_2 as photocatalysts

In collaboration with the work package on CO_2-reduction, TiO_2 nanocapsules were synthesized.

They were found to be more active for water splitting than commercial TiO_2. The presence of different amounts of ca. 20 nm silver nanoparticles (AgNPs) in and on the TiO_2 nanocontainers had no positive effect on the catalysis, which is why we are now studying the size effect of the AgNPs (Figure 5). The CO_2-reduction was shown to yield among other products also methanol.

Discovery of Fundamental Relations Between Impedance Spectra and Charge Transport Mechanisms

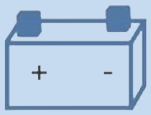

Scope of project

Impedance spectroscopy is a widely used technique for the investigation of charge- and mass-transport, as well as the associated degradation, in complex systems. It has become a key analytical tool for any group pursuing Li-ion battery research and development. Being a non-invasive method, it can provide valuable information from batteries under actual working conditions. However, there are still great challenges in this field, mainly related to the interpretation of impedance measurements.

Status of project and main scientific results of workgroups

Until recently, most models used in the parameterization of impedance data were based on the assumption that the transport is diffusive. For instance, the bulk impedance resulting from Li-ion intercalation, as ions are injected into the cathode through the solid-electrolyte interface, has been always modelled with the Warburg element, $Z \propto (iw)^{-1/2}$. However, experimental evidence indicates that not all data can be explained with circuits made of resistors, capacitors, inductors, and Warburg elements. Then, models have been proposed, which include constant-phase elements (CPEs), $Z \propto (iw)^{-n}$, where the phase is $-n\pi/2$, and the exponent $0 < n < 1$ that has no clear meaning.

In a previous work [1], we found that the general CPE can be understood based on a fundamental and more general formulation of the transport, which contains diffusion as a specific case. Within this framework, we showed that the constant-phase behaviour displayed by the impedance of battery parts have a universal statistical origin and that the value of the phase characterizes the type of transport in the system. Ion transport in the electrodes is in general non-diffusive, and this is characterized by the corresponding CPE exponent.

It was also shown that there are correlations of practical importance between n, the cell state of charge, and capacity loss. The new approach also links n with the dependence of the cell capacity on the charging rate. Larger deviations in the behavior from the diffusive limit will result in stronger rate-dependency of the capacity.

Applications in the analysis of battery performance and charge relaxation in ion conductors and dielectrics

As a continuation of this work, we were able to show that the laws that we previously applied to the transport of ions (involving hopping) can be extended to describe the orientation of localized dipoles [2]; a model meant to describe polymers widely used in electrochemistry.

This led us to discover universal constraints to the form of dielectric response spectra. In this extension of the work, phase exponents also play the essential role of characterizing the type of relaxation taking place in complex systems, allowing a clear identification of fast (exponentially) relaxing systems and slow (algebraically) relaxing ones.

The classification into slow and fast, based on the low-frequency behavior of the dielectric function, has a general mathematical origin and applies not only to dipolar systems but also to materials with moving ions such as electrodes. The conductivity relaxation in the diffusive limit is equivalent to the relaxation function of a dipolar system that satisfies Debye's model. Non-diffusive transport has a relaxation similar to dipolar glasses. The relevant exponents for dipolar systems correspond to the rising and lowering slopes of the loss-peak and can be extracted within a standard measurement of dielectric losses.

These results are being applied not only in our battery research, but also in the field of dielectric polymers for energy harvesting and actuators [3, 4].

List of abbreviations

CPE Constant-Phase Element

References

[1] E. Cuervo-Reyes, C.P. Scheller, M. Held, U. Sennhauser, J. Electrochem. Soc., 162, A1585 (2015).

[2] E. Cuervo-Reyes, Scientific Reports, 6, 29021 (2016).

[3] Y.S. Ko, E. Cuervo-Reyes, F.A. Nüesch, D.M. Opris, Proc. of SPIE., 9798, 97981I (2016).

[4] S.J. Dünki, E. Cuervo-Reyes, D.M. Opris, Polym. Chem., published online DOI: 10.1039/C6PY01917J.

Authors

Eduardo Cuervo-Reyes[1,2]
Marcel Held[2]
Evelyn Stilp[1,2]
Urs Sennhauser[2]

[1] Empa (Laboratory Materials for Energy Conversion)
[2] Empa (Laborarory Reliability Science and Technology)

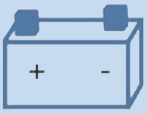

Manufacturing Technologies and Production Methods for Battery Cells

Scope of project

The focus of the team at the Bern University of Applied Sciences is on manufacturing technology and offers services to battery production industry, equipment manufactures for battery production and battery material suppliers in Switzerland. Emerging materials, e.g. developed by the partners within the SCCER, might benefit or even require prospective manufacturing technologies. Consequently, the focus lies on battery configurations and also on investigations regarding new battery components. The team combines machinery and process knowledge with holistic approach undertaking cooperation between industry and research studies for know-how transfer.

Status of project and main scientific results of workgroups

The Swiss government has decided to exit nuclear energy production until 2050. Changing the actual energy production completely to renewable requires energy storage since wind and sun is not constantly available. For instance the photovoltaic electricity production needs storage for night consumption.

This project is embedded in the Swiss Competence Center for Heat and Electricity Storage to make stationary battery storage more attractive from an economic point of view and to speed up the Swiss energy transition. Although the battery electro-chemistry is already available and constantly improving, resulting in high expectations, batteries need to be manufactured at extreme low cost and, for safety reasons, at very high quality level. Further, the productions of batteries depend on the design and therefore on the application.

Coming back to the photovoltaic application: For a system with uninterrupted power supply, the daily electricity demand needs to be stored and a high current needs to be provided, requiring more conducting surface and cross sections compared to a base load use.

A highly optimized and flexible battery production is needed to produce a wide range battery configuration according to different requirements and in different sizes and designs. The application of the ideas of the next industrial revolution will enable such production technology.

Currently, the activities concentrate on implementing a pilot production line for battery manufacturing. At this first stage the pouch cell design was chosen with industry partners as a common application of Li-ion battery. Specifically for the pouch cell type the cell manufacturing includes cutting, stacking and assembly. These are three important steps which have big improvement potential concerning the process parameters such as positioning and cutting accuracy, cutting speed etc. including particular quality control for self-adjusted process control.

The status of the project is shown at the following graph (Figure 1). The orange colored part shows the major steps for electrode production which will be studied in future. The current activities are focused at the blue part: the battery cell manufacturing and specifically cutting and stacking.

As a first part of the project a laser cutting unit for electrodes has been installed, cf. left side of the picture in Figure 1. Optimization studies for the operational parameters regarding to the demanding quality of the electrode cuts are ongoing. This requires some more work especially for copper foils, since the laser light is highly reflected by plain copper.

After the electrode cutting, anode and cathode sheets are assembled with a separator. Z-folding is one of the assembling methods [4] in which the separator foil is continuously folded surrounding anode and cathode sheets. As a second step for the pilot line the Z-folding module is initialized. Its assembly has begun in September 2016. As shown in Figure 1, at the current stage of this project the main structure of the Z-folding unit was established and building a handling system between two units is continuing in parallel.

The whole line was evaluated with Failure Modes and Effects Analyses (Process FMEA) in the recent months. The boundary conditions were checked against the specifications and the question how the manufacturing process can be improved in a safe manner.

Authors

A. Fuerst[1]
A. Haktanir[1]

[1] BFH (Bern University of Applied Sciences)

Manufacturing Technologies and Production Methods for Battery Cells

As a conclusion, this pilot line helps to get deeper understanding and serves as a showcase for industry partners and research groups. With the aid of modelling a virtual production line and integration of smart sensors to the system it will ensure an «Industrie 4.0» environment for the future applications and their developments.

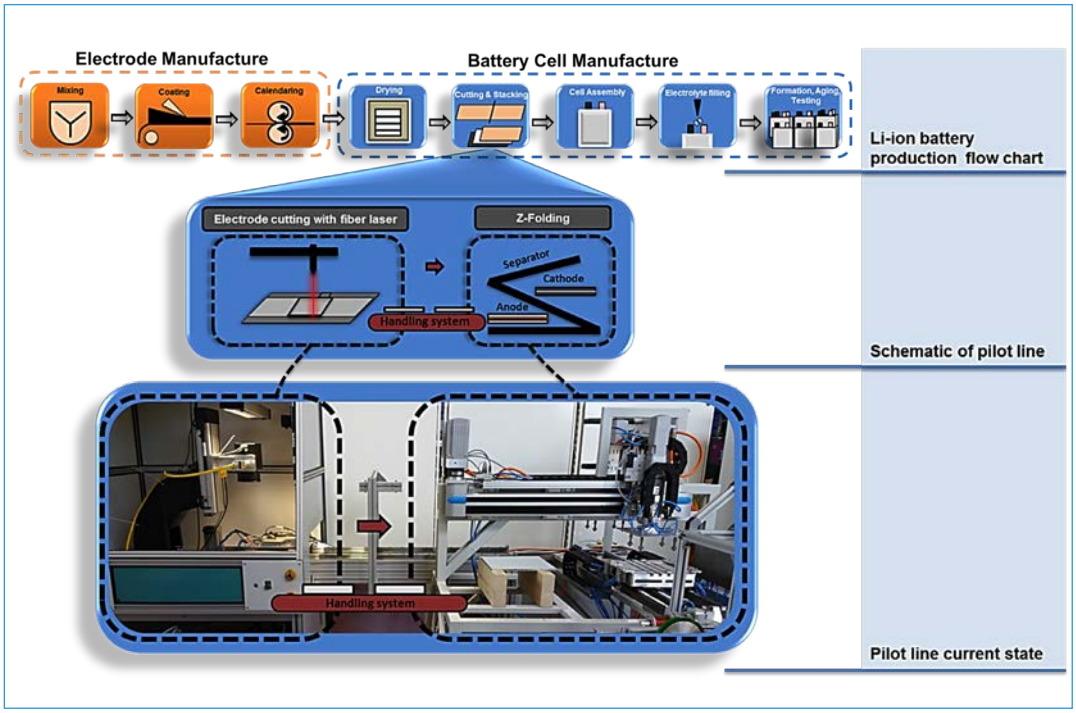

Figure 1:

Lithium-ion battery production steps and pilot production line (current state).

References

[1] A. Fuerst, hitech das Magazin für Technik und Informatik, 3|2014, BFH, Schweiz.

[2] A. Fuerst, A. Haktanir, H. Roth, B. Löffel, M. Müller, «Pilot production line for battery manufacturing». Book of Abstracts Heat & Electricity Storage, 4th Symposium, 2016.

[3] R. Korthauer (Hrsg), Handbuch für Lithium-Ionen-Batterien, Springer Vieweg, 2013.

[4] A. Techel (Hrsg), «Produktionstechnisches Demonstrationzentrum für Lithium-Ionen-Zellen». Ergebnisbericht zum Verbundvorhaben, Fraunhofer Verlag, 2011.

Hydrogen

Production and Storage

Work Package "Hydrogen" at a Glance

Hydrogen is an inherently clean energy vector provided the gas is produced from renewable sources or with the help of renewable energy.
The partners in this work package are focusing on the one hand on the production of hydrogen via water electrolysis as well as via a combined redox-flow cell/catalytic reactor. On the other hand, storage of hydrogen gas is addressed by developing advanced hydrides with increased storage capacities and the hydrogen storage in formic acid reaction cycle.

The large scale use of hydrogen for the storage of renewable energy requires large scale production of hydrogen, preferably in a dynamic process and large scale storage of hydrogen in an economic and dense form.

The production of hydrogen was investigated by a new approach based on the chemical discharge of the active material in the electrolyte of a redox flow battery. This method has several advantages: the redox flow battery tolerates a highly dynamic charge and discharge and is able to buffer the electrical energy from a fluctuating renewable source e.g. photovoltaic or wind. The new catalytic reaction developed allows to chemically react the charged electrolyte with water and directly produce hydrogen. The reaction products are recycled and returned into the redox flow battery. Since the reaction does not require any electrochemical installation it has a great potential for scaling up.

Electrolysers

Two types of electrolysers are commercialized today:

- the polymer electrolyte membrane (PEM) electrolyser and
- the alkaline electrolyser.

The main challenge is the large scale efficient electrolysis in the power range of > 1 MW. Alkaline electrolysers exist since more than 30 years with a power of > 4 MW and exhibit operational times of > 10 years before major revision is necessary. They reach efficiencies of > 80 % at a rather low current density of only 200 mA/cm^2. The resistance is due to the membrane and the overpotentials for the oxygen evolution reaction (OER).

New electrocatalytically active materials have been developed and investigated for the overpotential of the OER. Especially $Co_{0.11}Fe_{0.33}Ni_{0.55}$, a compound found in the Gibeon meteorite that landed 13'000 years ago in Western Africa. The unique microstructure and composition turned out to show a very low overpotential for the OER and is characterized as a model system within the SCCER HaE.

Hydrogen storage in complex hydrides

Hydrogen storage in complex hydrides allows to store hydrogen up to 20 mass% and 150 kg/m^3 in the host material. Many of the complex hydrides turned out to be rather stable compounds that release hydrogen only at elevated temperatures far above room temperature. However, with the development of a thermodynamic model to describe the stability of complex hydrides without the need to know the structure nor to synthesize the compounds and measure, it was possible to find many interesting new complex hydrides that are much less stable than the known ones – and some of them are even liquids at room temperature. The challenge is to handle and to investigate these compounds and to find new ways to stabilize complex hydrides. We have successfully stabilized $Ti(BH_4)_3$ by infiltration in a metal organic framework (MOF). The hydride, which spontaneously desorbs hydrogen at room temperature, became stable over several months by infiltration. This method offers a great advantage in order to investigate these compounds.

Hydrogen storage in liquids

Hydrogen storage in liquids has many advantages over solids, since a liquid can be pumped and any diffusion limitations can be overcome by convection. Beside the storage of hydrogen in Dibenzyltoluol (or Carbazol) the storage of hydrogen in formic acid only uses CO_2 and water and allows to store > 5 mass% of hydrogen. Non-noble metal based precatalysts have been developed for aqueous phase formic acid (FA) dehydrogenation. This required the synthesis of m-trisulfonated-tris[2-(diphenylphosphino)ethyl]phosphine sodium salt (PP3TS) as a water soluble polydentate ligand. New catalysts, particularly those with iron(II), were formed *in situ* and produced H_2 and CO_2 from aqueous FA solutions, requiring no organic co-solvents, bases or any additives. The catalysts are entirely selective and the gaseous products are free from CO contamination. To the best of our knowledge, these represent the first examples of first row transition metal based catalysts that dehydrogenate quantitatively formic acid in aqueous solution.

Illustration: Jeff Kubina

Metal Hydride Catalyst for Energy Storage

Scope of project

For heterogeneous hydrogenation reactions, for example, ammonia synthesis and reduction of carbon dioxide for energy storage (Figure 1), atomic hydrogen on the surface of a metal with high hydrogen solubility is of particular interest. [1] Ammonia is a transport form of hydrogen (17.8 wt% H_2, 121 kg H_2 m^{-3} for liquid), especially for medium to long term hydrogen trading and storage [2]. The hydrogenation of CO_2 is an alterative way for storing large quantities of hydrogen in hydrocarbons. This enables the utilization of carbon dioxide as a raw material and can be further expanded in the chemical industry. [3]

Status of project and main scientific results of workgroups

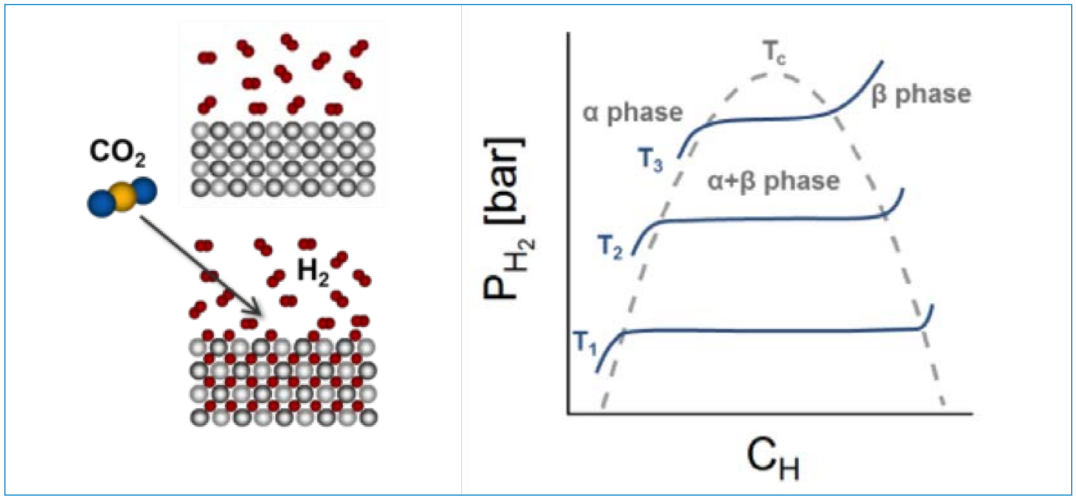

Figure 1:

Left: A metal hydride catalyst: during the hydrogen desorption, the metal hydride can deliver hydrogen to carbon dioxide at the surface, which is catalytically active in the reduction of carbon dioxide and formation of hydrocarbons.

Right: The pressure-composition isotherms (pcT) at three different temperatures ($T_1 < T_2 < T_3$).

One of the simplest hydrogenation reactions is the formation of water from oxygen and hydrogen. In the atmosphere with an excess of hydrogen, the formation of water on palladium is dominated by the transport of atomic hydrogen between the surface and the bulk, which was shown by using a molecular-beam relaxation technique under ultra-high vacuum conditions. [4]

In heterogeneous catalysis, palladium is one of the most important hydrogenation catalysts. However, it is generally not clear whether the formation of the metal hydride is important for industrially applied supported catalysts.

By using advanced *in situ* surface analysis methods, near-ambient pressure X-ray photoelectron spectroscopy (NAP-XPS) and time-of-flight secondary ion mass spectroscopy (ToF-SIMS), we have elucidated the origin of the catalytic activity of a metal hydride: since at the initial stage the dissociation of impinging hydrogen molecules is hindered by a high activation barrier of the oxidised surface, the atomic hydrogen flux from the metal hydride is crucial for the reduction of carbon dioxide and surface oxides at interfacial site.

The evolution of the oxidation state was analysed in detail by NAP-XPS *in situ*, with respect to the equilibrium hydrogen desorption pressures at different temperatures (Figure 2). To analyse hydrogen in the topmost layers of a solid surface, ToF-SIMS is a powerful tool (Figure 3). For ammonia synthesis, we further applied *in situ* ToF-SIMS surface analysis (in the course of hydrogen desorption) to investigate the formation of NH_x adsorbates on a metal hydride, *in situ* in gas (Figure 4). [5] While the industrial Haber-Bosch processes require high pressure (> 100 bar) and high temperature (> 400 °C), under our experimental conditions (at low pressure and low temperature), the formation of NH_x intermediates are thermodynamically possible, as we experimentally demonstrated [5]. In order to control heterogeneous catalytic reaction, metal hydride catalysts have great potential for various hydrogenation reactions.

List of abbreviations

NAP-XPS
: Near-Ambient Pressure X-Ray Photoelectron Spectroscopy

ToF-SIMS
: Time-of-Flight Secondary Ion Mass Spectroscopy

Authors

Shunsuke Kato[1]
Andreas Züttel[1]

[1] EPFL, Valais/Wallis

Metal Hydride Catalyst for Energy Storage

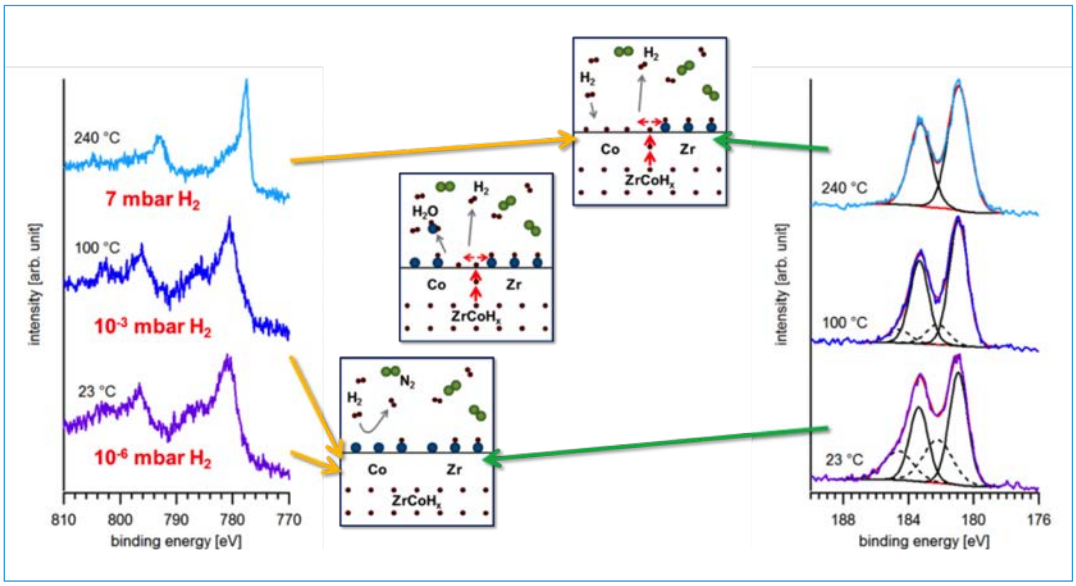

Figure 2:

Left: The Co 2p XP spectra of $ZrCoH_x$ measured in the atmosphere of a mixture of hydrogen (0.3 mbar) and nitrogen (0.6 mbar) at 23 °C, 100 °C and 240 °C, respectively.

Middle: The schematic representation of the surface reduction. When the hydrogen equilibrium pressure (red) exceeds the hydrogen partial pressure, the hydrogen desorption markedly occurs, leading to the reduction of cobalt and the formation of hydroxyl groups on zirconia.

Right: The Zr 3d XP spectra of $ZrCoH_x$.

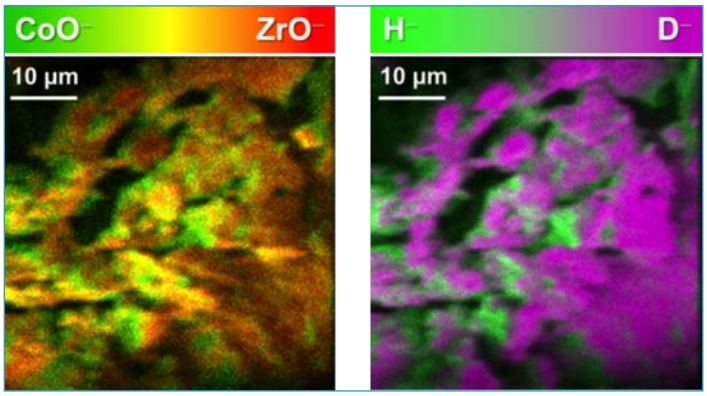

Figure 3:

A metal hydride catalyst: The ToF-SIMS chemical images of $ZrCoD_{1.2}$ powder, taken at 2×10^{-8} mbar and 25 °C. The distributions of ZrO-/CoO– (left) and D-/H- (right) on $ZrCoD_{1.2}$ are shown by labelling the hydrogen isotope. The distribution of deuterium correlates with that of zirconium oxides. [1]

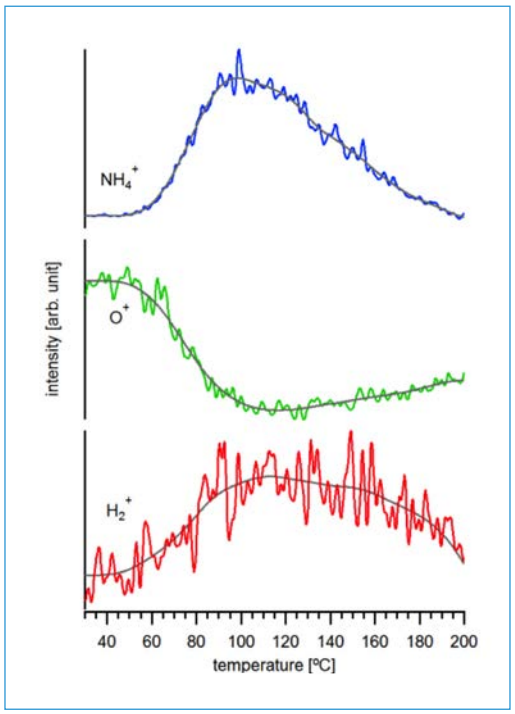

Figure 4:

The ToF-SIMS spectra of H_2^+, O^+ and NH_4^+ taken in the atmosphere of nitrogen (at 1×10^{-6} mbar). Above 60 °C, the recombination of hydrogen and the formation of NH_x proceed on the surface of $ZrCoH_x$. [5]

References

[1] S. Kato, S. Matam, P. Kerger, L. Bernard, C. Battaglia, D. Vogel, M. Rohwerder, A. Züttel, Angew. Chem. Int. Ed., 55, 6028–6032, 2016.

[2] R. Schögel, ChemSusChem, 3, 209, 2010.

[3] M.M. Halmann, M. Steinberg, «Greenhouse Gas Carbon Dioxide Mitigation: Science and Technology». CRC Press, Florida, 1999.

[4] T. Engel, H. Kuipers, Surf. Sci., 90, 181–196, 1979.

[5] S. Kato, L. Bernard, A. Züttel, et al., to be submitted.

Recent Activity for the Advances of Water Electrolysis Catalysts

Scope of project

The competence center dedicated to new water electrolysis catalyst testing, which opened last year in LIMNO at EPFL, has been fully equipped for electrode preparation (solution processable techniques, spin coater, electrodeposition setup, annealing under controllable atmosphere), characterization (XRD, Raman, microscopy) and catalytic performance assessment (potentiostats, transient / frequency modulated techniques). Several new equipment items, including a setup for ageing multiple electrodes under operating conditions, and novel skills, notably in metal electrodes preparation and atomic composition characterization, have been successfully added this year, enlarging the scope of potential materials and electrodes to inspect.

Status of project and main scientific results of workgroups

The first project of our group has been to study electrocatalysts for the water oxidation reaction (or oxygen evolution reaction). This process remains a technological challenge, considering the high overpotential required to drive this 4-electrons reaction, which limits the performance of an electrolyzer.

However, recent investigations on abundant 3d transition metal electrocatalysts, in particular NiFe, FeCo or NiCo, have shown impressive reduction of overpotentials and demonstrated cooperative function of the different metals when alloyed. Thus, we reported the electrocatalytic function of an iron-based Gibeon meteorite for the oxygen evolution reaction (OER) in alkaline medium in collaboration with the group of Paul Dyson. [3] This meteorite originates from sub-saharan Africa and has the largest strewnfield known with pieces discovered over 20 000 km^2 in Namibia and a total collected mass exceeding 21 tons. Examining this particular type of minerals is of interest for energy conversion applications given their unique atomic composition and formation history.

After 10 hours ageing under operational conditions in an alkaline electrolyte, an activity matching or possibly slightly superior to the best performing OER catalysts emerges, with stable overpotentials as low as 270 mV (for 10 $mA\,cm^{-2}$) and Tafel slopes of 37 $mV\,decade^{-1}$ (see Figure 1a). The Faradaic efficiency for OER was quantified as unity and no deterioration in performance was detected during the 1000 hours of OER operation tested at 500 $mA\,cm^{-2}$.

Spectroscopic analyses suggest an operando surface modification involving the for-

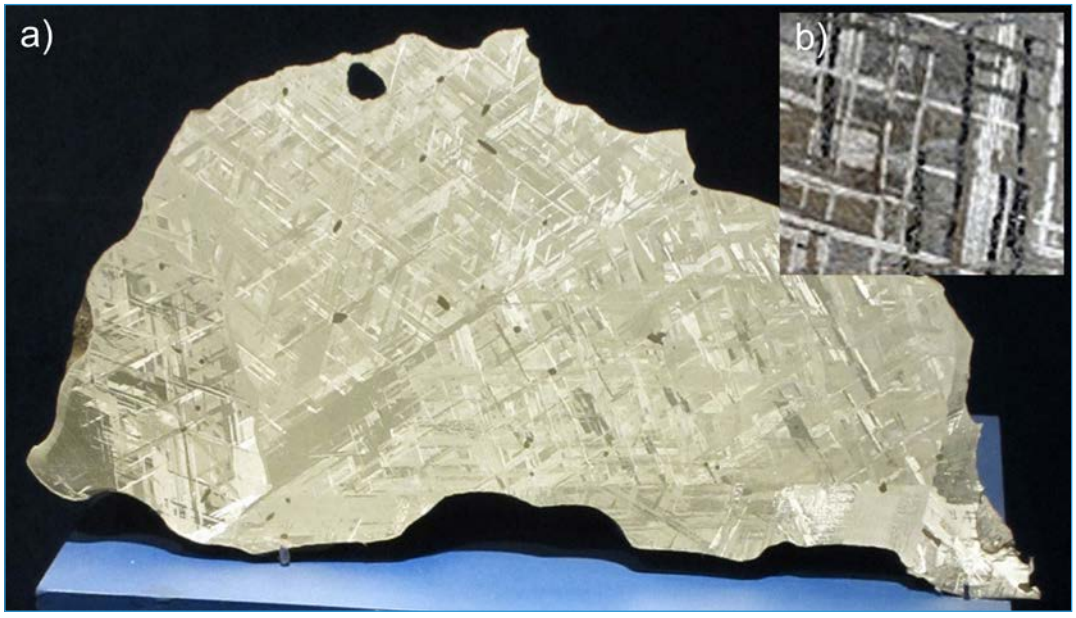

Figure 1:

a) Gibeon meteorite [1],

b) Widmanstätten texture in the surface of an etched meteorite from the Gibeon cluster, Namibia [2].

List of abbreviations

OER	Oxygen Evolution Reaction

Authors

Florian Le Formal[1]
Wiktor S. Bourée[1]
Mathieu S. Prévot[1]
Kevin Sivula[1]

[1] EPFL

Recent Activity for the Advances of Water Electrolysis Catalysts

mation of a 3D oxy(hydroxide) layer with a metal atom composition of $Co_{0.11}Fe_{0.33}Ni_{0.55}$, as indicated by Raman and XPS studies and trace Ir as indicated via elemental analysis. The growth of the catalyst layer was self-limiting to < 200 nm after ca. 300 hours of operation as indicated through XPS depth profiling and cyclic voltammetry, as shown on Figure 2b and c. The unique composition and structure of the Gibeon meteorite suggest that further investigation Co-Ni-Fe systems or other alloys inspired by natural materials for water oxidation are of interest.

Indeed, metal electrodes based on nickel and manganese containing stainless steel also evidence the *in situ* formation of a highly catalytic layer for OER in alkaline electrolyte, with overpotentials recorded below 250 mV. The formation of this layer is induced by selective dissolution of metal ions in solution and results in a porous, layered double hydroxide type structure. The composition of the active layer is shown to be enriched in nickel and manganese while iron and chromium contents are drastically decreased as compared to the initial stainless steel composition. Remarkably, the final composition shows little or no dependence on the initial composition and highlights the synergetic function of different metal atoms. These results emphasize and rationalize the potential use of inexpensive and earth abundant metals for alkaline OER catalysis.

The further characterization of the optimized atomic composition will give deep insights into the origin of the benchmark performance and offer routes for further improvement. These studies are underway in our laboratories.

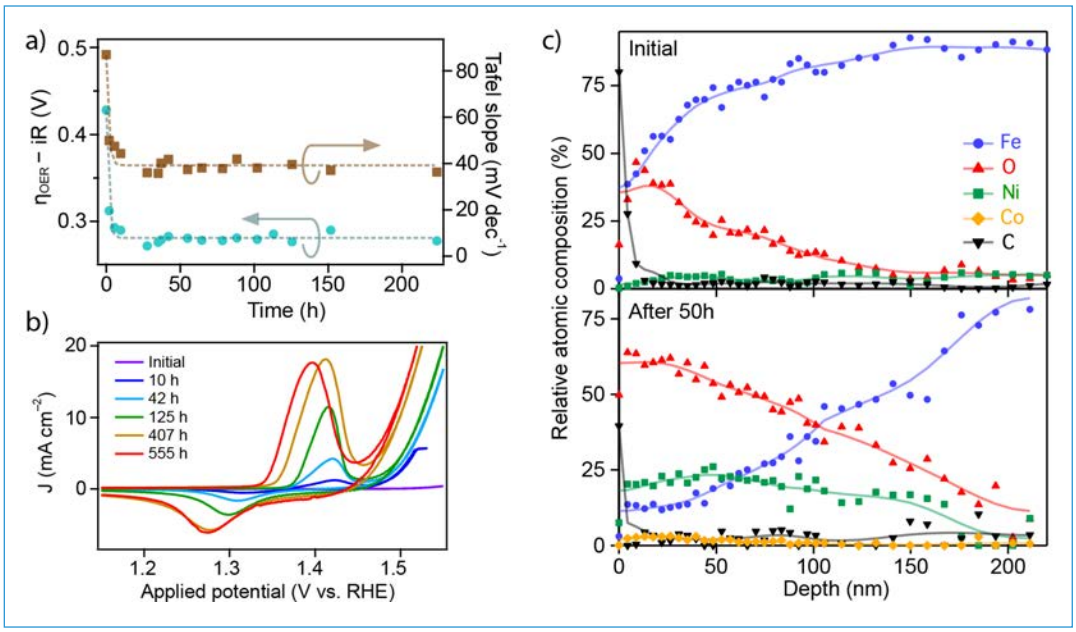

Figure 2:

a) Summary of the change in overpotential measured at 10 mAcm^{-2} (left axis) and Tafel slope (right axis) with OER operation time at 500 mAcm^{-2} in 1M NaOH

b) Examples of cyclic voltammograms of a Gibeon electrode measured at 10 mVs^{-1} after different oxidation periods.

c) Atomic composition profile obtained via XPS of a Gibeon sample before (top) and after 50 hours of OER operation.

References

[1] National Museum of Natural History, Washington D.C (Kinda Kinked – Flickr: IMG_1761)

[2] Kevin Walsh, https://www.flickr.com/photos/86624586@N00/10198012/

[3] F.L. Le Formal, N. Guijarro, W.S. Bourée, A. Gopakumar, M.S. Prévot, A. Daubry, L. Lombardo, C. Sornay, J. Voit, A. Magrez, P.J. Dyson, K. Sivula, Energy Environ. Sci., 9, 3448–3455, 2016.

Demonstration of a Redox Flow Battery to Generate Hydrogen from Surplus Renewable Energy

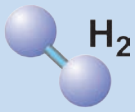

Scope of project

Redox flow batteries (RFBs) can be used in energy storage for stationary applications due to the independency between the power output and the energy capacity, which leads to a flexible design, but also due to their long lifetime (> 15 000 cycles claimed by suppliers), their easy maintenance and recyclability, and their secured operation. However, it is considered that RFBs suffer from a low energy density compared to alternative battery systems. In addition, their electrochemical energy efficiency remains still relatively low (80–85 %) compared to other batteries. Therefore, a large amount of research is conducted at the levels of the chemistry of the electrolytes, the materials of the electrodes, the design of the cells and the strategy of operation. Different directions of research for the increase of energy density of RFBs were explored during these last four years in the frame of the SCCER funding in our laboratory.

Status of project and main scientific results of workgroups

In a first direction, a demonstration system was developed for the production of hydrogen directly from a redox flow battery.

This allows a significant extension of the energy capacity (which depends on the capacity of the associated hydrogen storage) of a standard RFB system, while keeping a reasonable installation size. Indeed, hydrogen exhibits a much higher energy density than a RFB. Indirectly, this system therefore allows to increase the energy density of the RFB. Moreover, it provides on demand two products in one installation: electricity and hydrogen. Both products can also be obtained simultaneously.

The concept, called dual-circuit redox flow battery, is based on the production of hydrogen from the at least partially charged negative electrolyte of a RFB with a suitable electrochemistry. It is extensively described elsewhere [1–3], but, in a nutshell, the idea is to use the RFB in its typical electrochemical mode except when a surplus of (renewable) energy is available and the battery is already fully charged. In this particular case, a secondary circuit (see Figure 1) made of two catalytic beds enables an external chemical discharge of both electrolytes.

On the negative side (right circuit in Figure 1), the catalytic chemical discharge reaction is the reduction of proton by the V(II) species present in the electrolyte, generating hydrogen and regenerating the discharged V(III) species. The catalyst for this reaction is molybdenum carbide, which was chosen for its low price, its stability and its clear activity for the reaction of hydrogen evolution in an acidic V(II) solution.

On the positive side (left circuit in Figure 1), catalysts such as iridium dioxide (IrO_2) or ruthenium dioxide (RuO_2) are able to activate the oxidation of water by the Ce(IV) ions, generating oxygen and protons – that can cross the membrane and re-equilibrate the proton concentration on the negative electrolyte – and regenerating the discharged Ce(III) species. Both chemically discharged electrolytes return then to the RFB, which can be charged further, storing thus surplus energy in the form of hydrogen. The efficiency of this system in chemical discharge mode is calculated by comparison of the chemical energy capacity corresponding to the hydrogen produced and the electrical energy used for charging the V–Ce RFB. Using a bench-scale system, this efficiency was close to 50 %. When the V–Ce RFB is replaced by an all-vanadium RFB, as it is the most advanced type of RFBs and they are commercially available, it involves changing the reaction for the chemical discharge of the positive electrolyte.

In our demonstration system, a commercially available 10 kW / 40 kWh all-vanadium RFB was installed in 2014 with the aim of validating the feasibility of the dual-circuit concept at a larger scale. The chemical discharge of the negative electrolyte, that is the reaction of hydrogen evolution, was scaled-up to a medium-scale. The chemical discharge power was equivalent to 2.4 kW, that is the discharge of the whole battery in 17 h (1 L/min flow rate for full chemical discharge), in a specifically designed, vertical, segmented

List of abbreviations

PAN	Polyaniline
RFB	Redox Flow Battery

References

[1] V. Amstutz, K.E. Toghill, C. Comninellis, H.H. Girault, «Redox flow battery for hydrogen generation». WO Patent Application N° WO2013131836 A1, 2013.

[2] V. Amstutz, K.E. Toghill, F. Powlesland, H. Vrubel, C. Comninellis, X. Hu, H.H. Girault, «Renewable hydrogen generation from a dual-circuit redox flow battery». Energy Environ. Sci., 7, 2350–2358 (2014).

[3] P. Peljo, H. Vrubel, V. Amstutz, J. Pandard, J. Morgado, A. Santasalo-Aarnio, D. Lloyd, F. Gumy, C.R. Dennison, K.E. Toghill, H.H. Girault, «All-Vanadium dual circuit redox flow battery for renewable hydrogen generation and desulfurisation». Green Chem., 18, 1785-1797 (2016).

[4] C.R. Dennison, H. Vrubel, V. Amstutz, P. Peljo, K.E. Toghill, H.H. Girault, «Redox Flow Batteries, Hydrogen and Distributed Storage». Chimia, 12 (69), 753-756 (2015).

Authors

Véronique Amstutz[1]
Christopher Dennison[1]
Heron Vrubel[1]
Elena Zanzola[1]
Alberto Battistel[1]
Hubert H. Girault[1]

[1] EPFL Valais Wallis

Demonstration of a Redox Flow Battery to Generate Hydrogen from Surplus Renewable Energy

catalytic reactor. Concerning the chemical discharge of the vanadium based positive electrolyte, as water oxidation could not be performed using the V(V) electrolyte, the oxidation reactions of N_2H_4, SO_2 and H_2S were investigated [3]. The corresponding products of the reactions are N_2, SO_4^{2-} and S, respectively. Therefore, in the present state, the all-vanadium RFB can be discharged chemically on both sides, producing hydrogen and being able to completely remove sulfur species from a gas stream. This is a significant advance in the demonstration of the feasibility of the system, but also for the discussion of the integration of the system into specific energy networks.

As a follow-up of the successful demonstration of the feasibility of this concept, a research is aiming at optimising the positive side of the dual-circuit. Different approaches are being studied and evaluated. Using Ce as redox couple in the RFB remains an interesting direction and therefore, the chemistry and electrochemistry of cerium and its chemical discharge in the reaction of water oxidation was studied further. Moreover, a system involving an electrochemical cell to discharge the positive electrolyte of an all-vanadium RFB is also currently being studied.

A third research direction focussed on the increase of the energy density of the RFB through the addition of solid particles in the electrolyte tanks. The solid needs to be redox-active in the same range of potential as one of the redox couple of the RFB and needs to be chemically stable and to exhibit a low solubility limit in its both redox states. A screening through solids of different natures was conducted for several redox couples. One specific successful assembly was the redox couple Fe^{3+}/Fe^{2+} with a polyaniline (PAN) polymer. Preliminary studies showed that the electrolyte energy density can be increased by a factor of 3 if a suitable amount of stationary solid PAN is added in the electrolyte solution with no decrease for at least 20 charge-discharge cycles. This is a considerable increase of the RFB density at a low cost and involving only little change in a classical RFB.

All in all, these 3 years of SCCER Hae funding allowed a wide range of research on redox flow battery to be conducted, going from fundamental science to applied research, involving the building of a demonstration project and leading to multiple communications and publications and to the initiation of new promising projects for the continuation of this research on electrochemical energy storage and hydrogen storage in our laboratory.

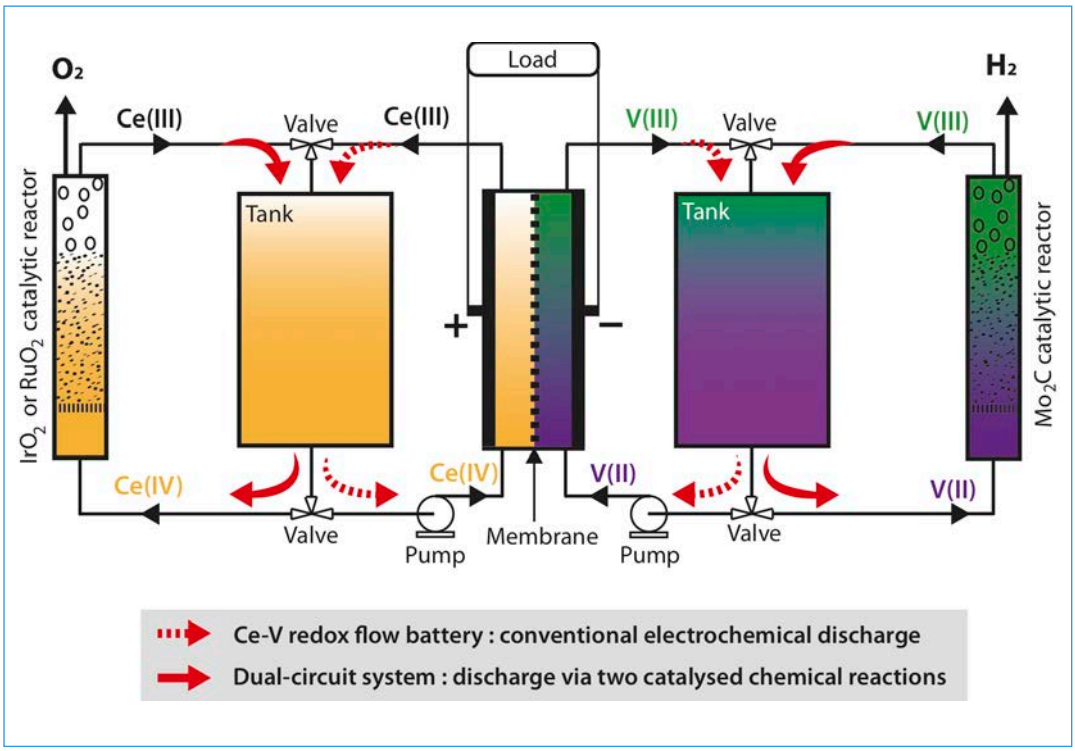

Figure 1:

Concept of the dual-circuit RFB. Hydrogen is generated by the chemical discharge of the negative electrolyte.

Hydrogen / Energy Storage and Production with the Carbon Dioxide / Formic Acid Systems

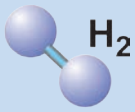

Scope of project

The reversible catalytic reduction of CO_2 with hydrogen to formic acid (FA, HCOOH) under mild conditions offers a convenient solution to store H_2 with a comparably high volumetric energy density (4.3 %wt H_2, 7.5 MJL^{-1}). Formic acid is a moderately toxic [1, 2] liquid at room temperature and used as feedstock chemical for industries. [3, 4] Finally, formic acid can be decomposed to H_2, releasing only CO_2 as the by-product on demand. If the CO_2 is recycled a carbon-neutral hydrogen storage cycle is established. [5–8]

Status of project and main scientific results of workgroups

Recently the successful disproportion of formic acid into methanol, realized at ambient temperatures and in aqueous, acidic media employing an iridium catalyst was published. [9]

Based on literature findings, it became evident that iridium-pentamethylcyclopentadienyl dimers are promising starting materials for efficient catalysis. [10–16]

The combination with bidentate nitrogen donors afforded a series of powerful catalysts for CO_2/bicarbonate hydrogenation and FA dehydrogenation in the past. [12, 15, 17]

Li et al. reported in 2015 on achieving unprecedentedly high formic acid dehydrogenation activity on an Ir complex bearing an N,N′-diimine ligand in water without the addition of bases or additives. [18]

This observation triggered the investigation of a variety of Pentamethylcyclopentadienyl-N,N′-diimine ligand based catalysts with Ir or Rh center with the N,N′-diimine ligand as variable $[Cp^*MCl_2]_2$ (M = Ir or Rh, Cp* = Pentamethylcyclopentadienyl), see Figure 1.

The details of used methods instruments and chemicals can be found in our publication. [19]

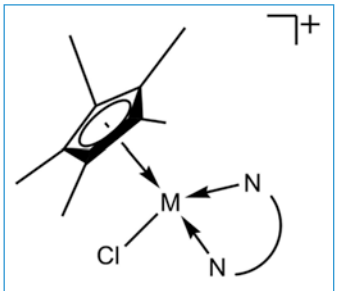

Figure 1:
$[Cp^*M(N–N')Cl]^+$.

^1H NMR spectroscopy was used to follow up formic acid dehydrogenation online. The reaction occurred in sealed

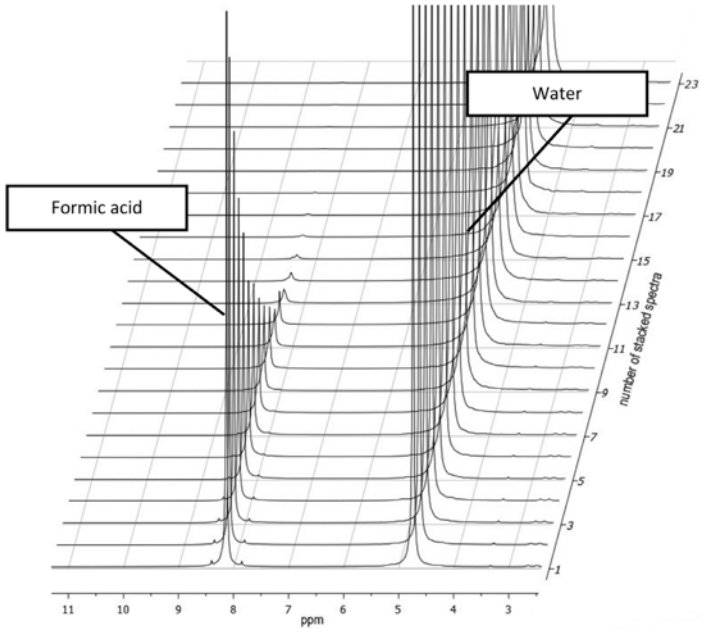

Figure 2:
^1H NMR (400 MHz, 10 mm) stacked spectra;
4.5 M FA in D_2O at 60 °C;
c(Ir) = ethylenediamine = 0.009 M;
FA dehydrogenation is recorded as a function of time;
the interval between two consecutive spectra is 450 s.

List of abbreviations

FA	Formic Acid (HCOOH)
NMR	Nuclear Magnetic Resonance
TOF	Time of Flight

References

[1] «Chemistry and its elements – formic acid», http://www.rsc.org/chemistryworld/podcast/CIIEcompounds/transcripts/formic_acid.asp, (accessed 30. July, 2016).

[2] H.W. Gibson, Chem. Rev., 69, 673–692, 1969.

[3] A.A.N. Afshar, «Chemical profile: formic acid», http://chemplan.biz/chemplan_demo/sample_reports/Formic_Acid_Profile.pdf, (accessed 02. Nov., 2016).

[4] Formic Acid Market worth $618,808.7 Thousand by 2019, http://www.marketsandmarkets.com/PressReleases/formic-acid.asp, (accessed 02. Nov., 2016).

[5] A. Boddien, F. Gärtner, C. Federsel, P. Sponholz, D. Mellmann, R. Jackstell, H. Junge, M. Beller, Angew. Chem., Int. Ed., 50, 6411–641 (2011).

[6] P.H. Dixneuf, C. Bruneau, «Ruthenium in Catalysis», Springer International Publishing (2014).

[7] M. Grasemann, G. Laurenczy, Energy Environ. Sci. 5, 8171–8181 (2012).

[8] G. Papp, J. Csorba, G. Laurenczy, F. Joó, Angew. Chem., Int. Ed. 50, 10433–10435 (2011).

[9] K. Sordakis, A. Tsurusaki, M. Iguchi, H. Kawanami, Y. Himeda, G. Laurenczy, Chem. – Eur. J. 22, 15605–15608 (2016).

Authors

Gábor Laurenczy[1]
Cornel Fink[1]

[1] EPFL

Hydrogen / Energy Storage and Production with the Carbon Dioxide / Formic Acid Systems

vessels and was kept at a constant temperature during the whole experiment. Among the 13 investigated N,N′-diimine ligands, the 1,2,Diaminocyclohexane (an aliphatic nitrogen diastereomer) shows by far the highest turnover frequency (3278 h^{-1}) at 90 °C in acidic media.

The NMR spectra in Figure 2 shows the reaction progress at 60 °C. The impact of different temperatures on the dehydrogenation rate is depicted in Figure 3 visualizing the dependency of the reaction rate on the temperature.

Based on temperature variation, the activation parameters were obtained by an Arrhenius plot (Figure 4) and determined an apparent activation energy of $E_a = 77.94 \pm 3.2\ kJ\,mol^{-1}$, which is in good agreement with literature findings such as 76.4 $kJ\,mol^{-1}$ for [Ir(Cp*)(2,2′,6,6′-tetrahydroxyl-4,4′-bipyrimidine)(H_2O)]SO_4 by Himeda et al. [17] or for the Fe(II)·PP_3/propylene carbonate system by Beller et al. (77 ± 0.4 $kJ\,mol^{-1}$). [20]

In conclusion, we synthesized a series of compounds by reacting $[Cp^*MCl_2]_2$ (M = Ir or Rh) with bidentate nitrogen donor ligands and examined their catalytic activity in formic acid dehydrogenation. In most cases, the Rh analogues decomposed quickly and were in all cases less performant than iridium based catalysts. The highest TOF of 3278 h^{-1} was obtained with the complex featuring 1,2-diaminocyclohexane as the ligand. By investigating the activity of the catalyst at different temperatures, we determined an activation energy of $E_a = 77.94 \pm 3.2\ kJ\,mol^{-1}$ for formic acid dehydrogenation.

A generally observed issue with this type of structure is the instability at increased temperatures and elevated hydrogen pressures, leading to the reduction of the metal central ion and thereby to a partial deactivation of the catalyst.

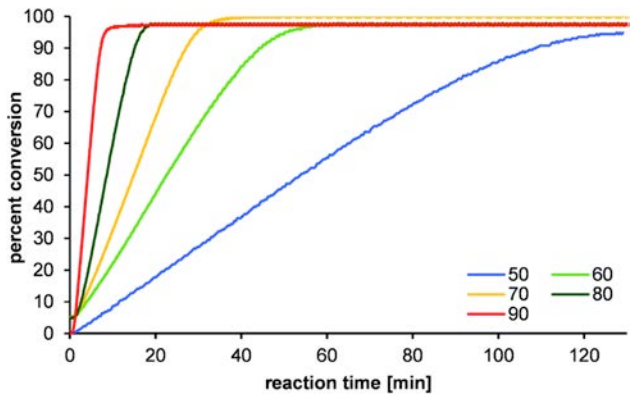

Figure 3:

Pressure increase due to catalytic FA decomposition to CO_2 and H_2 as a function of time at different temperatures (50–90 °C).

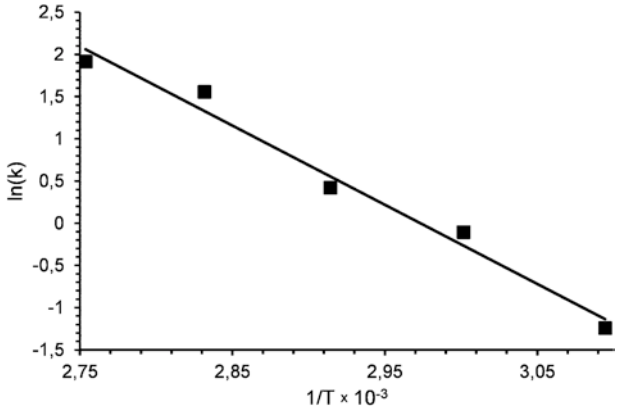

Figure 4:

Arrhenius plot for $[Cp^*Ir(III)(N\text{–}N')Cl]Cl_2$, to estimate the activation energy ($R^2 = 0.991$).

References

[10] J.F. Hull, Y. Himeda, W.-H. Wang, B. Hashiguchi, R. Periana, D.J. Szalda, J.T. Muckerman, E. Fujita, Nat. Chem. 4, 383–388 (2012).

[11] Y. Manaka, W.-H. Wang, Y. Suna, H. Kambayashi, J.T. Muckerman, E. Fujita, Y. Himeda, Catal. Sci. Technol., 4, 34–37 (2014).

[12] Y. Himeda, Green Chem. 11, 2018–2022 (2009).

[13] S. Fukuzumi, T. Kobayashi, T. Suenobu, J. Am. Chem. Soc.132, 1496–1497 (2010).

[14] J.H. Barnard, C. Wang, N.G. Berry, J. Xiao, Chem. Sci., 4, 1234–1244 (2013).

[15] Y. Himeda, S. Miyazawa, T. Hirose, ChemSusChem 4, 487–493 (2011).

[16] J.H. Shin, D.G. Churchill, G. Parkin, J. Organomet. Chem. 642, 9–15 (2002).

[17] W.-H. Wang, S. Xu, Y. Manaka, Y. Suna, H. Kambayashi, J.T. Muckerman, E. Fujita, Y. Himeda, ChemSusChem 7, 1976–1983 (2014).

[18] Z. Wang, S.-M. Lu, J. Li, J. Wang, C. Li, Chem. – Eur. J. 21, 12592–12595 (2015).

[19] C. Fink, G. Laurenczy, Dalton Transactions, 46,1670–1676 (2017).

[20] A. Boddien, D. Mellmann, F. Gärtner, R. Jackstell, H. Junge, P.J. Dyson, G. Laurenczy, R. Ludwig, M. Beller, Science 333, 1733–1736 (2011).

Synthetic Fuels

Development of Advanced Catalysts

Work Package "Synthetic Fuels" at a Glance

Although CO_2 is an energetically very stable gas, pathways to reconvert the molecule into a syn-thetic fuel are very attractive as they offer the potential to close the CO_2 cycle, i.e., developing overall CO_2 neutral processes.
In this work package two general routes are followed to produce synthetic fuels: On the one hand, homogeneously and heterogeneously catalyzed pathways are followed in order to produce high value fuels and chemicals.
On the other hand, a direct electrochemical reduction pathway (co-electrolysis) is followed to produce chemical feedstock. In both routes, the focus is centered around the development of highly active and selective catalyst systems.

Indeed, a wide and diverse range of approaches are under evaluation within the work package, with the ultimate aim of discovering highly efficient and selective electrochemical and catalytic processes and applying them in demonstrators.

Electrochemical approaches to reduce CO_2 are the focus of the groups at PSI and the University of Bern, with contributions from EPFL and ETHZ. Indeed, electrochemical CO_2 reduction reaction (CO_2RR) is a complex reaction which must be carried out in a highly selective and efficient manner and various methods are being explored to develop catalysts with improved reaction selectivity and efficiency. However, CO_2RR kinetics and product identification and quantification are mostly carried out in half-cell configurations using liquid electrolytes. This fundamental approach of studying CO_2RR is limited by the low solubility of CO_2 in water, the maximum CO_2 reduction current reported in the literature being in the range of 0.01–0.02 A/cm^2. In order to overcome the solubility problem and to reach higher operating current densities, CO_2 reduction can be carried out in a co-electrolysis system where pure or diluted gaseous CO_2 is used. At PSI, research efforts were focused on the design of electrochemical cells for co-elecrolyser operating at high-current density with high product selectivity. The most promising result was obtained with a bipolar membrane used as a solid electrolyte. The cell consists of two metallic gold-coated flow fields, two electrodes and a bipolar membrane (Fumasep® FBM 130 µm thickness). The alkaline side of the bipolar membrane was used at the cathode to keep a high pH value. Au mesh (Goodfellow®) and Pt/C gas diffusion electrodes were used as cathode and anode, respectively. Humidified CO_2 was fed to the cathode side at 10 mL/min and the anode side was fed with pure H_2 at 50 mL/min. With such a cell configuration both high current densities and reaction product selectivity were achieved. CO and H_2 were the only products obtained in this configuration using Au mesh electrodes.

At the University of Bern improved carbon-supported oxidic nanoparticles (SnO_2NPs@rGO) and metal foam catalysts (oxide-derived Cu foams) were developed. Catalyst degradation pathways were also studied under *in operando* conditions using Raman spectroscopy. The potential-dependent stability of SnO_2-NPs was monitored *in operando* and correlated to the resulting Faradaic efficiency towards formate production ($FE_{formate}$). The SnO_2-NPs undergo first a partial electrochemical reduction to transient SnO in the potential regime where the highest $FE_{formate}$ is observed. It may be concluded that the most active catalyst contains both Sn(IV) and Sn(II) species at its interface to the working electrolyte. At most negative potentials the SnO_2 catalyst undergoes a full reduction to metallic tin which is accompanied by a drastic drop of $FE_{formate}$ from 75 % (Sn(IV/Sn(II) composite)) to 25 % at pH 8.5. This complete reduction process to metallic tin also involves an irreversible structural degradation of the NPs. Attempts to recover the SnO_2 catalysts by switching back the potential into the thermodynamic stability regime of SnO_2 indeed leads to the reappearance of SnO_2-NPs, which have a different size distribution to the as synthesized NPs. These smaller SnO_2-NPs show a higher FE towards hydrogen evolution reaction (HER) on the expense of $FE_{formate}$. Further stability measurements of the SnO_2-NPs demonstrate that their partial reduction to the transient SnO is, in contrast, fully reversible over a number of potential cycles. These in operando degradation studies confining the optimum potential window for operating this type of oxidic NP catalysts with regard to both catalyst stability and Faradaic efficiency.

High-surface area Cu foams obtained by an additive-controlled electrodeposition process have been demonstrated as excellent CO_2 reduction catalysts affording C_2H_4 and C_2H_6. Various factors have been characterized as important for the resulting FE_{C2} such as the annealing pre-treatment in air and the mean surface pore size of the Cu foams. Maximum FE_{C2} reach values of 55 % under optimum condi-

Illustration: BeholdingEye / iStock

tions. These Cu foams can be deposited not only on planar surfaces but also on 2D-Cu meshes (Figure 2) or on 3D Cu-skeletons which is important for future applications in flow cell devices.

Catalytic approaches to produce fuels from CO_2 and hydrogen were undertaken at ETHZ and EPFL. At ETHZ, research has been focused on heterogeneous catalysts for the direct hydrogenation of CO_2 and also dry reforming processes. It was shown that in both cases the interface between the copper particles and the support play an essential role in controlling the activity and the selectivity of the processes. In the particular case of supported Cu nanoparticles, ETHZ has been able to explain why zirconia is among the best supports for Cu using a combined computational and spectroscopic approach. In brief, Cu activates H_2 and CO_2 at the interface with Zirconia facilitating hydrogenation; this molecular level understanding of the elementary steps provide new guidelines to develop improved catalysts. This was possible through a collaboration with Prof. Urukawa (ICIQ), who developed *in situ* IR characterization of reaction intermediates under high pressure. For dry reforming, ETHZ has also shown that supported FeNi NPs show much improved stability over pure Ni catalysts, because the Fe present is continuously oxidized by CO_2 to generate FeO, which subsequently reacts with carbon deposits thus avoiding coke formation. In addition, ETHZ has developed preparation methods to prepare supported Cu NPs on carbon with high loadings, which are currently being evaluated in the electroreduction of CO_2 to methanol (collaboration with PSI and Uni Bern). In parallel, it has been found that the corresponding silica-supported copper NPs display very high selectivity in the semihydrogenation of alkynes.

In addition, a hybrid material for the conversion of CO_2 to organic compounds (collaboration with EPFL) and formic acid derivatives (collaboration with P. von Rohr) has been developed. These results pave the way to develop catalysts for the efficient conversion of CO_2 to fuels and chemicals using thermal and electrochemical processes.

At EPFL efforts to develope so-called ‹soft› two-step catalytic approaches to convert CO_2 into methanol have progressed. In the first step CO_2 is incorporated into energy-rich nucleophilic molecules such as amines to afford formamides, which can then be converted into methanol in a second step by hydrogenolysis of the newly formed N-C bond. Several catalysts were developed that can reductively functionalize amines with CO_2 to obtain formamides under mild conditions, including two new classes of catalysts for this reaction, one based on naturally occurring organic compounds and the other on palladium NPs. Investigation of ionic liquid catalysts revealed a strong anion dependency on the reaction rate in the order $I^- < Br^- < Cl^- < F^- \sim OH^-$, and based on these data together with spectroscopic and computational studies, a molecular-level understanding of the reaction mechanism was obtained and a new catalytic system operating at ambient conditions was subsequently developed.

In another two-step approach, CO_2 can be reacted with epoxides or diols to afford cyclic carbonates and, the subsequent hydrogenolysis of these compounds affords methanol. A number of new ionic polymer catalysts for the synthesis of cyclic carbonates from CO_2 and epoxides were developed and the importance of functional groups as well as cross-linking for catalytic activity and for product separation were demonstrated. Carbenes were found to be highly active catalysts for the reaction of CO_2 with diols. Notably, a cheap thiazolium carbene was used as the catalyst allowing the carbonate to be obtained in excellent yield. Moreover, it was found that air could be used as the CO_2 source in the reaction involving epoxides. Hence, the resulting catalytic process can be used to scrub CO_2 directly from air as it passes through the ionic liquid catalyst containing the epoxide substrate. A pilot-scale prototype reactor for this process is under construction.

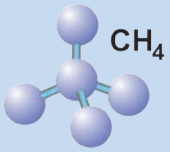

Catalytic approaches to convert CO_2 into fuels

List of abbreviations

IL Ionic Liquid

Scope of project

We have continued our research on the development of new catalytic strategies for the transformation of CO_2 into fuels. Various classes of catalysts are under investigation, including ionic liquid and polymer organocatalysts, homogeneous and heterogeneous metal-based catalysts and electrocatalysts. In collaboration, we have also studied the electrocatalytic water oxidation reaction to generate hydrogen. A summary of the main results from 2016 is provided below.

Status of project and main scientific results of workgroups

The direct reduction of CO_2 into methanol is an energy intensive process, owing to the high thermodynamic stability of CO_2. In principle, the transformation could be facilitated by initially incorporating CO_2 into energy-rich nucleophilic molecules such as amines, as formamides, which can then be converted into methanol in a second step (Scheme 1).

In the last year, we have discovered a plethora of catalysts that can reductively functionalize amines with CO_2 to obtain formamides under mild conditions (Scheme 1). In 2016 we reported two new classes of catalysts for this reaction, one based on naturally occurring organic compounds and the other on palladium nanoparticles. [1, 2] Investigation of ionic liquid (IL) catalysts revealed a strong anion dependency on the reaction rate in the order $I^- < Br^- < Cl^- < F^- \sim OH^-$ (Table 1). Based on the data, novel understanding of the reaction mechanism and a new catalytic system operating at ambient conditions was developed. [3]

We also found out that several crystalline and amorphous variants of earth-abundant metal salts in nanoscale or bulk form based on Co, Zr, Mo, Mn, Ti, Y, Bi, Fe, Ni, Cu and Ce, could selectively catalyze the N-formylation reaction using CO_2 at ambient conditions with very low catalytic loadings.

In the future, our studies will focus on the second step of the cycle shown in Scheme 1, i.e. developing catalysts for the hydrogenolysis of the formamide to release MeOH and regenerate the amine starting material.

Incorporating CO_2 to produce cyclic carbonates from epoxides or diols and the subsequent hydrogenolysis of these compounds to afford methanol is another alternative to the direct reduction of CO_2 to MeOH that we are also working on. We have developed a number of new ionic polymer catalysts for the synthesis of cyclic carbonates from CO_2 and epoxides (CCE reaction) and demonstrated the importance of functional groups as well as cross-linking for catalytic activity and for product separation. [4, 5] When diols are used as starting materials a catalytic cyclic may be imagined where the diol product is recycled (Scheme 2), and methanol may be produced via the hydrogenolysis of the carbonate product. This approach is similar to that proposed in Scheme 1. For this reaction, ILs were not suitable catalysts,

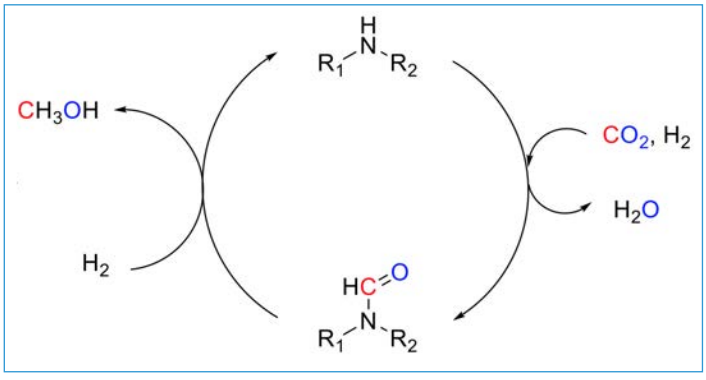

Scheme 1 (top):

Two step reduction of CO_2 into methanol via formamides.

Table 1 (bottom):

N-formylation reaction yields with tetrabutylammonium ionic liquid catalyst demonstrating the halide trend.
(* duration of experiment)

Entry	Catalyst	T* [h]	Yield [%]
1	[TBA]I	20	2
2	[TBA]Br	20	6
3	[TBA]Cl	20	65
4	[TBA]F.3H$_2$O	2	66
5	[TBA]OH.30H$_2$O	2	73
6	[TBA]F.3H$_2$O	6	99

Author

Paul J. Dyson[1]

[1] EPFL

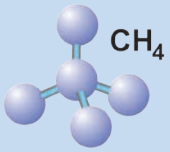

Catalytic approaches to convert CO_2 into fuels

but carbenes were highly active when combined with suitable additives. A cheap thiazolium carbene was employed and the carbonate could be obtained in moderate to good yields starting from the diol product. [6]

In the electrochemical reduction of CO_2 to CO (generation of CO from CO_2 and H_2 from water is viewed as an alternative way to make synthetic fuels, i.e. CO/H_2 is syngas used in Fischer-Tropsch chemistry), we recently deciphered the mechanism by which imidazolium salts lower the overpotential in the electrochemical reduction of CO_2 to CO. [7] Following on from these studies, we have developed a series of new ILs based on triazolium and pyrazolium cations, which show superior properties to the imidazolium variants. Triazolium ILs possess an unusual quasi-reversible current-potential curve, which probably can explain the IL activity by its participation in the CO_2 reduction as a redox mediator. Catalysis proceeds with excellent Faradaic efficiencies, which was confirmed by gas chromatography measurements (Figure 1).

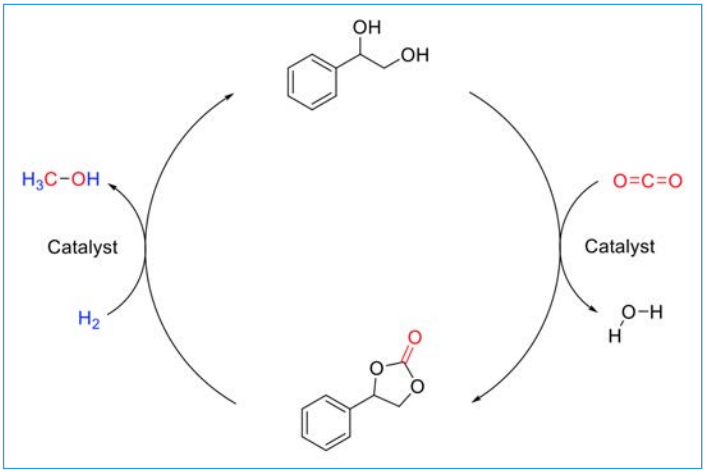

Scheme 2:
Two-step synthesis of methanol from cyclic carbonates.

In collaboration with Prof. Sivula, we demonstrated the potential of naturally occurring minerals, i.e. an iron-nickel containing Gibeon meteorite, as state-of-the-art electrocatalyst for water oxidation reaction to produce hydrogen. [8]

References

[1] S. Das, F.D. Bobbink, S. Bulut, M. Soudani, P.J. Dyson, Chem. Commun., 52, 2497 (2016).

[2] S. Das, F.D. Bobbink, A. Gopakumar, P.J. Dyson, Chimia, 69, 765–768 (2015).

[3] M. Hulla, F.D. Bobbink, S. Das, P.J. Dyson, ChemCatChem., 8, 3338–3342 (2016).

[4] F.D. Bobbink, Z. Fei, R. Scopelliti, S. Das, P.J. Dyson, Helv. Chim. Acta., 99, 821–829 (2016).

[5] F.D. Bobbink, A.P. Van Muyden, A. Gopakumar, Z. Fei, P.J. Dyson, Chemplusschem., 81, 1–9 (2016).

[6] F.D. Bobbink, W. Gruszka, M. Hulla, S. Das, P.J. Dyson, Chem. Commun., 52, 10787–10790 (2016).

[7] G.P.S. Lau, M. Schreier, D. Vasilyev, R. Scopelliti, M. Grätzel, P.J. Dyson, J. Am. Chem. Soc., 138 (25), 7820–7823 (2016).

[8] F.L. Formal, N. Guijarro, W.S. Bourée, A. Gopakumar, M.S. Prévot, A. Daubry, L. Lombardo, C. Sornay, J. Voit, A. Magrez, P.J. Dyson, K. Sivula, Energy Environ. Sci., 9, 3448 (2016).

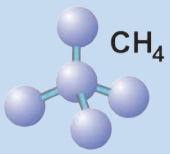

From Electro to Thermocatalytic CO_2 Conversion Processes via Material and Surface Chemistry

List of abbreviations

DFT	Density Function Theory
DRM	Dry Reforming of Methane
HAADF-STEM	High Angle Annular Dark Field - Scanning Transmission Electron Microscopy
HTE	High-Throughput Experimental
IR	Infra Red
NMR	Nuclear Magnetic Resonance
NP	Nanoparticle
OER	Oxigen Evolution Reaction
PHIP	Parahydrogen-Induced Polarization
TEM	Transmission Electron Microscopy

Status of project and main scientific results of workgroups

Electrocatalyst

Complementary to CO_2 electroreduction (vide infra), efficient OER materials based on high surface IrO_x were prepared via a simple and scalable modified Adams fusion method. This method yielded highly OER active iridium oxide nanoparticles of various size and shape, allowing the effects of particle size, morphology, and the nature of the surface species on the OER activity of IrO_2 to be investigated. Iridium oxide synthesized at 350 °C from $Ir(acac)_3$, consisting of 1.7 ± 0.4 nm particles with a specific surface area of 150 $m^2 g^{-1}$, shows the highest OER activity ($E = 1.499 \pm 0.003$ V at 10 $A g_{ox}^{-1}$; Figure 1). Operando X-ray absorption spectroscopy and X-ray photoelectron spectroscopy studies indicate the presence of iridium hydroxo (Ir–OH) surface species, which are strongly linked to the OER activity. Preparation of larger IrO_2 particles using higher temperatures results in a change of the particle morphology from spherical to rod-shaped particles. A decrease of the intrinsic OER activity was associated with the predominant termination of the rod-shape particles by highly ordered (110) facets in addition to limited diffusion within mesoporous features. [1]

Furthermore, in order to decrease the amount of IrO_x, IrO_2 was combined with a TiO_2 support. Using the Adams method described above, it was possible to generate high surface area IrO_2–TiO_2 mixed oxides. While anatase is formed in the absence of Ir, both anatase and rutile phases of TiO_2 were identified by XRD for 40 % IrO_2 – 60 % TiO_2. Analysis of the material via HAADF-STEM microscopy shows the formation of small IrO_2 particles of ca. 1 nm in diameter, in all compositions of IrO_2–TiO_2. The materials display sufficient electrical conductivity, which can be described using a simple equation derived from percolation theory (Figure 1e). This allows for electrochemical applications for materials containing only 40 molM% IrO_2. [2] In parallel, we have been developing Cu-based electrocatalyst for the CO_2 electroreduction.

Dry reforming catalyst

When considering only the metal (Ni), the CO_2 adsorption strength and reactivity increases in the order Ni(111) < Ni(211) < Ni55 < Ni13 where the edges of nanoparticles, especially of subnanometric ones, are the most reactive. However, when considering the support, here γ-Al_2O_3, the binding energy is significantly higher than on the bare nanoparticles, which is attributed to an increased electron transfer from both the nanoparticle and the support to the CO_2 molecule. The most active site toward CO_2 activation is present at the interface between the Ni55 particle and the 110 surface of γ-Al_2O_3: it is associated with the lowest activation energy (32 kJ mol^{-1})

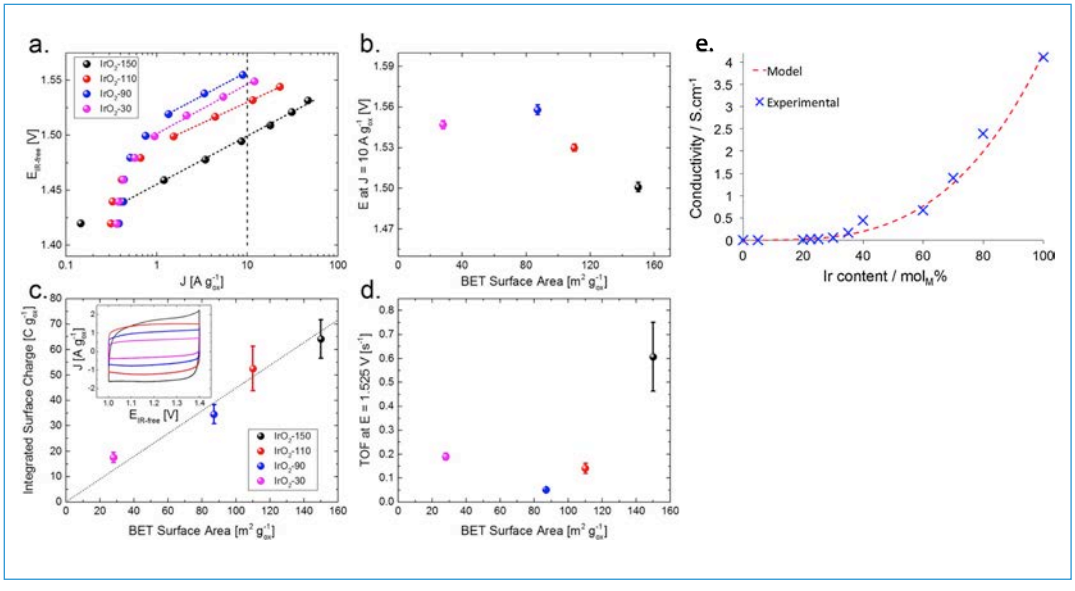

Figure 1:

OER Tafel plots showing:

a) the steady-state current density recorded after 1 min in 0.1 M $HClO_4$;

b) OER activity (E at J = 10 $A g^{-1}$) as a function of surface area;

c) integrated surface charge extracted from cyclic voltammograms recorded at 10 $mV s^{-1}$ plotted as a function of the surface area; inset shows the cyclic voltammograms for each electrode at 10 $mV s^{-1}$;

d) the turnover frequency calculated at E = 1.525 V as a function of surface area;

e) Experimental and modelled conductivity of IrO_2–TiO_2 materials in dependence of Ir content.

Authors

C. Copéret[1]
K. Larmier[1]
E. Lamm[1]
D. Lebedev[1]
N. Kaeffer[1]
R. Kissner[1]
H.K. Lo[1]
E. Oakton[1]
S. Tada[1]
P. Wolf[1]

[1] ETHZ

From Electro to Thermocatalytic CO_2 Conversion Processes via Material and Surface Chemistry

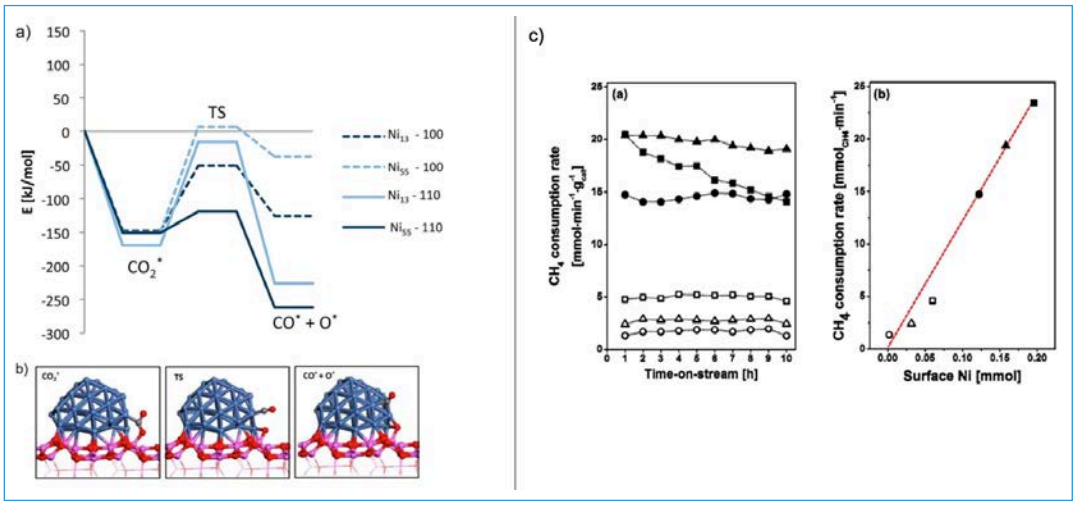

Figure 2:

a) Energy profile for the CO_2 activation on the Ni13 and Ni55 clusters supported on the (100) and the (110) surface of γ-Al_2O_3.

b) Geometries for the CO_2 cleavage on the Ni55 particle supported on the 110 surface of γ-Al_2O_3.

c) Rate of methane consumption as (a) function of TOS and (b) rate of methane consumption (after 1 h TOS) as a function of the quantity of surface Ni: (■) Ni-MA, (▲) Ni4Fe1-MA, (●) Ni3Fe1-MA, (□) Ni1Fe1-MA, (Δ) Ni1Fe3-MA and (○) Fe-MA.

and the most favored thermodynamics for the CO_2 dissociation ($E_{diss} = -262\ kJ\,mol^{-1}$; Figure 2). This work shows how support–metal interactions can provide more favorable activation pathways, thus opening the path for the design of more active metal/oxide interfaces toward CO_2 activation. [3]

Introducing Fe in Ni dry reforming catalysts increases catalytic performance, in particular the stability. Using Ni-Fe nanoparticles supported on $Mg_xAl_yO_z$ as prototypical DRM catalysts, we have shown that the best catalysts correspond to a Ni/(Ni + Fe) ratio of 0.8 (Figure 2c). Using operando X-ray synchrotron-based studies complemented by *ex situ* characterization techniques and DFT calculations has shown that under DRM conditions:

1. Ni remains at oxidation state 0 whether it is alloyed with Fe or not;
2. the deactivation of monometallic Ni is due to the formation of graphitic coke and whiskers;
3. the role of Fe, which is inactive for DRM, is to improve the stability of Ni-based catalysts and the optimal catalyst composition is Ni4Fe1;
4. Fe in NiFe alloys is partially oxidized to FeO, which induces a partial de-alloying and the formation of a Ni-richer Ni-Fe alloy;
5. FeO, located preferentially at the surface as small domains of a few atom layer thickness covering a fraction of the Ni-rich particles, reacts with carbon deposits and reduces coke formation.

These findings explain the increased catalytic stability of bimetallic NiFe catalysts via a $Fe^{2+}O/FeO$ redox cycle. This study also illustrates how important dynamic phenomena are, even for such supported bimetallic nanoparticle catalysts. [4]

CO_2 hydrogenation

Cu is well known for its catalytic activity regarding CO_2 hydrogenation, but the nature of its active sites is highly debated. First, by combining experimental and theoretical approaches, it was possible to rationalize the number of exposed/reactive copper atoms in supported small copper nanoparticles: the reaction of H_2 and N_2O allows the selective titration of surface Cu atoms, with defined but different stoichiometry of $1\,O/2\,Cu_S$ and $1\,H_2/2.2\,Cu_S$. This study has also shown that determining surface sites from simple spherical model and particle size distribution from TEM leads to an over estimation of surface sites (Figure 3). Conversely, determining particle size from chemisorption is not possible for Cu, although it provides relevant information regarding the number of active sites and sintering for instance. This study clearly supports the need to use complementary methods to understand surface sites and describe catalyst behavior. [5]

By the same approach, we have also been able to understand the support effect in CO_2 hydrogenation, and in particular the increase production rate in methanol upon addition of ZrO_2. Using computational chemistry combined with *in situ* IR and *ex situ* NMR spectroscopy, it was possible to show that the formate species formed under a broad

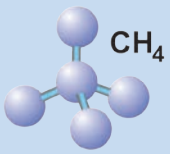

From Electro to Thermocatalytic CO_2 Conversion Processes via Material and Surface Chemistry

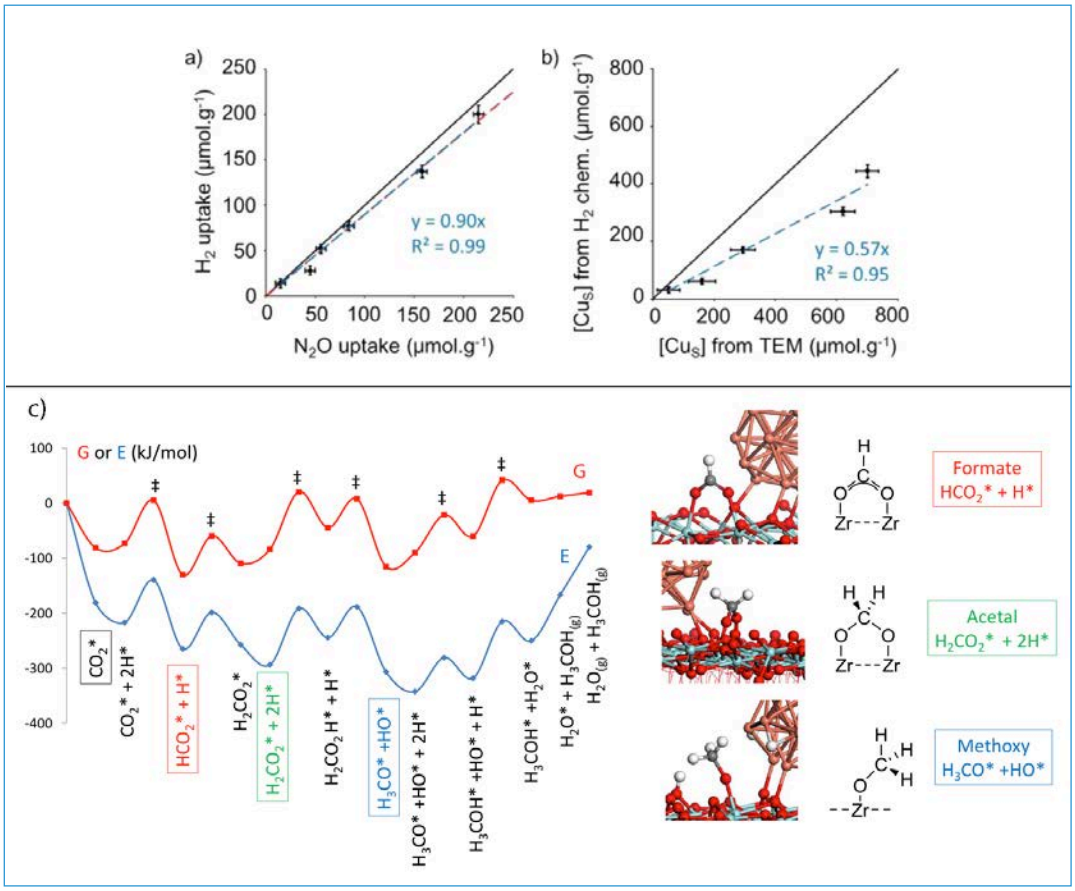

Figure 3:

a) Correlation plots for the specific N_2O and H_2 uptakes determined by N_2O titration and H_2 chemisorption, respectively (marks) (black solid line: expected correlation for a 1 : 1 stoichiometry (eqs 1 and 2); red dotted line: experimental correlation; blue dotted line: expected correlation with the DFT-calculated stoichiometry).

b) Correlation plot for the specific concentration of CuS (marks, given in $\mu mol \cdot g^{-1}$) determined by TEM and H_2 chemisorption (solid line: 1 : 1 ratio; blue dotted line: experimental trend).

c) Potential energy surface derived from computation chemistry and intermediates monitored by *in situ* IR and *ex situ* NMR spectroscopic measurements.

range of pressure readily convert to methoxy species under high pressure (> 5 bars) via an acetal intermediate. Detailed labelling studies have shown that only the formate and the methoxy species can be observed by spectroscopic methods, while the acetal is only an instable reaction intermediate. The proposed mechanism (Figure 3c) is reminiscent of what has been recently proposed for a ruthenium molecular catalyst, bridging the gap between molecular and heterogeneous catalysis. [6] These results clearly point to the crucial molecular role of the interface between the copper particles and zirconia, [7, 8] and is an important guide for a rational development of efficient heterogeneous CO_2 hydrogenation catalysts. [9]

Other discoveries

Following the development of Cu-based catalysts for CO_2 reduction, it was also possible to identify selective semihydrogenation of alkynes via High-Throughput Experimental (HTE) approach. The high-throughput ligand screening approach applied to a heterogeneous catalyst allowed identifying tricyclohexylphosphine as a potent ligand to increase the chemoselectivity of alkyne semihydrogenation (Figure 4a). The optimal catalyst Cy_3P–Cu / SiO_2–700 is thus an efficient, practical, sustainable, and cheap alternative to the Lindlar catalyst. [10]

The reaction mechanisms of the selective semihydrogenation of alkynes with silica-supported Cu nanoparticles and parahydrogen were further investigated. Parahydrogen-induced polarization (PHIP) effects were observed for the hydrogenation of 1-butyne on Cu/SiO_2-700 and were very minor for the hydrogenation of 1-butene and not observed for 2-butyne hydrogenation, indicating that different mechanistic manifolds operate with these substrates. Modification of the Cu/SiO_2-700 catalyst with PCy_3 leads to an increase in the selectivity of 1-butyne hydrogenation to nearly 100 % (with by-products below the detection limit of NMR), although it was found to make this catalyst significantly less active. The remarkable selectivity of Cy_3P–Cu / SiO_2-700 also manifested in no activity in the hydrogenation of 1-bu-

From Electro to Thermocatalytic CO_2 Conversion Processes via Material and Surface Chemistry

tene, and no formation of butane from 2-butyne. Cy_3P–Cu/SiO_2-700 provided no less than 2.7 % pairwise hydrogen addition to 1-butyne, with the actual value likely to be higher due to polarization losses via relaxation (Figure 4b). Our results demonstrate that copper-based catalysts are promising inexpensive alternatives to heterogeneous noble metal catalysts for the semihydrogenation of alkynes in the flow and the production of hyperpolarized gases. [11]

Collaboration network

In situ IR characterization of reaction intermediates for the hydrogenation of CO_2 with supported catalysts (collaboration with A. Urukawa, ICIQ) and approach to supported Cu nanoparticles on carbone with high loading was developed. This is currently being evaluated in the electroreduction of CO_2 to methanol (collaboration with T.J. Schmidt and P. Broekmann). In addition, hybrid material for the conversion of CO_2 to organic compounds (collaboration with P. Dyson) and formic acid derivatives (collaboration with P. von Rohr) was developed. These results pave the way to develop catalysts for the efficient conversion of $C2_2$ to fuels and chemicals using thermal and electrochemical processes.

Part of this work was carried out in collaboration with Profs. P. Broeckmann (University of Bern), P. Dyson (EPFL), C. Müller (ETHZ–D-MATV), F. Ribeiro (Purdue University, USA), P. von Rohr (ETHZ–D-MATV), T.J. Schmidt (PSI), A. Urukawa (ICIQ, Spain).

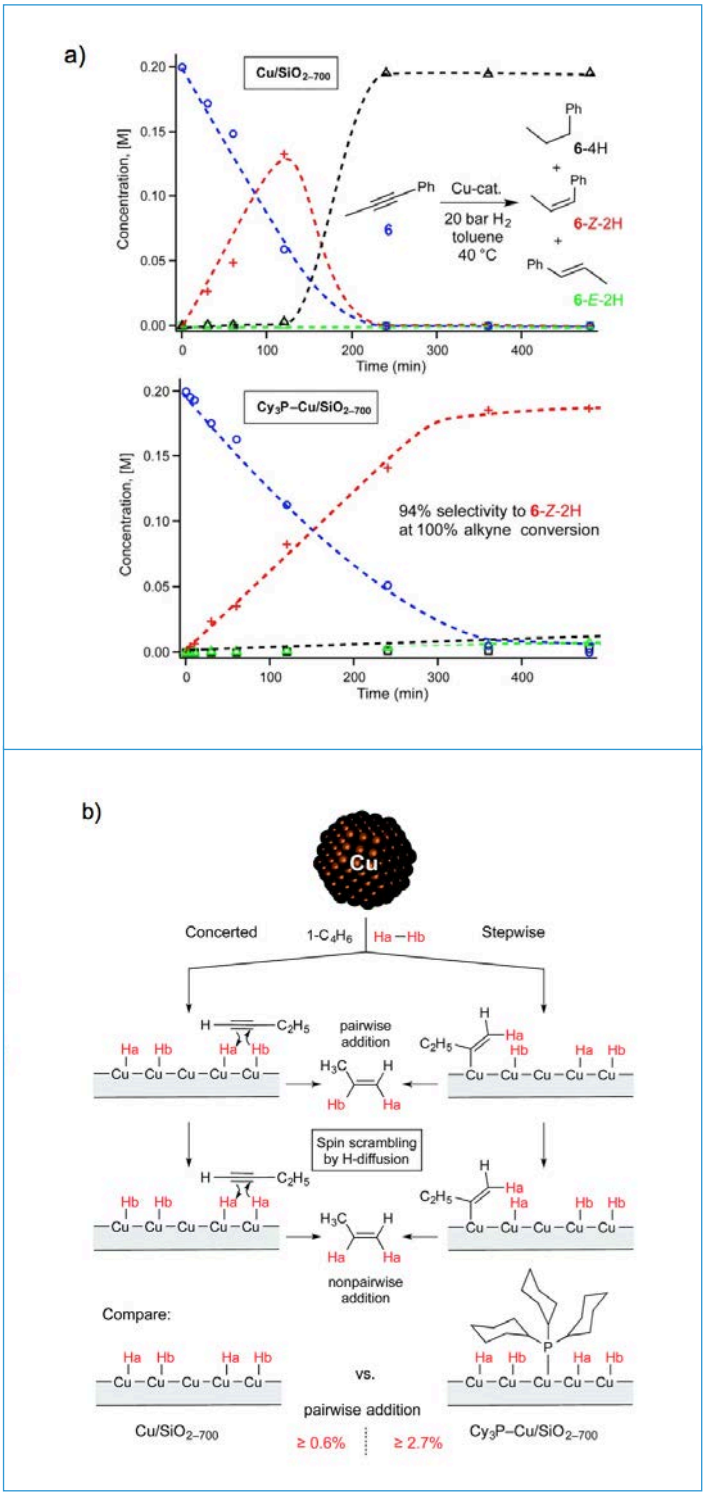

Figure 4:

a) Evolution of concentration with time for the hydrogenation of 1-phenyl-1-propyne with Cu/SiO_2–700 (0.375 mol %, top) and Cy_3P–Cu/SiO_2–700 (0.18 mol %, bottom) with dotted lines added to guide an eye.

b) Non-pairwise and pairwise routes of hydrogen addition to 1-butyne over Cu/SiO_2-700 and Cy_3P–Cu/SiO_2-700 catalysts.

References

[1] D.F. Abbott, D. Lebedev, K. Waltar, M. Povia, M. Nachtegaal, E. Fabbri, C. Copéret, T.J. Schmidt Chem. Mater. 28, 6591–6604 (2016).

[2] E. Oakton, D. Lebedev, A. Fedorov, F. Krumeich, J. Tillier, O. Sereda, T.J. Schmidt, C. Copéret, New J. Chem. 40, 1834–1838 (2016).

[3] M.-C. Silaghi, A. Comas-Vives, C. Copéret, ACS Catal. 6, 4501–4505 (2016).

[4] S.M. Kim, P. Abdala, T. Margossian, D. Hosseini, L. Foppa, A. Armutlulu, W. van Beek, A. Comas-Vives, C. Copéret, C. Mueller, J. Am. Chem. Soc. in press (2017).

[5] K. Larmier, S. Tada, A. Comas-Vives, C. Copéret, J. Phys. Chem. Lett., 7, 3259–3263 (2016).

[6] S. Wesselbaum, V. Moha, M. Meuresch, S. Brosinski, K.M. Thenert, J. Kothe, T.V. Stein, U. Englert, M. Holscher, J. Klankermayer, W. Leitner, Chem. Sci., 6, 693–704 (2015).

[7] F. Frusteri, G. Bonura, C. Cannilla, G.D. Ferrante, A. Aloise, E. Catizzone, M. Migliori, G. Giordano, Appl. Catal. B, 176, 522–531 (2015).

[8] F. Arena, G. Italiano, K. Barbera, S. Bordiga, G. Bonura, L. Spadaro, F. Frusteri, Appl. Catal. A, 350, 16–23 (2008).

[9] K. Larmier, W.-C. Liao, S. Tada, E. Lam, R. Verel, A. Bansode, A. Urakawa, A. Comas-Vives, C. Copéret, Angew. Chem. Int. Ed., in press (2017).

[10] A. Fedorov, H.-J. Liu, H.-K. Lo, C. Copéret, J. Am. Chem. Soc. 138, 16502–16507 (2016).

[11] O.G. Salnikov, H.-J. Liu, A. Fedorov, D.B. Burueva, K.V. Kovtunov, C. Copéret, I.V. Koptyug, Chem. Sci., DOI: 10.1039/c6sc05276b (2017).

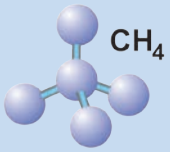

Metal Hydrides for Electrochemical CO_2 Reduction

List of abbreviations

DoS	Density of States
HER	Hydrogen Evolution Reaction
MH	Metal Hydride
SHE	Standard Hydrogen Electrode

Scope of project

Carbon dioxide concentration in the atmosphere is continuously increasing and corresponds to 750×10^{12} kg C. However, most of the CO_2 on the Earth is stored in the ocean ($41'031 \times 10^{12}$ kg C). At the same time, the contribution of renewable energy (e.g. solar, wind and hydropower) is growing worldwide and substitute energy from fossil fuels potentially decreasing the CO_2 emission. The storage of renewable energy requires the conversion of electricity into an energy carrier, for example hydrogen. Moreover, the reduction of CO_2 with hydrogen to hydrocarbons (synthetic fuels) allows storing renewable energy with the same energy density as fossil fuels. Therefore, electrochemical CO_2 reduction to specific hydrocarbons after its extraction from the air is of great importance for the future energy economy based on renewable energy. The direct electrochemical CO_2 reduction from seawater would be an even more attractive and efficient process. In order to reach this goal it is necessary to use a catalyst, which is active for the CO_2 reaction on the surface and provides H for the formation of hydrocarbons. Metal hydrides allow to split water and adsorb atomic hydrogen at the surface.

We have designed and prepared new catalytic copper-containing electrode materials, which form a hydride and offer highly active surface sites for the adsorption and reduction of CO_2 with atomic hydrogen.

Status of project and main scientific results of workgroups

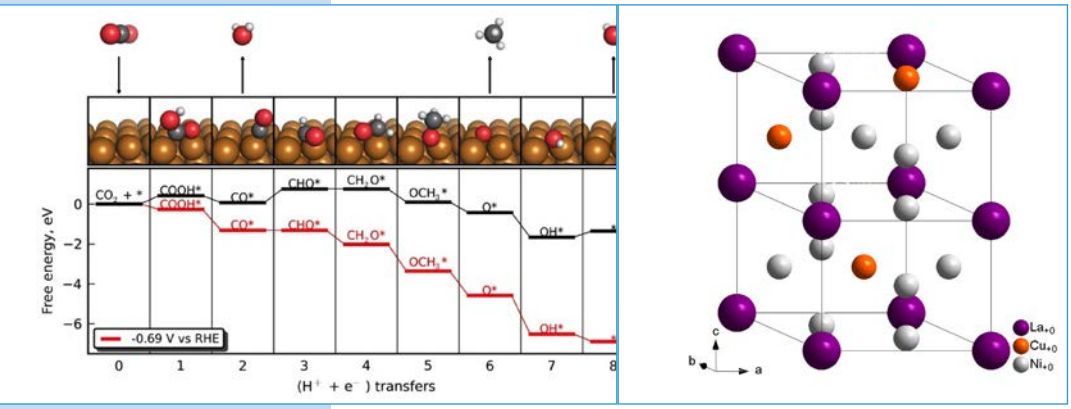

Figure 1:

Left: Calculated for the lowest energy pathway of CO_2 reduction on copper to CH_4. The black (higher) pathway represents the free energy at 0 V vs. RHE and the red (lower) pathway the free energy at the indicated potential [2].

Right: Crystal structure of $LaNi_4Cu$ alloy (• La, • Ni, • Cu) unit cell (schematic view).

The advantage of the simultaneous electrochemical reduction of CO_2 and H_2O allows the direct synthesis of hydrocarbons from electricity. The reaction is more efficient since no hydrogen gas phase is formed and therefore the entropy change is minimal.

Furthermore, the co-electrolysis may allow the production of hydrocarbons directly from seawater, subject of a large research program in the US [1].

The electrochemical CO_2 reduction in acidic electrolyte involves the dissociation of water and the reduction of H^+ to atomic hydrogen at the cathode:

$$H^+ + H^+ \rightarrow H_2\uparrow$$

The CO_3^{2-} ion in the electrolyte moves to the anode, where oxygen is evolved.

$$CO_2 + H_2O \leftrightarrows H_2CO_3 \leftrightarrows H^+ + HCO_3^- \leftrightarrows H^+ + CO_3^{2-}$$

Therefore, only the neutral CO_2 molecules dissolved in the electrolyte are available on the cathode for reduction. The CO_2 bound to the surface is electronically connected to the potential of the electrode, i.e. the chemical potential of the bound CO_2 follows the electrode potential. The reduction reaction of CO_2 with H requires the carbon atom bound to the surface and atomic hydrogen close to the oxygen atoms. Metal hydrides (MH) are substrates that can bind CO_2 and provide atomic hydrogen at the surface. In the reduction reaction there is a competition between O-H, C-H and C-C bond formation. While O-H and C-H bond formation requires large activity of hydrogen, the C-C bond formation requires the absence of oxygen and surface bound carbon close to each other.

The mechanism of C-C coupling on the surface and further formation of *CO and *CHO was described by the group of Norskov on a copper electrode. They show that the kinetics of C-C coupling during electrochemical CO_2 reduction

Authors

Mariana Spodaryk[1]
Andreas Züttel[1]

[1] EPFL Valais/Wallis

Metal Hydrides for Electrochemical CO_2 Reduction

strongly depends on the applied potential [2] (Figure 1 left). Therefore, the control of the potential allows to tune the reduction process towards the desired product.

The product distribution in CO_2 reduction varies widely, depending primarily on the electrode metals and the electrolyte used for the process. The key factor in determining the product distribution in CO_2 reduction is the cathode material. Among the other metals copper is a unique metal on which hydrocarbons can be obtained according to the one of the early work of Hori [3]. At the same time hydrides of metals [4] and alloys [5] according to the literature have ability to adsorb CO_2 and may be ideal catalysts for the reaction as well as a source of atomic reactive hydrogen at the surface. Ohkawa et al. [4] studied the electrochemical behavior of CO_2 on hydrided Pd electrodes and showed that the activity for CO_2 reduction increases with higher hydro-

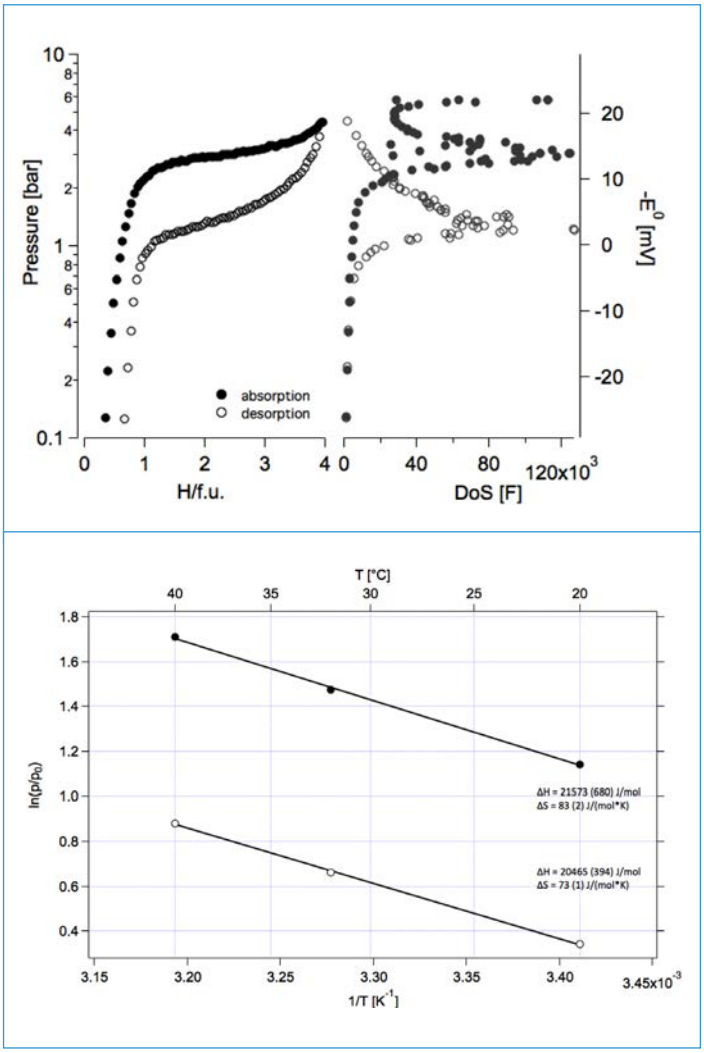

Figure 2:

Top: Equilibrium charge/discharge curves of $LaNi_4Cu$ alloy electrode with corresponding density of states (DoS) of hydrogen in alloy at 20 °C.

Bottom: Van't Hoff plot of $LaNi_4Cu$ alloy. Filled markers in both graphs represent charge (absorption) process, empty markers represent desorption (discharge) process.

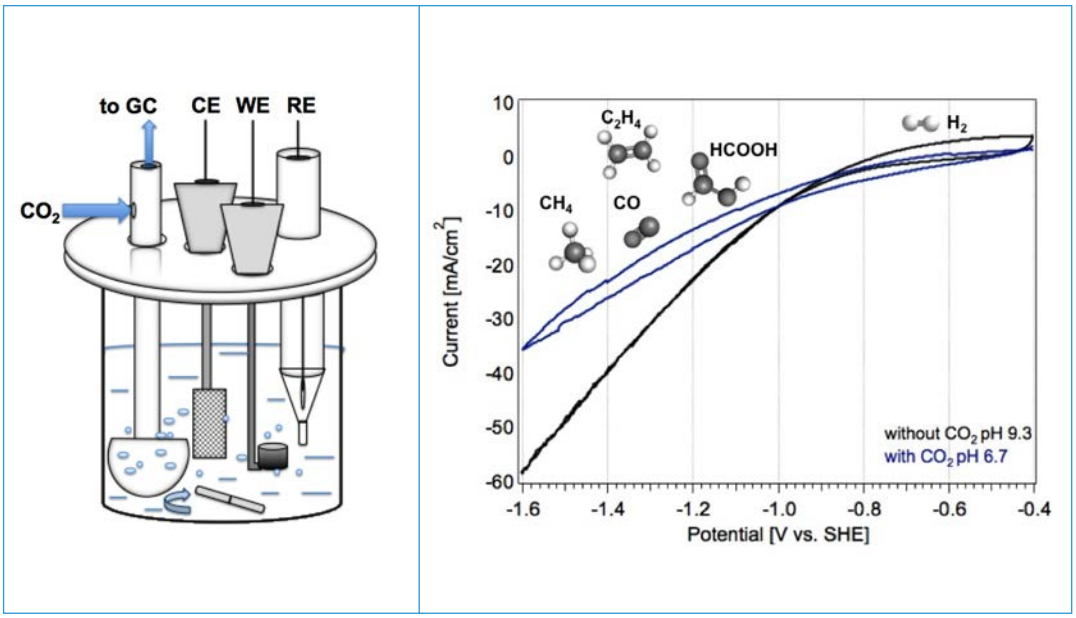

Figure 3:

Left: Schematic view of electrochemical cell for CO_2 reduction.

Right: Cyclic voltammograms obtained at scan rate of 1 mV/s on the surface of $LaNi_4Cu$ electrodes without CO_2 (pH 9.3) and with CO_2 (pH 6.7) in 0.1 M $KHCO_3$ and indicated products of electrochemical CO_2 reduction

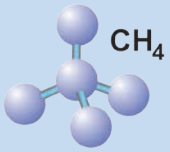

Metal Hydrides for Electrochemical CO_2 Reduction

References

[1] http://www.nrl.navy.mil/media/news-releases/2012/fueling-the-fleet-navy-looks-to-the-seas.

[2] A.A. Peterson, F. Abild-Pedersen, F. Studt, J. Rossmeisl, J.K. Nørskov, «How copper catalyzes the electroreduction of carbon dioxide into hydrocarbon fuels», Energy Environ. Sci., 3 (9), 1311–1315, 2010.

[3] Y. Hori, K. Kikuchi, S. Suzuki, «Production of co and ch4 in electrochemical reduction of co2 at metal electrodes in aqueous hydrogencarbonate solution», Chem. Lett., 14 (11), 1695–1698, Nov. 1985.

[4] K. Ohkawa, K. Hashimoto, A. Fujishima, Y. Noguchi, S. Nakayama, «Electrochemical reduction of carbon dioxide on hydrogenstoring materials: Part 1. The effect of hydrogen absorption on the electrochemical behavior on palladium electrodes», J. Electroanal. Chem., 345, (1), 445–456, 1993.

[5] S. Kato et al., «The Origin of the Catalytic Activity of a Metal Hydride in CO_2 Reduction», Angew. Chem., 128 (20), 6132–6136, 2016.

[6] K. Ohkawa, Y. Noguchi, S. Nakayama, K. Hashimoto, A. Fujishima, «Electrochemical reduction of carbon dioxide on hydrogen-storing materials: Part 3. The effect of the absorption of hydrogen on the palladium electrodes modified with copper», J. Electroanal. Chem., 367 (1), 165–173, 1994.

gen content in Pd. Moreover, it is declared by authors that the hydrogen absorbed on the Cu-modified Pd electrodes participates in the electrochemical reduction of CO_2 via surface adsorption or reacts with the intermediates directly [6].

A series of $LaNi_{(5-X)}$ Cu_X-type alloys with partially substituted nickel by copper were synthesized by arc melting under Ar atmosphere and single phase was detected by means of XRD. All obtained alloys have a hexagonal $CaCu_5$ structure (space group P6/mmm) and show random distribution of Cu on Ni sites. The crystal structure of alloys is presented on the example of $LaNi_4Cu$ alloy unit cell and is shown in Figure 1. The La and Ni atoms, which form the interstitial sites hosting hydrogen atoms, are the source of atomic hydrogen on the electrode surface while copper atoms represent active sights for CO_2 binding. This unique combination forms a new type of highly active catalytic sites.

The cold pressed pellet electrodes from the grinded copper-containing alloys were fully activated during 30 charge/discharge cycles in 6 M KOH electrolyte in standard electrochemical cell (Ni plate as a counter electrode, Hg/HgO as reference electrode). Afterwards, the equilibrium potentials of electrodes were measured with pulsed cycle method at different temperatures (20 °C, 30 °C, 40 °C). The equilibrium charge (absorption)/discharge (desorption) curves obtained at 20 °C and corresponding density of states (DoS) for hydrogen in $LaNi_4Cu$ alloy are presented in Figure 2 left. Maximum of the DoS corresponds to the equilibrium pressure of plateau (3.129 bar for absorption, 1.406 bar for desorption). Based on the obtained (electrochemically at different temperatures) absorption/desorption curves the Van't Hoff plot was evaluated and enthalpies together with entropies for both absorption and desorption processes were calculated (Figure 2 right).

According to [5] the atomic hydrogen flux from the metal hydride is crucial for the reduction of carbon dioxide and surface oxides, especially at grain boundaries or adlineation sites, while at the initial stage, the dissociation of hydrogen molecules from the gas phase is hindered by the high activation barrier on the oxidized surface. The higher the hydride composition, the higher the concentration of active sites and hence, the better the activity that increases with metal hydride composition. This indicates that the activity of the surface for the CO_2 reduction strongly depends on the hydrogen concentration in the metal hydride (between 2 and 4 H/f.u., Figure 2 left).

The electrochemical CO_2 reduction was carried out in the standard three electrode electrochemical cell (WE–MH alloy electrode, CE–Pt mesh, RE–Ag/AgCl in 3 M KCl solution) using 0.1 M $KHCO_3$ electrolyte (Carl Roth, 99.9 %) with continuous CO_2 bubbling through it in order to saturate the electrolyte by supplying neutral CO_2 to the working electrode and homogenization by a magnetic stirrer at the bottom of the cell to avoid locally increasing pH close to the electrode during the reduction process (Figure 3 left). After saturation of the electrolyte for 30 minutes the pH of the electrolyte was slightly acidic (6.65–6.8). On the cyclic voltammograms (Figure 3 right) obtained without and with CO_2 on $LaNi_4Cu$ electrode the potential region at which electrochemical conversion of CO_2 with hydrogen results in HCOOH, CO, C_2H_4, CH_4 (listed in sequence of reaction potential decreasing) is indicated.

Since all the products listed above are formed under potentials lower than hydrogen evolution reaction (HER) (starts at –0.414 V vs. SHE at 25 °C and pH 7 according to Pourbaix diagram) the main byproduct of CO_2 reduction on copper-containing MH electrodes, as well as on pure Cu, is hydrogen. Suppressing the HER and therefore, increasing the faradaic efficiency of the formation of hydrocarbons is challenging and a crucial task, which is of our interest for further investigation of these materials.

Towards *in operando* Characterization of High Surface Area Catalysts for Electrochemical CO_2 Conversion

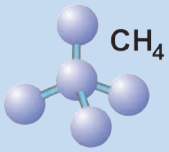

Scope of project

In the focus of the SCCER project were two types of catalyst materials for CO_2 electroconversion:

- carbon-supported oxidic nanoparticles (SnO_2NPs@rGO) and
- metal foam catalysts (oxide-derived Cu foams).

Synthesis strategies for both were further improved during the last project year. In addition, catalyst degradation pathways were studied under *in operando* conditions by means of Raman spectroscopy.

Status of project and main scientific results of workgroups

In the focus of this SCCER project is the conversion of the environmentally unfriendly green house gas CO_2 into high value products (e.g. ethylene, methanol, formic acid etc.) by means of electrochemical processing. The particular technological challenge is related to the extraordinary stability of the CO_2 molecule thus requiring extremely high over potentials for its electrochemical reduction. Only by the use of proper catalysts the CO_2 reduction can be accelerated so that the process might become feasible from an economic point of view. Up to now, only copper based catalysts show a promising activity towards the CO_2 conversion into hydrocarbons whereas tin based catalysts are the most promising candidates for formate production. [1, 2]

A number of catalyst specific issues, however, still need to be addressed which are related to a lack of selectivity in the case of Cu and a lack of stability in case of carbon-supported SnO_2-NPs. For a more tailored design of catalysts it is important to know which surface sites and which particular chemical states of the catalyst are the most active ones towards CO_2 electroreduction. In particular, oxidic catalysts might undergo changes of their chemical state, their composition and morphology under those harsh experimental conditions which are relevant for the CO_2 conversion. Therefore *in operando* approaches are important to characterize the catalyst under reactive conditions.

SnO_2-NPs@rGO catalysts for CO_2 conversion

The potential dependent stability of SnO_2-NPs was monitored by *in operando* Raman spectroscopy and correlated to the resulting Faradaic efficiency towards formate production ($FE_{formate}$). [3, 4] It turned out that the SnO_2-NPs undergo first a partial electrochemical reduction to transient SnO in the potential regime where the highest $FE_{formate}$ is observed. From this study it can therefore be concluded that the most active catalyst contains both Sn(IV) and Sn(II) species at its interface to the working electrolyte. At most negative potentials the SnO_2 catalyst undergoes a full reduction to metallic tin which goes along with a drastic drop of $FE_{formate}$ from 75 % (Sn(IV/Sn(II) composite)) down to 25 % at pH 8.5. [3, 4]

This complete reduction process to metallic tin also involves a structural degradation of the NPs which has to be considered as irreversible. Attempts to recover the SnO_2 catalysts by switching back the potential into the thermodynamic stability regime of SnO_2 indeed leads to the reappearance of SnO_2-NPs which, however, show a changed size distribution as compared to the as synthesized NPs. The appearance of sub-4 nm SnO_2-NPs during the recovery process can be monitored by the *in operando* Raman spectroscopy through appearance of a characteristic broad Raman feature in the range between 400 and 800 cm^{-1} (Figure 2). Unfortunately, these smaller SnO_2-NPs show a higher FE towards HER on the expense of $FE_{formate}$.

Further stability measurements of the SnO_2-NPs demonstrate that their partial reduction to the transient SnO is, by contrast, fully reversible over number of potential cycles.

These *in operando* degradation studies allow confining the optimum potential window for operating this type of oxidic NP catalysts with regard to both catalyst stability and Faradaic efficiency.

Oxide-derived Cu foam catalysts for CO_2 conversion

High surface area Cu foams obtained by an additive controlled electrodeposition pro-

List of abbreviations

FE	Faradaic Efficiency
HER	Hydrogen Evolution Reaction
NP	Nanoparticle
SEM	Scanning Electron Microscopy

References

[1] Y. Hori, A. Murata, Y. Yoshinami, J. Chem. Soc. Faraday Trans., 87, 125–128 (1991).

[2] K.J.P. Schouten, Y. Kwon, C.J.M. van der Ham, Z. Qin, M.T.M. Koper, Chem. Sci., 2, 1902–1909 (2011).

[3] A. Dutta, A. Kuzume, M. Rahaman, S. Vesztergom, P. Broekmann, ACS Catal., 5, 4798–7502 (2015).

[4] A. Dutta, A. Kuzume, V. Kaliginedi, M. Rahaman, S. Vesztergom, P. Broekmann, Acc. Chem Res. (invited, submitted for publication).

[5] A. Dutta, M. Rahaman, N.C. Luedi, M. Mohos, P. Broekmann, ACS Catal., 6, 3804–3814 (2016).

Author

A. Dutta[1]
A. Kuzume[1]
M. Rahaman[1]
V. Kaliginedi[1]
A. Zanetti[1]
N. Luedi[1]
M. Mohos[1]
P. Broekmann[1]

[1] University of Bern

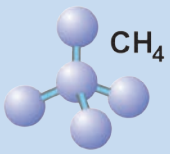

Towards *in operando* Characterization of High Surface Area Catalysts for Electrochemical CO_2 Conversion

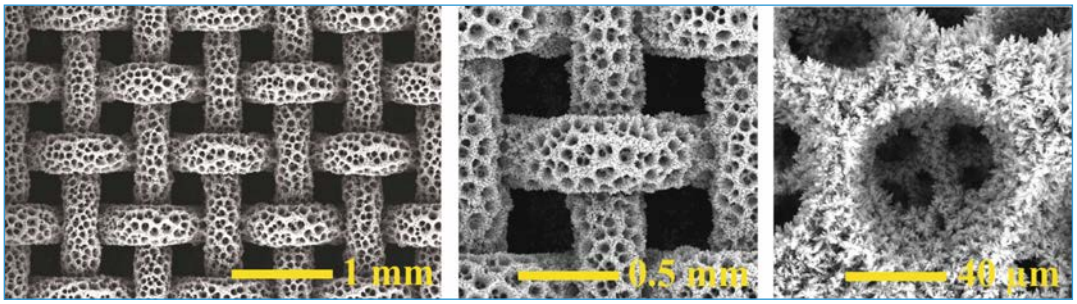

Figure 1 :

a) Three-dimensional surface plot of Raman intensities created by a continuous acquisition of Raman spectra as the electrode potential was slowly stepped from less (–0.25 V) to more negative values (–1.55 V vs. Ag | AgCl).

b) The intensities of SnO_2 and SnO related peaks as a function of electrode potential; the lines here correspond to those shown on the surface plot in (a).

c) Potential-dependent Raman spectra recorded on the course of stepping the potential back from –1.55 V to –0.25 V vs. Ag | AgCl.

d) The intensity of the SnO_2 related wave as a function of electrode potential; the line here corresponds to the one shown on the surface plot in (c).

cess have been demonstrated as excellent CO_2 catalysts towards C_2 (C_2H_4, C_2H_6) product formation. [5]

Various factors have been characterized as important for the resulting FE_{C_2} such as the annealing pre-treatment in air and the mean surface pore size of the Cu foams. Maximum FE_{C_2} reach values of 55 % under optimum conditions. Important for future applications in flow cell devices is that these Cu foams can be deposited not only on planar surfaces but also on 2D Cu-meshes (Figure 2) or on 3D Cu-skeletons.

Conclusions and next steps

In operando Raman spectroscopy will be applied to study the role of oxide species on Cu foam catalysts. In addition the Cu-foam on Cu-mesh catalyst needs to be tested with respect to their FE_{C_2}.

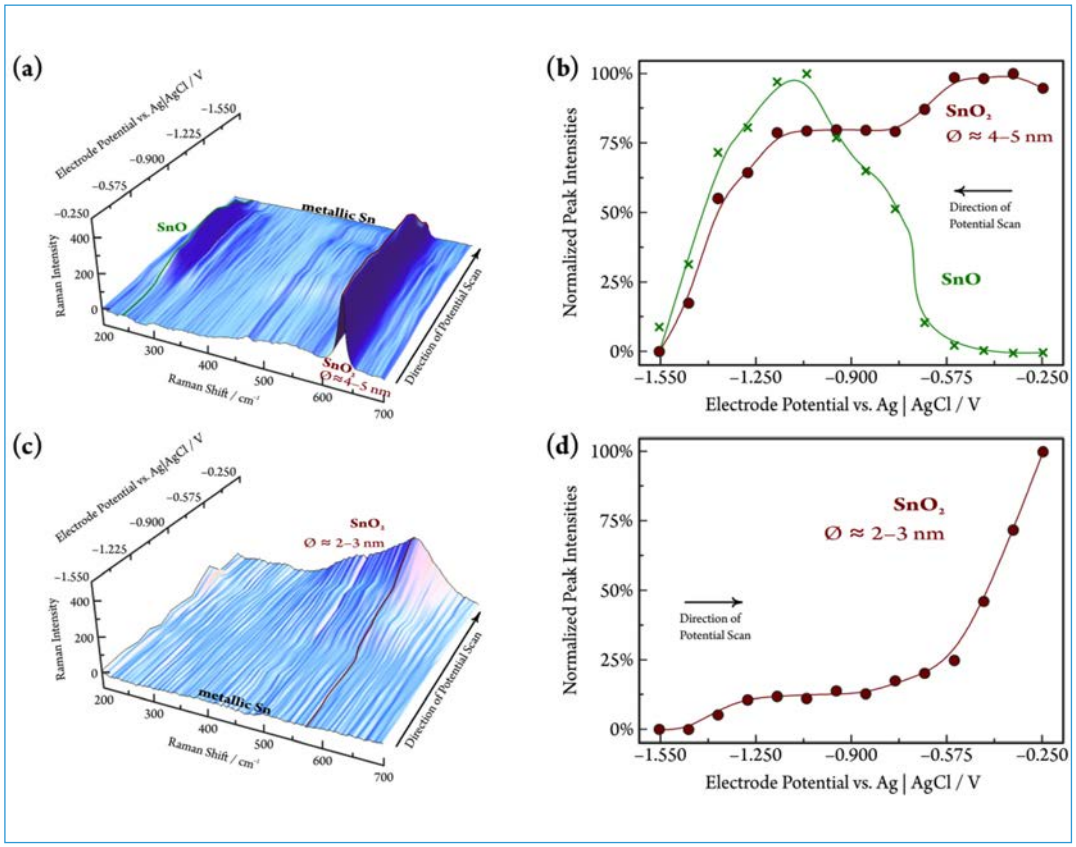

Figure 2 :

Series of SEM micrographs showing a Cu foam deposited on a 2D Cu mesh.

Electrochemical Cell Configuration for CO_2 Reduction in Gas Phase at Low Temperature

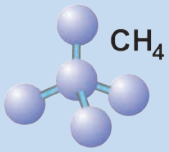

Scope of project

The electrochemical production of chemical products like syngas, format, methane, ethylene, methanol or other transportation fuels starting from CO_2 reactant appears like a suitable technology to recycle and reduce this greenhouse gas. However, a suitable process using only CO_2, water and renewable energy is currently not available. Only few models of co-electrolysis cells exist but they are limited by factors like energetic efficiency, reaction products selectivity and cost [1,2]. So far only carbon monoxide and formate products appear to be economically interesting when produced by electrochemical CO_2 reduction compared to other well established chemical processes [3]. As the catalyst used for CO_2 reduction reaction (CO_2RR) is crucial for selectivity but also for the energetic efficiency of the whole process (i.e. kinetic overpotentials), a majority of the studies aim towards high-performance catalyst development [4,5]. Product selectivity as a function of electrode material was established by Hori [6] and this is generally accepted by the scientific community. For example Au, Ag, Zn are widely known to be efficient for CO formation.

However, the overall efficiency of the process is not entirely dependent on the catalyst nature; mass transport phenomena and pH conditions are equally crucial parameters for an optimal CO_2 conversion process.

The direction of this work package was oriented on the production of CO starting from CO_2 in the gas phase using typical membrane electrolyzer cells. Au electrodes were chosen for their selectivity against CO but also for their chemical stability in a broad pH range. Various cell configurations using solid polymer electrolyte are discussed.

Status of project and main scientific results of workgroups

The process from CO_2 to syngas (H_2 + CO) in gas phase takes place in an electrochemical reactor / electrochemical cell. The electrochemical cell consists of two metallic gold coated flow fields, two electrodes and different solid electrolytes / membranes. To efficiently design such a system we first focused on finding the appropriate solid electrolytes. With this respect, various cell configurations, electrolyte's pH and operation conditions (temperature, pressure and current densities) were studied in order to achieve efficient CO_2 conversion to CO.

Since the starting of the project, many activities have successfully been started with a wide variety of results:

- design of electrocatalyst systems with high selectivity in the CO_2 reduction;
- development of polymer electrolyte based electrochemical cell.
- development of analytical tools for online and operando detection of reaction products in the electrochemical reduction of CO_2;

The results related to co-electrolysis cell design are exemplified in the following.

Experimental

Au mesh (Goodfellow®) and Pt/C gas diffusion electrode were used as cathode and anode, respectively. The electrodes area was 0.5 cm^2. Various membranes were used as solid electrolyte: proton exchange membrane Nafion® XL 100 (30 µm thickness), anions exchange membrane Fumasep® AA (130 µm thickness) and bipolar membrane Fumasep® FBM (130 µm thickness). The anion exchange membrane was pretreated in 0.5 M $KHCO_3$ solution for 24 h before utilization.

For comparison, a cell configuration containing a buffer layer between the cathode and the proton exchange membrane was tested [6]. The buffer layer was a Watman® paper impregnated in 0.5 M $KHCO_3$ solution in order to mimick a bipolar membrane architecture.

CO_2 was fed to the cathode side at 10 mL/min, whilst the anode side was fed with pure H_2 at 50 mL/min. Gas humidification was achieved by passing through a water-bubbling system; their temperature was set to yield 100 % humidification values. The cells were operated at 40 °C and ambient pressure. Polarization curves were measured galvanostatically. For each data point, the cell current was stabilized for 5 minutes and the data were averaged from the last 3 minutes. The gas product from cathode was analyzed by mass spectroscopy (MS Prisma).

List of abbreviations

AEM	Anionic Exchange Membrane
CEM	Cation Exchange Membrane
CO_2RR	CO_2 Reduction Reaction

References

[1] D.T. Whipple et al., Electochem. Solid-Sate Letters, 13 (9), B109–B111 (2010).

[2] C. Delacourt et al., J. Electrochem. Soc., 155 (1), B42–B49 (2008).

[3] J. Durst et al., Chimia 69 (12), 1–8 (2015).

[4] J. Herranz et al., Nano Energy 29, 4–28 (2016).

[5] J. Rosen et al., ACS Catalysis, 5, 4293–4299 (2015).

[6] Y. Hori et al., «Electrochemical CO_2 reduction on metal electrodes. Modern aspects of electrochemistry», Springer, 89–189 (2008).

Author

Alexandra Pătru[1]
Thomas J. Schmidt [1]

[1] PSI

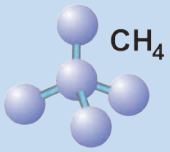

Electrochemical Cell Configuration for CO_2 Reduction in Gas Phase at Low Temperature

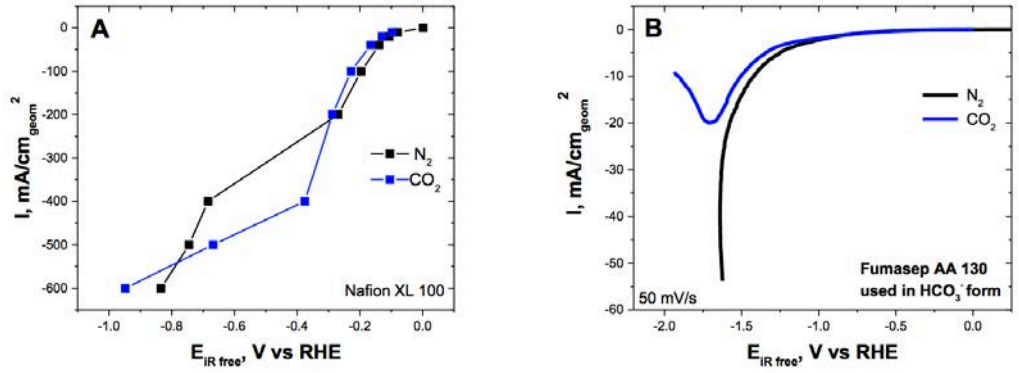

Figure 1:

Potential of the cathode obtained using CEM cell configuration (A) and AEM cell configuration (B). Cathode: Au mesh; flow 10 mL/min N_2/CO_2. Anode: Pt/C gas diffusion electrode; flow 50 mL/min H_2. Tcell 40 °C, p ambient, full humidification.

Results

Standard cell configurations – acidic vs alkaline system

When CO_2RR takes place at the gold cathode the principal electrochemical reactions are:

in alkaline environment

$$CO_2 + H_2O + 2e^- \rightarrow CO + 2OH^- \quad E = -0.932\ V/RHE \quad [1]$$

$$2H_2O + 2e^- \rightarrow H_2 + 2OH^- \quad E = -0.828\ V/RHE \quad [2]$$

or in acidic environment

$$CO_2 + 2H^+ + 2e^- \rightarrow CO + H_2O \quad E = -0.104\ V/RHE \quad [3]$$

$$2H^+ + 2e^- \rightarrow H_2 \quad E = 0\ V/RHE \quad [4]$$

Cation exchange membrane (CEM) and anionic exchange membrane (AEM) were used for CO_2 reduction from the gas phase. The polarization curves obtained under N_2 and CO_2 are shown in Figure 1. In the case of CEM configuration high currents densities were obtained under CO_2 at low overpotential (–400 mA/cm² at –0.4V/RHE). Despite the good electrochemical performances achieved using a CEM cell configuration, H_2 was the majority reaction product obtained as shown by the MS results (Figure 2). In view of this result, it is likely that the acidity of the membrane shifts the cathode selectivity toward hydrogen evolution. Contrary, in the case of AEM configuration low current densities are obtained at high reaction overpotential. Moreover, an increase in membrane high frequency resistance (up to 15 Ωcm²) and losses of membrane stability were observed. A product analysis was not possible under these conditions by MS.

However, the use of AEM configuration can be interesting for CO_2 reduction from gas phase due to the pH increase, but membranes with improved stability, lower resistance and better affinities for carbonate and bicarbonate species must be found. Another possible limitation of this kind of system can be the anode reaction when a complete co-electrolyser is used (i.e. oxygen evolution reaction at the anode side). In this case, HCO^{3-}, CO_3^{2-} and OH^- are possible charge carriers and CO_2 can be produced at the anode side according to reactions 5 and 6.

A considerable production of CO_2 at the anode side will obviously lead to an inefficiency of the system.

$$2HCO^{3-} \rightarrow \tfrac{1}{2}O_2 + H_2O + 2e^- + 2CO_2 \quad E = -0.765\ V/RHE \quad [5]$$

$$CO_3^{2-} \rightarrow \tfrac{1}{2}O_2 + 2e^- + CO_2 \quad E = -0.692\ V/RHE \quad [6]$$

Figure 2:

Ion current recorded by MS for different mass fraction (m/z) showing the formation of H_2 (m/z = 2) when a Nafion® XL membrane is used.

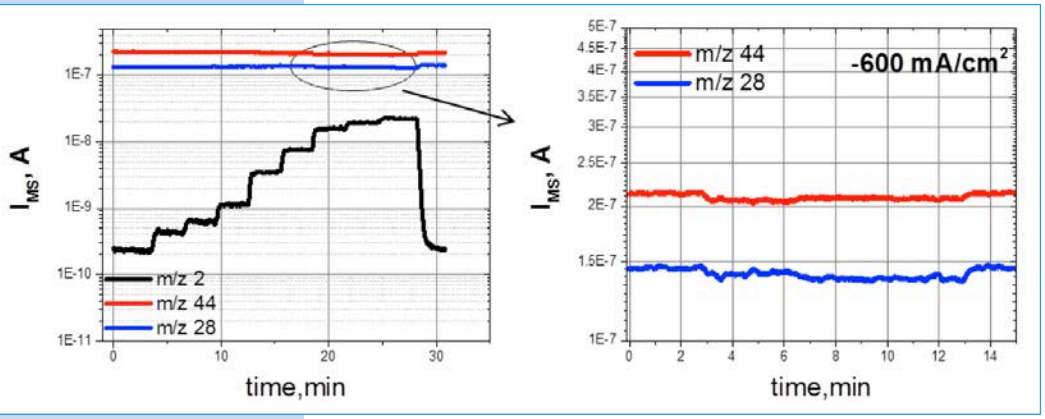

Electrochemical Cell Configuration for CO_2 Reduction in Gas Phase at Low Temperature

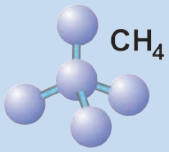

Alternative cell configurations

A buffer layer cell configuration was also used for CO_2 reduction in gas phase [6]. The polarization curves are shown in Figure 3 and the results are comparable with the available literature data [6].

With this cell configuration current densities >200 mA/cm² were achieved with reasonable overpotentials. The consumption of CO_2 (m/z 44) was observed by MS (Figure 4). CO and H_2 were the only products obtained in this configuration using Au mesh electrodes. The CO selectivity calculated from the mass spectrometer signal was ca. 35% at −400 mA/cm².

Currently, the buffer layer cell configuration is only a proof of concept, the cell stability being a major issue in this case. Therefore new stable layered cell configurations are needed.

With this in mind, bipolar membranes were tested. The alkaline side was used at the cathode. The polarisation curves are compared against the buffer layer cell configuration in Figure 3. Using this type of membrane high current densities were achieved, but with higher overpotentials (most probably due to the high membrane resistance, ca. 5 Ωcm²). The CO selectivity was 23% at −400 mA/cm².

Outlook

Various cell configurations for reduction of CO_2 in gas phase have been presented and their performances compared. For convenience, only Au mesh was used as cathode catalyst for CO_2 reduction to CO.

A membrane electrolyzer like configuration using CEM was shown to be unfavorable for CO_2 reduction, leading to H_2 evolution only. The same configuration using a commercially available AEM (Fumasep® AA 130) was not successful due to high membrane resistance and a loss of membrane stability. That said, we believe that this configuration can be improved by using different alkaline membranes.

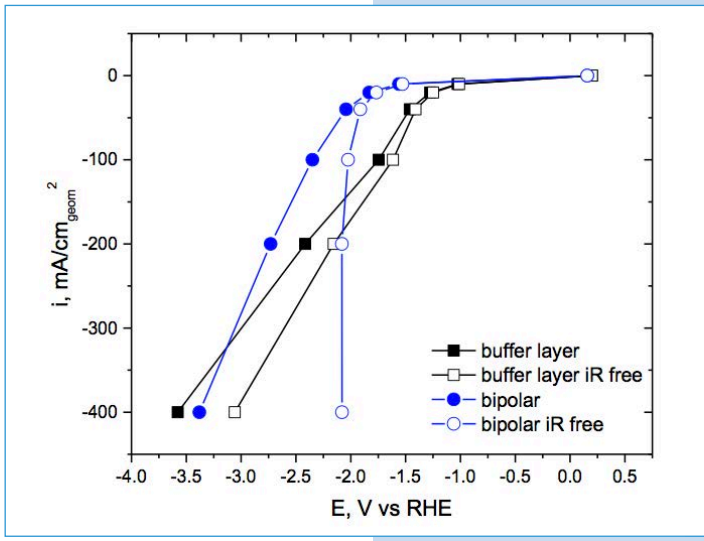

Figure 3:

Performances of alternatives cell configurations: buffer-layer cell vs bipolar membrane cell. The raw data (full symbols) are compared with the iR corrected data (empty symbols). Same conditions for anode and cathode as in Figure 1.

Alternative cell configurations were also tested and it was proved that by using a bipolar membrane system (alkaline side used at the cathode) high current densities are achieved and the cathode selectivity to CO is enhanced. This first promising result shows the feasibility of using such a system for electrochemical CO_2 conversion from gas phase. However at this point the energetic efficiency is low and optimisation work must be carried out in order to reduce the high cathode overpotentials.

Figure 4:

Ion current recorded by MS for m/z 44 and m/z 28 recorded in an electrochemical cell using a bipolar membrane (Fumasep® FBM) at different current densities and under cell operation at −400 mA/cm² proving the formation of CO.

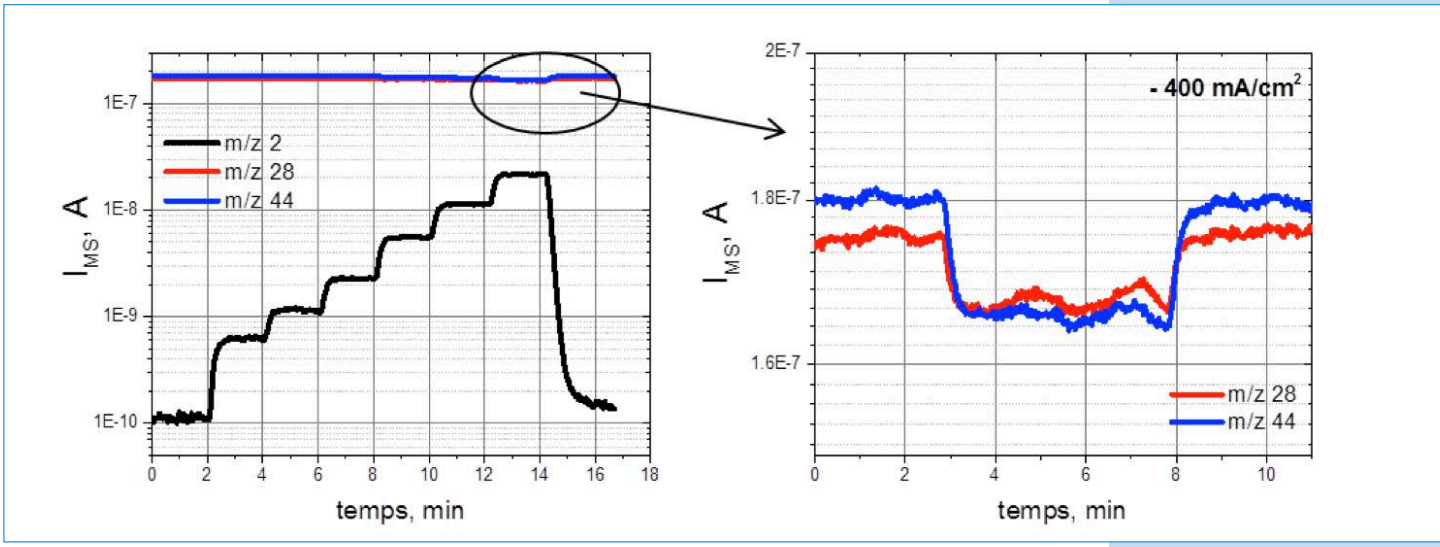

Assessment

Interactions of Storage Systems

Work Package Assessment of Storage Systems at a Glance

This work package can be considered as our ‹door towards the applications› since different application- and system-near projects are combined. Different aspects of energy storage systems are studied in techno-economic and environmental analyses with the focus Switzerland, as well as applied power to gas systems.
This work package is very important as it does and will be in the future the SCCER's platform combining projects in the highest technology readiness levels.

Within the work package a combined techno-economic and environmental assessment method for energy storage was developed and applied. Based on this method different energy storage technologies and applications were assessed. While energy storage is being proposed in the context of climate change mitigation, typically linked with renewable energy, past evaluations have mainly focused on the techno-economic aspects, and rarely differentiated the implications of the various applications and storage technologies. The results found within this work package thus help to inform the current storage debate about the integrated impacts of different technologies and applications from both, techno-economic and environmental perspectives. The work contributes to a better informed decision analysis of the role of energy storage technologies towards the energy transition in Switzerland.

Stationary storage technologies including pumped hydro storage (PHS), advanced adiabatic and isothermal compressed air energy storage (AA- and I-CAES), power-to-gas-to-power (P2G2P) and Li-ion battery (nickel cobalt aluminum / lithium titanate (NCA/LTO)) are compared in terms of levelised cost and life cycle greenhouse gas emissions (GHG). The scenarios include three applications representing frequency control, arbitrage and seasonal storage, as well as two system scales (1 and 100 MW).

We have also focused on particular storage technologies such as power-to-gas, power-to-heat, and residential batteries for various scenarios under the Swiss context. The role of energy storage for communities from a techno-economic, environmental and social perspective was also reviewed.

With the commissioning of Switzerland's first power-to-methane plant, Hochschule IET-HSR established itself as a competence centre for the practical application of power-to-gas on a system level. In the last two years, tests were performed on the plant and experience with practical aspects of power-to-gas was collected. Different sources of CO_2 were investigated and the product gas was used for mobility applications as well as for grid injection.

Illustration: AF-Studio / iStock

A Uniform Techno-Economic and Environmental Assessment for Electrical and Thermal Storage in Switzerland

Scope of project

A comprehensive methodology combining techno-economic analysis and life cycle assessment for storage technology assessment is demonstrated. While energy storage solutions are being proposed in the context of climate change mitigation, typically linked with renewable energy technologies, energy storage evaluations have mainly focused on the techno-economic implications of energy storage technologies. Therefore, the current debate has neglected so far the environmental impacts of the potential penetration of various energy storage technologies. The results created in the context of this work package help to inform the current storage debate about the integrated impacts of various technologies and therefore contribute to a more comprehensive decision analysis of the role of energy storage technologies towards the energy transition in Switzerland.
This report describes the work undertaken at the University of Geneva, at Paul Scherrer Institut and at Hochschule Luzern in 2016. All institutions contribute as a team to the development and assessment of different energy storage (ES) technolo-gies and applications.

Status of project and main scientific results of workgroups

Integrated economic and environmental assessment of energy storage technologies for different time scales

This ongoing study compares pumped hydroelectric energy storage (PHS), advanced adiabatic and isothermal compressed air energy storage (CAES), power-to-gas-to-power (P2G2P) and lithium-ion batteries for three different storage scenarios characterized by storage discharge time scale (TS) and for two different storage system scales. In particular, short-term (< 1 min), medium-term (4.5 hr) and long-term (seasonal) storage time scales are compared for systems with a power rating of 1 MW and 100 MW corresponding to distributed and bulk ES respectively.

The preliminary results (Figure 1) of the analysis show that (with the Swiss electricity consumption mix with an assumed price of 0.10 EUR/kWh) for the short time scale battery

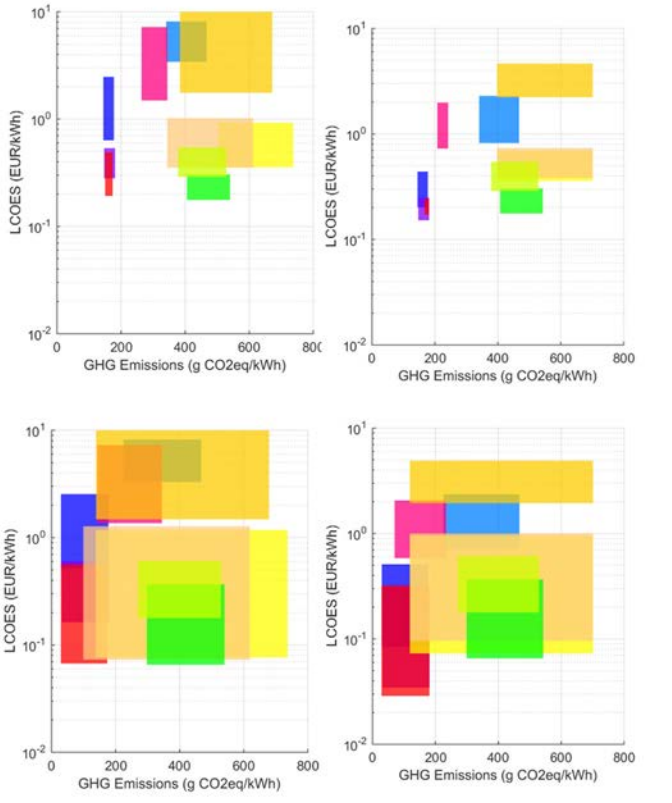

Figure 1:

Preliminary results: Integrated economic and environmental evaluation of electricity storage for different system sizes (1 MW, left, and 100 MW, right) and time scales (TS) considering technical factors including lifetime, efficiency, and cost (above), and technical factors as well as electricity price range and types (Swiss wind electricity and Swiss grid supply based on consumption mix) (below). GHG emissions are based on Life Cycle Assessment (LCA).

List of abbreviations

BESS	Battery Energy Storage System
CAES	Compressed Air Energy Storage
CAPEX	Capital Expenditure
CCU	CO_2 Capture and Utilization
CES	Community Energy Storage
DSO	Distribution System Operator
ES	Energy Storage
GHG	Greenhouse Gas
LCOES	Levelised Cost of Electricity
LVOES	Levelised Value of Electricity
LCA	Life Cycle Assessment
OPEX	Operational Expenditure
P2G	Power-to-Gas
P2G2P	Power-to-Gas-to-Power
P2H	Power-to-Hydrogen
P2M	Power-to-Methane
PHS	Pumped Hydroelectric Energy Storage
PV	Photovoltaics
PVCts	avoidance of curtailment
PVts	energy time shift
SNG	Synthetic Natural Gas
TS	Time Scale
T&D	Transmission and distribution grid.

Authors

D. Parra[1]
M.K. Patel[1]
X. Zhang[2]
C. Bauer[2]
A. Abdon[3]
J. Worlitschek[3]

[1] University of Geneva
[2] PSI
[3] HSLU

A Uniform Techno-Economic and Environmental Assessment for Electrical and Thermal Storage in Switzerland

technology is the most attractive option, whereas for medium time scale both PHS and CAES are more attractive due to comparable cost but lower emissions. The long time scale results show that PHS is more attractive than P2G2P due to significantly lower emissions in large scale system, and the preference between these two technologies for small scale systems is rather unclear, and depends on the relative weighting factor between LCOES and life cycle GHG emissions of the decision making. In the case of storing 100 % renewable electricity with low or zero marginal cost and low emissions associated with the electricity being stored, P2G2P gains significant attractiveness and may even be competitive with other technologies for medium and long time scales.

Integrated technoeconomic and environmental assessment of power-to-gas systems

Interest in power-to-gas (P2G) as an energy storage (and energy conversion) technology is increasing, since it allows to utilize the existing natural gas infrastructure as storage medium, which is supposed to reduce capital investments and facilitate its deployment. P2G systems using renewable electricity can also substitute fossil fuels used for heating and transport. In this study, both techno-economic and life cycle assessment (LCA) are applied to determine key performance indicators for P2G systems generating hydrogen or methane (synthetic natural gas – SNG) as main products. The proposed scenarios assume that P2G systems participate in the Swiss wholesale electricity market and include several value-adding services in addition to the generation of low fossil-carbon gas.

We find that none of the systems can compete economically with conventional gas production systems when only selling hydrogen and SNG. For P2G systems producing hydrogen, four other services such as heat and oxygen supply are needed to ensure the economic viability of a 1 MW power-to-hydrogen (P2H) system, while for SNG with CO_2 captured from the atmosphere there is no economic case yet. The CAPEX and OPEX contribute 28 % and 72 % of the levelised cost for the P2H system, while the CAPEX share increases to 48 % for P2M with CO_2 from the atmosphere (see Figure 2).

As for environmental performance, only the input of «clean» renewable electricity to electrolysis results in environmental benefits for P2G compared to conventional gas production. In particular, the electricity supply to electrolysis for hydrogen production, and the source of CO_2 in case of SNG dominate the environmental performance of P2G (see Figure 3).

Interdisciplinary review of energy storage for communities: challenges and perspectives

Given the increasing penetration of renewable energy technologies as distributed

Figure 2 (upper):

Levelised cost for different cost components (both CAPEX and OPEX) as a percentage of the total for a 1 MW P2H system and a 1 MW P2M system capturing CO_2 from the air.

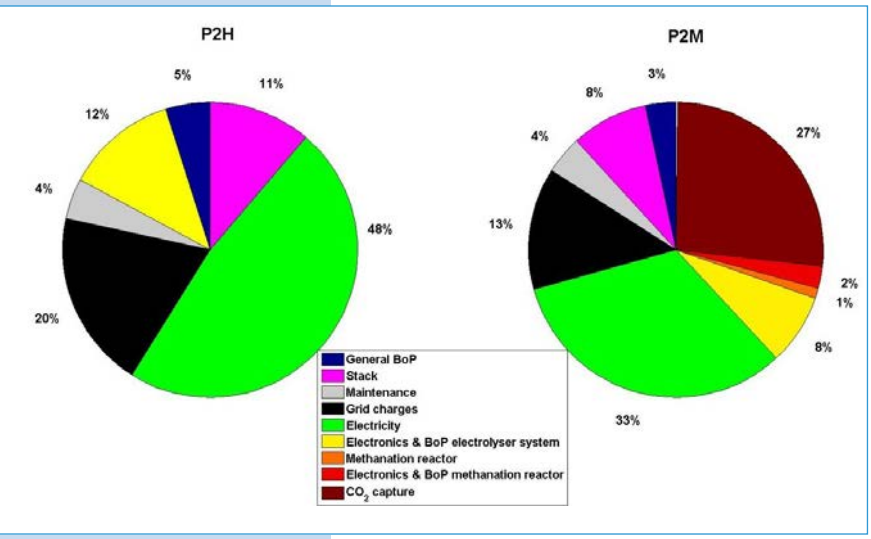

Figure 3 (lower):

LCIA results for Hydrogen Generation (PEM electrolyser: 1 MW) with different electricity supplies to the electrolyser.

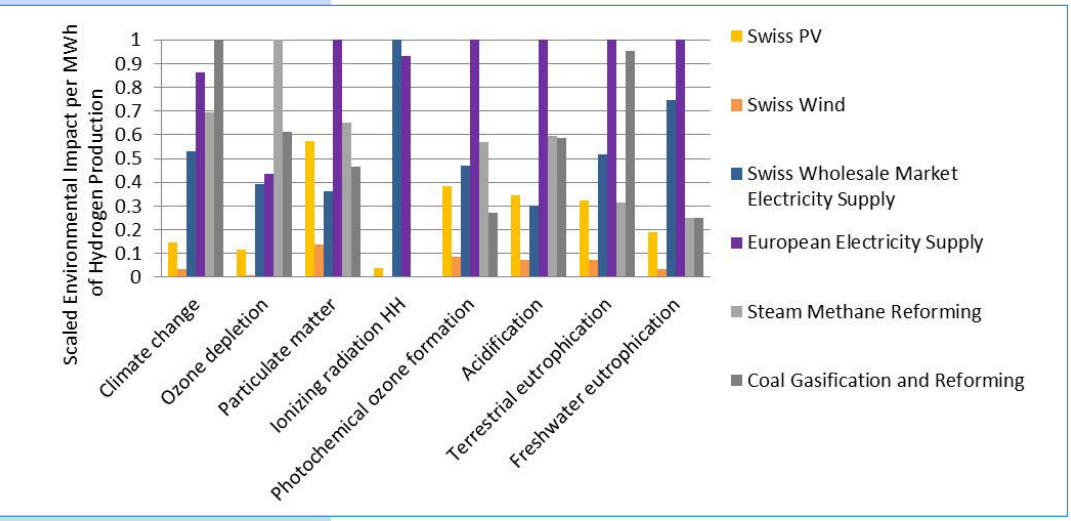

A Uniform Techno-Economic and Environmental Assessment for Electrical and Thermal Storage in Switzerland

generation embedded in the consumption centres, there is growing interest in energy storage systems located very close to consumers (see Figure 4).

These systems allow to increase the amount of renewable energy generation consumed locally, they provide opportunities for demand-side management and help to decarbonise the electricity, heating and transport sectors.

An interdisciplinary review of community energy storage (CES) with a focus on its potential role and challenges as a key element within the wider energy system was compiled. The discussion includes:

- the whole spectrum of applications and technologies with a strong emphasis on end user applications;
- techno-economic, environmental and social assessments of CES;
- an outlook on CES from the customer, utility company and policy-maker perspectives.

Currently, in general only traditional thermal storage with water tanks is economically viable.

However, CES is expected to offer new opportunities for the energy transition since the community scale introduces several advantages for electrochemical technologies such as batteries. Technical and economic benefits over energy storage in single dwellings are driven by enhanced performance due to less spiky community demand profile and economies of scale, respectively.

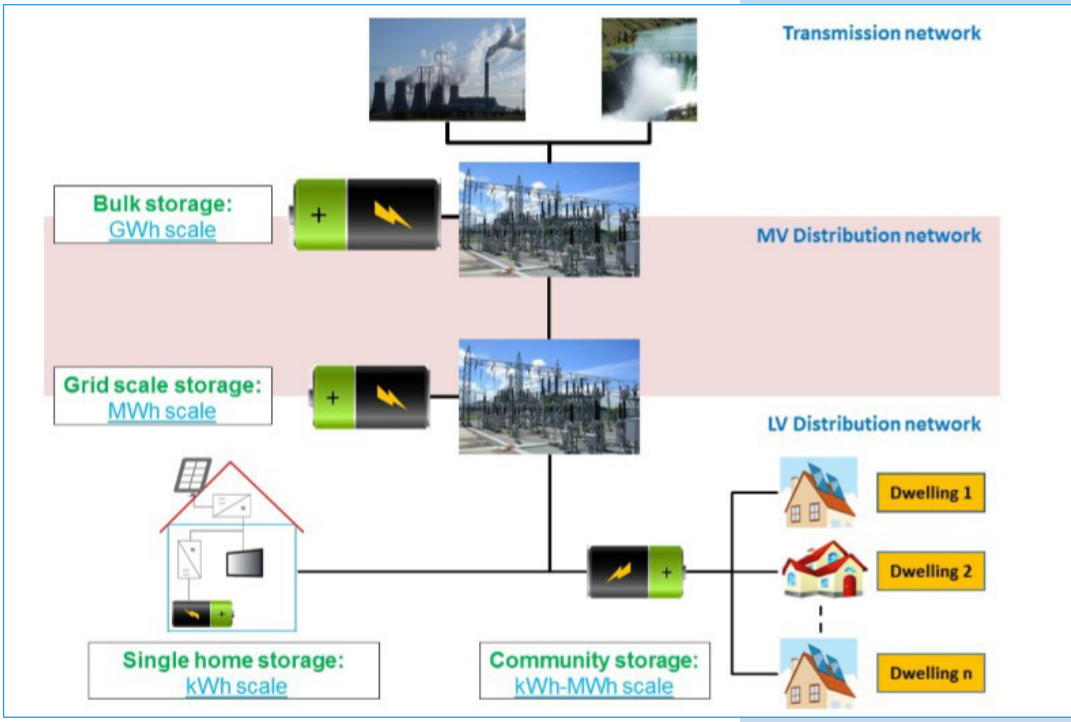

Figure 4:

Schematic representation of the scale of CES studied in this paper in comparison with single home and grid-scale ES.

In addition, CES brings new opportunities for citizen participation within communities and helps to increase awareness of energy consumption and environmental impacts.

Life cycle assessment of power-to-gas: approaches, system variations and their environmental implications

This recently published work provides a comprehensive environmental evaluation of P2G with insights into methodological aspects as well as various technology options. The study focuses on the following three aspects:

1) discussion of differences as consequence of the approach applied for CO_2 Capture and Utilization (CCU);
2) evaluation of technology variations including supply of electricity, alternative system processes (electrolysis technologies and CO_2 sources), product gases (hydrogen and methane), and comparison of these P2G systems with conventional technologies;

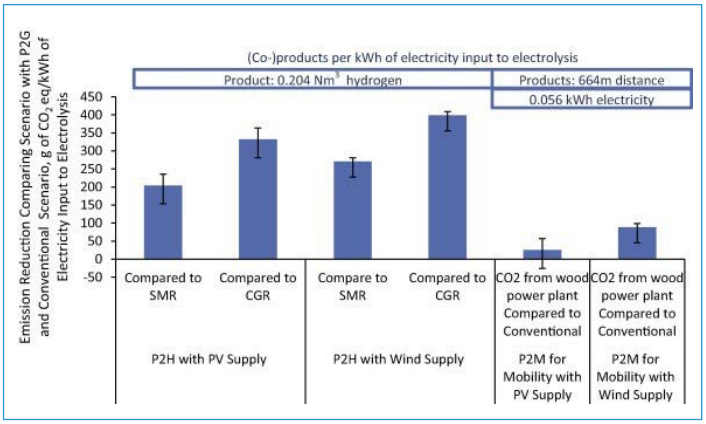

Figure 5:

Life cycle GHG emission reduction comparing P2H and P2M for mobility with conventional scenarios (fossil fuel pathways): with PV and wind electricity supply to 100 kW PEM electrolyzer; error bars indicate variability of GHG intensity of electricity from PV and wind in Switzerland. SMR = steam reforming, CGR = coal gasification and reforming.

A Uniform Techno-Economic and Environmental Assessment for Electrical and Thermal Storage in Switzerland

Scenario	A	B	C	D	E
Solution	BESS	BESS	BESS	curtailment	curtailment
Location	substation	substation	dwellings	dwellings	dwellings
Owner/Operated by	DSO	DSO	end user	DSO	end user
Electricity price	wholesale	wholesale	retail	wholesale	wholesale
Size/Control	optimised	fixed	optimised	dynamic	fixed
Service benefits	PVts and PVCt	PVts, PVCt and T&D	PVts and PVCt	T&D	T&D
Economic benefits	PVts and PVCt	PVts, PVCt and T&D	PVts and PVCt	T&D	-

Table 1:

Various scenarios and related implications for BESSs and curtailment strategies considered in this study regarding the location, stakeholder and control respectively.

PVts means energy time shift, PVCt means avoidance of curtailment, T&D denotes as transmission and distribution grid.

3) investigation of further environmental impacts of P2G in addition to the impact of global warming potential.

We found that in case of power to methane (P2M), system expansion provides more meaningful results than subdivision for CCU, since it reflects the added value of CO_2 utilization providing electricity or cement with low GHG intensity. The results of system variations show that P2G can, depending on electricity supply and CO_2 source, reduce GHG emission compared to conventional gas production technologies, and that P2H has higher potential of emission reduction than P2M.

Concerning other impact categories, P2H can have lower impacts than conventional hydrogen production, while P2M most often has higher impacts than using conventional natural gas (see Figure 5).

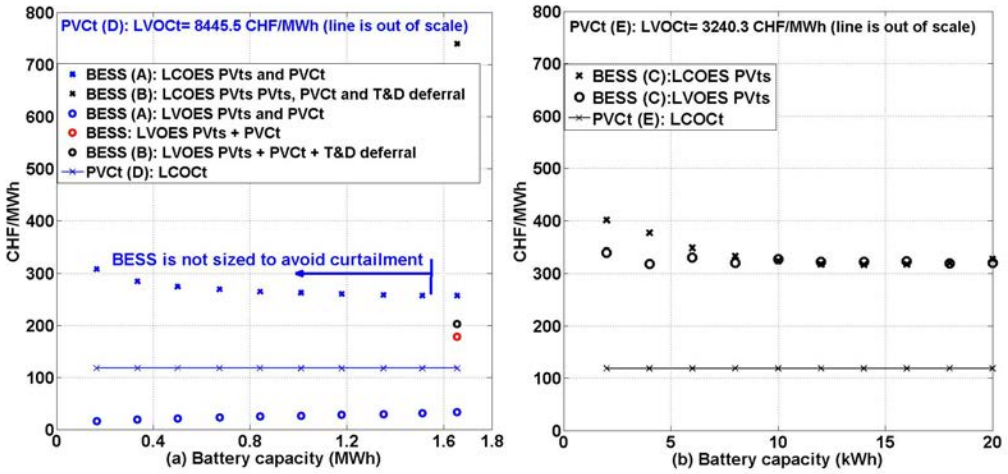

Figure 6:

Levelised cost, LCOES (CHF/kWh), and levelised value, LVOES (CHF/kWh), as a function of the battery capacity for:

(a) A BESS connected to the distribution transformer depending on whether the battery capacity is selected to avoid any PV curtailment (i.e. the BESS is only charged when surplus PV energy exceeds the nominal power of the transformer); or a BESS is charged whenever there is surplus PV energy. The capacity, without assuring that the PV reverse power, exceeds the nominal capacity of the transformer. For the latter, 10 battery capacities are tested, the largest having the same capacity as the first scenario.

(b) A residential BESS connected to the PV system of a dwelling. 10 battery capacities are tested up to 20 kWh. For PV curtailment, the levelised cost, LCOCt (CHF/kWh), and levelised value, LVOCt (CHF/kWh), are also given as straight lines. PVts means energy time shift, PVCt means avoidance of Curtailment, T&D denotes as transmission and distribution grid.

Techno-economic analysis of battery storage and curtailment in a distribution grid with high PV penetration

Global solar PV capacity continues growing and this technology is a central solution for the global energy transition based on both economic growth and decarbonisation. However, it is an intermittent source as well as mainly installed next to the consumption centres therefore requesting the redesign of distribution networks. In this study, battery storage and PV curtailment are compared for a residential area in Zurich (Switzerland) with large PV penetration. The techno-economic analysis focuses on the implications of the location (and related size) of battery storage (BESS) and the type of curtailment control (fixed versus dynamic) for the end user and distribution network operator. PV energy time-shift, the avoidance of PV curtailment and the upgrade deferral of the distribution transformer are the energy services provided by battery systems. All the various implications of the BESS' location and PV curtailment strategies are given in Table 1.

According to Figure 6, residential batteries offer more value for PV management than grid-scale solutions despite higher levelised cost but PV curtailment is the most cost-effective solution since only up to 3.2 % of total PV electricity generation in energy terms should be curtailed for avoiding the transformer upgrading. Shared ownership models for PV curtailment could much improve its acceptance among end users.

Practical Aspects of Power-to-Methane

Scope of project

Power-to-gas is a process for storing the energy from renewable electricity from summer to winter in the form of chemical energy as hydrogen or methane. The required technologies and the main infrastructures required for its implementation already exist today. New and improved technologies from research laboratories and start-up companies will appear on the market in the next few years. The Institute for Energy Technology (IET) has used the funds from the SCCER to build up a group of experts in the domain of the practical application of power-to-gas plants. One important activity is the commissioning and operating of the first power-to-methane plant in Switzerland as a pilot and demonstration plant.

Status of project and main scientific results of workgroups

Figure 1:

Aerial view of Switzerland's first Power-to-Methane plant operated in Rapperswil by IET-HSR.

1: PV installation,
2: CO_2 adsorption from the atmosphere using technology from Climeworks,
3: 25 kW Power-to-Gas-container provided by Etogas containing an electrolyser and methanation reactors,
4: Fuelling station,
5: Methane driven car provided by Audi and Amag.

Renewable electricity is provided by Elektrizitätswerke Jona-Rapperswil EWJR, published in [1] and [2].

In the SCCER's annual report 2015, the pilot and demonstration plant power-to-methane at IET-HSR (Figure 1) was presented together with its goals, industry partners, technical data and first results. 2016 was the second year of operation. Testing on the behaviour of the reactor under different conditions was continued and the grid injection was completed and commissioned.

A new CO_2-collector built by Climeworks and provided to IET-HSR by Audi was integrated. Fundamental considerations and the summary of learnings were published in the report of Friedl, Meier, Ruoss and Schmidlin «Thermodynamik von Power-to-Gas», published on the website of IET-HSR, 20 October 2016.

Complementary activities were continued: In addition to the 500 visitors mentioned in the annual report 2015, 230 more people visited the plant during 2016. The steering committee met in February and November. The exchange of experience continued in including further parties (Umweltarena, EPFL from Martigny) and meetings took place in April, June and September. The conference «Expertengespräche Power-to-Gas» was organised the fourth time, but unfortunately almost no participants from the French speaking part of Switzerland enrolled and the simultaneous translation into French was cancelled.

The year 2016 lead to new industry co-operations with KVA Linth, Hitachi Zosen Inova, Groupe e, Biogas Zürich and Nordur. Due to delays in commissioning and testing at the plant Hybridwerk Aarmatt built by Regio Energie Solothurn, no analysis of data could be performed nor published. A feasibility study of a large-scale power-to-methane

List of abbreviations

IET Institute for Energy Technology

Authors

Markus Friedl[1]
Boris Meier[1]
Elimar Frank[1]

[1] HSR

Practical Aspects of Power-to-Methane

References

[1] G. Benjaminsson, J. Benjaminsson, R. Boogh Rudberg, «Power-to-Gas – A technical review», Swedish Gas Technology Centre, SGC, Report 2013:284, 2013.

[2] S. Schmitz, «Schlussbericht Projekt Innovationsforum 'Power to Gas to Power'», Deutsches Brennstoff Institut Gas- und Umwelttechnik GmbH (DBI-Gut), 32, Nov. 22, 2013.

[3] E. Giglio, A. Lanzini, M. Santarelli, P. Leone, «Synthetic natural gas via integrated high temperature electrolysis and methanation». Journal of Energy Storage, Number 1, 22–37, May 2015.

installation at the waste incineration plant KVA Linth showed that power-to-methane is very close to profitability.

To our own judgement, large-scale application of power-to-methane has reached the following status in Switzerland. A large scale power-to-gas plant can be close to profitability under the condition that:

a) the electricity used is renewable and free from fees for the usage of the electricity grid;
b) the plant can operate in full load during more than 5'000 hours per year;
c) income can be generated from selling the gas as renewable and maybe «Swiss Made» for a premium price;
d) additional income is generated from providing a service to the electricity grid e.g. in the form of secondary balance energy.

Electricity is only free from fees for the usage of the electricity grid, if the power-to-gas plant is located on the same ground as the production of renewable electricity. The requirement of than 5'000 operating hours per year excludes PV installations as the only source of renewable electricity for a power-to-methane plant, because in Switzerland PV only reaches 1'000 full load hours.

Support of the investment e.g. by the pilot, demonstration and beacon programme of the Swiss Federal Office of Energy (SFOE) and other benefits like the recognition of the CO_2 used in the methanation when calculating the CO_2-emissions of an importer's fleet can make a power-to-gas installation profitable. In comparison to Germany, Switzerland offers favourable conditions for large-scale power-to-gas installations and several projects are being discussed by different parties. However, the uncertainties about future regulations and about energy prices (gas, renewable gas and electricity) are a problem for launching large-scale power-to-gas projects.

Our investigations have shown, that the cost of electricity (including fees for utilisation of the electricity grid if applicable) are the dominant cost factor and determine the business case. Furthermore, the emissions for the production of the electricity used are dominant when assessing the environmental impact of the gas produced in a power-to-gas plant, e.g. in a life cycle analysis.

Hence the future development on a system level has to go towards higher efficiencies, which at the moment is at 53% (upper heating value of gas produced divided by the electricity used). The efficiency of power-to-methane can be increased in using a high temperature electrolysis (solid oxide electrolyser cell = SOEC, [1–3] and www.helmeth.eu).

IET-HSR participates in the EU-funded project «Pentagon» (www.pentagon-project.eu), part of which is building a small-scale power-to-methane installation as a co-operation of IET-HSR and EPFL, where a SOEC is integrated. IET-HSR has done extensive modelling and calculations on the thermodynamics of this plant in order to be able to define the installation's layout early 2017.

ESI – Energy Systems Integration Platform

Scope of project

The Energy Systems Integration (ESI) Platform at the Paul Scherrer Institute (PSI) provides a basis for research and technology transfer activities for the SCCERs «Heat and Electricity Storage» (HaE) and «Biomass for Swiss Energy Future» (BIOSWEET). Main topics so far are power-to-gas processes and conversion of biomass.

Status of project and main scientific results of workgroups

Work in 2016 focussed on finishing the hardware infrastructure on the platform and on commissioning both the basic platform infrastructure (support structure for individual sub-systems, supply of media-gases, (cooling) water and electricity, safety system & controls) and the first sub-systems. In parallel, intensive interactions have started between the technology oriented sub-systems and the teams working on cross-cutting scientific topics such as catalysis research (synthesis and characterization), process diagnostics tools (sampling, analysis, process validation) and energy system modelling (energy scenarios, technology assessment, life cycle analysis).

Electrochemical systems

The polymer electrolyte membrane (PEM) based electrolyser and the connected gas cleaning system are now fully operational and can convert electric energy to dry, pure hydrogen and oxygen in 100 kW scale. In the first series of experiments, the system is characterized with respect to system efficiencies at various load points, dynamic system response (load ramps) and operational limits.

The two gas tanks for hydrogen and oxygen are prepared to be filled the first time in early 2017. With this sub-system, storage of even highly fluctuating electricity will be realised in pilot scale which subsequently could be used for mobility purposes (fuel cell cars) or for re-electrification, especially as positive balancing power service.

The fuel cell system on the ESI platform which will allow dynamic and highly efficient re-electrification of the stored hydrogen and (pure) oxygen without significant emissions is close to mechanical completion. Four pilot scale PEM fuel cell stacks will be installed and all necessary subsystems are already in place. Commissioning will start in spring 2017.

SNG production routes

Catalytic fluidised bed reaction systems are being used to on the ESI platform to convert hydrogen and carbon oxides to methane, i.e. synthetic natural gas, SNG. This way, hydrogen can not only be stored in dedicated gas tanks or as limited addition (< 2 %) to natural gas in the existing gas grid, but in unlimited amount. As source for the carbon oxides, biogas from anaerobic digestion or CO_2 separated from industrial flue gas are being investigated. Additionally, the conversion of (simulated) producer gas from biomass gasification to SNG is possible as well, both with and without hydrogen addition.

For the investigation of these synthesis processes, two plants have been built in conjunction with the ESI platform. The smaller one in 10 kW scale, referred to as *COSYMA*, is a fully automated, mobile system in a container which was commissioned successfully on the ESI platform and then transferred to a biogas plant in Zürich (in January 2017) in order to demonstrate direct methanation of real biogas in a 1000 h operation campaign.

A 160 kW pilot scale system, referred to as *GanyMeth*, will be used to investigate scale-up effects in these synthesis processes and to deliver realistic data for model validation. The main parts of *GanyMeth* were delivered in autumn 2016. The next steps are the mechanical and electrical completion, followed by the commissioning.

Hydrothermal gasification allows converting wet or liquid biomass (such as algae, sewage sludge, manure or residuals from food production) to methane / SNG. A fully automated, mobile system in a container is in operation on the ESI platform and was already used successfully for tests with food production residues

List of abbreviations

BIOSWEET	Biomass for Swiss Energy Future
CEDA	Coherent Energy Demonstrator Assessment
HaE	Heat and Electricity Storage
SCCER	Swiss Competence Center for Energy Research
PEM	Polymer Electrolyte Membrane
SNG	Synthetic Natural Gas

Author

P. Jansohn[1]
M. Hofer[1]
T. Schildhauer[1]

[1] PSI

ESI – Energy Systems Integration Platform

as well as for investigation of power-to-gas applications.

In the next phase 2017–2020, a scale-up of the technology to 100 kW scale is planned.

Integrated operation

Subsequently to the start-up of the individual sub-systems, integrated operation of several systems is prepared for 2017, e.g. combined electrolysis to convert electricity to hydrogen and its further conversion to SNG. The platform infrastructure has significant flexibility to accommodate additional technologies in the next phase 2017–2020.

One goal is to close the link between SNG production and storage in the gas grid on the one hand, and flexible re-electrification in combined heat and power (CHP) systems, on the other hand. For this, conversion technologies like micro gas turbines or internal combustion engines are being considered for complementation of the test infrastructure.

Outlook

Within joint activities of several SCCERs – coherent energy demonstrator assessment (CEDA) – intra-platform data handling procedures and data evaluation standards will be developed and applied for data generated at ESI.

Figure 1 :
The ESI installations at PSI.

Appendix

Photo: olaser / iStock

Conferences

- Expertengespräche «Power-to-Gas». 13.04.2016, Umwelt Arena Spreitenbach, HSR.
- 32nd PSI Electrochemistry Symposium, «Electrolytes: The Underestimated Player in Electrochemical Processes». 27.04.2016, PSI.
- SCCER Summer School 2016: Energy Storage in Batteries Materials, Systems, and Manufacturing, 11.–15.07.2016, Möschberg.
- 3rd Swiss Symposium Thermal Energy Storage, 22.01.2016, Luzern.
- 15th International Symposium on Hydrogen-Metal Systems, 07.08.2016, Interlaken.
- Swiss Mobility Days, 07.04.2016, Martigny.
- International Summer School on CO_2 Conversion: From Fundamentals towards Application, 9.08.–02.09.2016, Villars-sur-Ollon.

Presentations

Work Package «Heat – Thermal Energy Storage»

- S. Binder, S. Haussener, «Encapsulation Strategy for Metallic Phase Change Materials used for High Temperature Heat Storage». Material Science & Technology, November 2016, Salt Lake City, USA.
- D. Perraudin, S. Binder, E. Rezai, A. Ortona, S. Haussener, «High Temperature Heat Storage Material-Systems: Design, Stability, and Performance». SCCER Symposium, Oct. 2016, Luzern, Switzerland.
- D. Perraudin, S. Haussener, «Coupled Radiation Conduction Heat Transfer in Participating Macroporous Media». 8th Interpore Conference, May 2016, Cincinnati, USA.
- S. Binder, D. Perraudin, S. Haussener, «Phase Change Material Systems for High Temperature Heat Storage». Swiss Thermal Energy Storage Symposium, January, 2016, Luzern, Switzerland.
- P. Gantenbein, X. Daguent-Frick, M. Rommel, B. Fumey, R. Weber, K. Goonesekera, «Seasonal Solar Thermal Energy Absorption Storage with Aqueous Sodium Hydroxide Sorbent and Water Vapour Sorbate». Gleisdorf Solar 2016. 12. Internationale Konferenz für solares Heizen und Kühlen. June 8–10, 2016, Gleisdorf, Austria.
- M. Dudita, X. Daguenet-Frick, P. Gantenbein, «Seasonal Thermal Energy Storage with Aqueous Sodium Hydroxide – Experimental Methods for Increasing the Heat and Mass Transfer by Improving Surface Wetting». 11th ISES EUROSUN Conference, Oct. 11–14, 2016, Palma, Spain.
- A. Haselbacher, «Stromspeicherung über adiabatische Luftkompression Energiespeicher: Treiber oder Bremser der Energiewende?». Sessionsveranstaltung der Parlamentarischen Gruppe «Erneuerbare Energien», August 2016, Bern, Switzerland.
- S. Stroehle, A. Haselbacher, Z. Jovanovic, A. Steinfeld, «High-temperature thermochemical energy storage: Getting the most of it». AIChE Annual Meeting, 2016,San Francisco, CA, USA.
- A. Haselbacher, A. Steinfeld, «Die Rolle von Hochtemperatur-Wärmespeicherung». ESC Symposium on «Die Zukunft der Energiespeicher». Dec. 2016, ETH, Zürich, Switzerland.

Work Package «Batteries – Advanced Batteries and Battery Materials»

- M.V. Kovalenko, 18th International Meeting on Lithium Batteries, June 19–24, 2016, Chicago, USA.
- M.V. Kovalenko, Fall Meeting of the European Materials Research Society, Sept. 19–22, 2016, Warsaw, Poland.
- M.V. Kovalenko, 1st International Symposium on Magnesium Batteries (Mag-Batt), July 21–22, 2016, Blautal/Ulm, Germany.
- H. Yao, «Ionic liquids based on crown ether as electrolyte for batteries». SCCER WP1 meeting, Jan. 21, 2016, Fribourg, Switzerland.
- S. Maharajan, «Sn/C composite anode material for high energy batteries». SCCER WP1 meeting, Jan. 21, 2016, Fribourg, Switzerland.
- N. Herault, «TiO_2 nanocontainers and nanospheres as photocatalysts for photoelectrochemical water splitting». SCCER WP1 meeting, Jan. 21, 2016, Fribourg, Switzerland.
- S. Maharajan, «Sn/C composite anode material for high energy batteries». SCCER WP1 meeting, July 7, 2016, ETHZ, Zürich, Switzerland.
- N.H. Kwon, «Post Lithium batteries: Li-O_2 and Li-water battery. New Cathodes of Li-ion battery». SCCER WP1 meeting, July 7, 2016, ETHZ, Zürich, Switzerland.
- N.H. Kwon, «Preferred Orientation of Li^+ Diffusion in Nano-$LiMnPO_4$». Aug. 28 – Sept. 01, 2016, ECM-30, Basel, Switzerland.
- N. Herault, «TiO_2 nanocontainers and nanospheres as photocatalysts for photoelectrochemical water splitting: Structural modification». Aug. 28 – Sept. 01, 2016, ECM-30, Basel, Switzerland.
- N. Herault, «TiO_2 nanocontainers and nanospheres as photocatalysts for photoelectrochemical water splitting: Structural modification». SCS Fall Meeting, Sept. 15, 2016, Zurich, Switzerland.
- S. Maharajan, «Sn/C composite anode material for high energy batteries». SCCER WP1 meeting, Oct. 19, 2016, ETHZ, Switzerland.
- N.H. Kwon, «Nanomaterials and nanostructured composites of cathode for lithium ion batteries». Japanese-Swiss Workshop on «Hydrogen Technologies and Energy Storage», Oct. 3 – 6, 2016, Tokyo, Japan.
- S. Maharajan, «Running out of fuel!! Find a socket.» 4th Symposium of SCCER Hae, Science slam, Oct. 24, 2016, Lucerne, Switzerland.

Presentations

- N.H. Kwon, «Nanomaterials and nanostructured composites of cathode for lithium ion batteries». Metrohm user meeting, Oct. 28, 2016, Zofingen, Switzerland.
- N.H. Kwon, «Rechargeable Li-air batteries». Metrohm user meeting, Oct. 28, 2016, Zofingen, Switzerland.

Work Package «Hydrogen – Production and Storage»

- H.H. Girault, V. Amstutz, A. Battistel, A.N. Colli, C.R. Dennison, P.E. Peljo, H. Vrubel, «Redox electrocatalysis and indirect water electrolysis for charging electric vehicles». 67th Annual Meeting of the International Society of Electrochemistry, Aug. 21–26, 2016, The Hague, The Netherlands.
- V. Amstutz, H. Vrubel, F. Gumy, C. Dennison, P. Peljo and H.H. Girault, «Demonstration of the synergies between hydrogen generation and a flow battery». International Flow Battery Forum, June 07–09, 2016, Karlsruhe, Germany.
- C.R. Dennison, A. Battistel, P. Peljo, H. Vrubel, V. Amstutz, H.H. Girault, «Solid-phase charge storage in redox mediated flow batteries». International Flow Battery Forum, June 07–09, 2016, Karlsruhe, Germany.
- V. Amstutz, H. Vrubel, A. Battistel, F. Gumy, C. Dennison, P. Peljo and H.H. Girault, «Indirect water electrolysis: principle and applications». 67th Annual Meeting of the International Society of Electrochemistry, Aug. 21–26, 2016, The Hague, The Netherlands (Presentation).
- H.H. Girault, «Grid-to-Mobility». SCCER Hae 4th Symposium, Oct 24, 2016, Lucerne, Switzerland.
- V. Amstutz, H.H. Girault, «Redox flow et production d'hydrogène». Atelier Batteries Redox Flow, Dec. 01, 2016, Paris, France.
- H.H. Girault, «From grid to mobility. The challenge of re-charging electric vehicles». Lancaster University Christmas Conference 2016, Dec. 20, 2016, Lancaster, UK.

Work Package «Synthetic Fuels – Development of Advanced Catalysts»

- K. Larmier, S. Tada, E. Lam, A. Comas-Vives, C. Copéret, «Supported Cu nanoparticles for the hydrogenation of CO_2 to Methanol». SCCER CO_2 conversion meeting, January 28–29, 2016, Les Diablerets, Switzerland.
- A. Comas Vives, «The Role of the Interface on the CO_2 Activation on Oxide-Supported Nanoparticles: Insights from Ab Initio Calculations». SCCER CO_2 conversion meeting, January 28–29, 2016, Les Diablerets, Switzerland.
- H.-J. Liu, «Synthesis of Supported Copper Nanoparticles for Electro-Reduction of CO_2». SCCER CO_2 conversion meeting, January 28–29, 2016, Villars, Switzerland.
- K. Larmier, «Improving CO_x conversion Catalysts by Controlling Surface Interactions via a Molecular Approach». CO_2 Catalysis Conference, Apr. 16, 2016, Albufeira, Portugal.
- C. Copéret, «The role of the interface in supported metal catalysis: Water Gas Shift, Dry Reforming and CO_2 hydrogenation, CO_2 conversion». From Fundamentals towards Applications Meeting, Aug. 29 – Sept. 2, 2016, Villars, Switzerland
- P.J. Dyson, «Enhancing sustainable catalytic processes with ionic liquids». Swiss Chemical Society Spring Meeting, April 2016, University of Zürich, Zürich, Switzerland.
- P.J. Dyson, «Ionic liquids: properties and applications in CO_2 capture and valorization». International Summer School on CO_2 Conversion, Aug. 2016, Villars-sur-Ollen, Switzerland.
- P.J. Dyson, «Enhancing sustainable catalytic processes with ionic liquids». 18th E. Hála Lecture at the Institute of Chemical Process Fundamentals, Sept. 2016, Czech Academy of Sciences, Prague.
- P.J. Dyson, «From Swiss alpine forests to Zika control: the role of green chemistry». Oct. 2016, University of York, UK.
- F.D. Bobbink, «Synthesis of Cross-Linked Ionic Polymers for DMC production». SCCER Meeting, Jan. 2016, Les Diablerets, Switzerland.
- F.D. Bobbink, «Catalysts for converting CO_2». «My Thesis in 180 Seconds-MT180» competition, EPFL Rolex Center, October 2015, Lausanne, Switzerland.
- F.D. Bobbink, P.J. Dyson, «Synthesis of imidazolium-based cross-linked ionic polymers and their application in CO_2 fixation». Swiss Snow Symposium, Jan. 2016, Saas Fee, Switzerland.
- F.D. Bobbink, A. Redondo, P.J. Dyson, «Synthesis and characterization of novel imidazolium-based ionic poly(styrenes) and their application as supports for Pd nanoparticles». SCS Fall Meeting, Sept. 15, 2016 University of Zurich, Zürich, Switzerland.

Presentations

- A. Gopakumar, P.J. Dyson, «Earth-abundant metal oxide nanoparticles as recyclable catalysts for N-methylation and N-formylation reactions using CO_2 as C1 source in mild conditions». SCS Fall Meeting, Sept. 15, 2016 University of Zurich, Zürich, Switzerland.
- D. Vasilyev, P.J. Dyson, «Triazolium ionic liquids for electrochemical reduction of CO_2». SCS Fall Meeting, Sept. 15, 2016 University of Zurich, Zürich, Switzerland.
- M. Hulla, P.J. Dyson, «CO_2 based N-formylation of amines catalyzed by Fluoride and Hydroxide ions». SCS Fall Meeting, Sept. 15, 2016, University of Zurich, Zürich, Switzerland.
- T.J. Schmidt, «Elektrochemie: Lösungen für die Langzeitspeicherung». Symposium «Die Zukunft der Energiespeicher – Trends und offene Fragen». Dec. 14, 2016, Zürich, Switzerland.
- T.J. Schmidt, «Oxygen Evolution Electrocatalysis on Perovskites». University of Birmingham School of Chemistry, Dec 02, 2016, Birmingham, UK.
- T.J. Schmidt, «Hydrogen Production by Electrolysis: Recent Progress on Closing Gaps». UK Energy Storage Conference 2016, Nov. 30 – Dec. 02, 2016, Birmingham, UK.
- T.J. Schmidt, «Technologien für Dezentrale Speicherlösungen – Eine Übersicht. Energiespeichersysteme – Dezentrale Batteriespeicherlösungen». Hightech Zentrum Aarau AG, Oct. 18, 2016, Brugg, Switzerland.
- T.J. Schmidt, «Materials for PEM Water Electrolysis». EMRS Fall Meeting, Sept. 19–22, 2016, Warsaw, Poland.
- T.J. Schmidt, «Oxygen Evolution on Nano-Sized Non-Noble Metal Catalysts». International Conference on Advances in Semiconductors and Catalysts for Photoelectrochemical Fuel Production, Sept. 05–06, 2016, Berlin, Germany.
- T.J. Schmidt, «Water Electrolysis: Gaps for New Innovations». Workshop Breakthrough Innovations, Aug. 23, 2016, Park InnovAare, Villigen, Switzerland.
- T.J. Schmidt, «Water Electrolysis: From Materials to Systems». Seminar at DTU Physics, Lyngby, Aug. 18, 2016, Denmark.
- T.J. Schmidt, «Power-to-Hydrogen-to-Power». Open Workshop Energy Storage in the Electricity Grid, March 23, 2016, Dublin, Ireland.
- T.J. Schmidt, «Insights into Oxygen Evolution Electrocatalysis on Perovskites». 80. Jahrestagung der DPG und DPG Frühjahrstagung 2016, March 06–11, 2016, Regensburg, Germany.
- T.J. Schmidt, «Technische Optionen der Energiespeicherung». Technische Gesellschaft Zürich, March 07, 2016, Zürich, Switzerland.
- T.J. Schmidt, «Development of Advanced Water Splitting Electrocatalysts». NCCR Marvel Workshop, March 3, 2016, Villigen, Switzerland.
- T.J. Schmidt, «Oxygen Evolution on Non-Noble Metal Electrocatalysts». Workshop Munich ECS Student Chapter, Feb. 15, 2016, Munich, Germany.
- T.J. Schmidt, «H_2 Production by Electrolysis». Workshop on Electrolysis, Aalborg University, Feb. 9, 2016, Copenhagen, Denmark.

Work Package «Assessment – Interactions of Storage Systems»

- M.J. Friedl, «Die zukünftige Rolle von Power-to-Gas in einer nachhaltigen Energieversorgung der Schweiz». Veranstaltung der Parlamentarischen Gruppe Erneuerbare Energien und aee Suisse (Agentur Erneuerbare Energie), March 16, 2016, Switzerland.
- M.J. Friedl, «Power-to-Gas: Speicherung von überschüssigem Strom als synthetisches Gas». Veranstaltung der Parlamentarischen Gruppe Erneuerbare Energien und aee Suisse (Agentur Erneuerbare Energie), March 16, 2016, Bern, Switzerland.
- M.J. Friedl, «Power-to-Gas will save us all». Science Slam at the SCCER Heat and Electricity Storage 4th Symposium, Oct. 24, 2016, Horw, Switzerland.
- M.J. Friedl, «Power-to-Gas – Etat de la recherche». Séminaire 2016 des dirigeants des Gaziers Romands, February 3, 2016, Glion, Switzerland.
- M.J. Friedl, «Power-to-Gas-Technologien: aktueller Stand und Herausforderungen». Erdgastagung 2016, March 11, 2016, Kantonsratssaal St.Gallen, Switzerland.
- E. Frank, «Power-to-Gas plants in Switzerland – operational experiences». OTTI Conference on Power-to-Gas and Power-to-X for Europe's Energy Transition, March 16, 2016, Düsseldorf, Germany.
- B. Meier, «Hybridwerk Aarmatt: Die Energiezukunft wissenschaftlich begleitet». FOGA Forschungstag, June 6, 2016, Zürich, Switzerland.

Presentations

- B. Meier, «Power-to-gas: Speicherung von erneuerbarer Energie als Gas». Bau und Energie Messe, Dec. 10, 2016, Bern, Switzerland.
- P. Schuetz, D. Gwerder, L. Gasser, L. Fischer, B. Wellig, J. Worlitschek, 10th International conference of renewable energy storage, 2016, Düsseldorf, Germany.
- A. Abdon, X. Zhang, D. Parra, M. K. Patel, C. Bauer, J. Worlitschek, «Techno-economic and environmental assessment of energy storage technologies for different storage time scales». 2016, 10th International Renewable Energy Storage Conference (IRES 2016).
- C. Bauer, X. Zhang, C. Mutel, «Life Cycle Assessment of Energy Storage: A Case Study for Power-to-Gas». LCA XV, Oct. 6–8, 2016, Vancouver, Canada.
- X, Zhang, C. Bauer, «Life Cycle Assessment of Electricity Storage Technologies for Different Discharge Durations and Scales». 22nd SETAC Europe LCA Case Study Symposium, Sep. 20–22, 2016, Montpellier, France.
- A. Abdon, X. Zhang, D. Parra, M. K. Patel, C. Bauer, J. Worlitschek, «Techno-Economic and Environmental Assessment of Energy Storage Technologies for Different Storage Time Scales». 10th International Renewable Energy Storage Conference (IRES), 2016, Düsseldorf, Germany.
- S. Maranda, F. Eckl P. Schütz, L. Fischer, J. Worlitschek, «Quasi-stationary modeling of melting and solidification inside a latent heat storage system». 10th International Renewable Energy Storage Conference (IRES), 2016, Düsseldorf, Germany.
- P. Schütz, D. Gwerder, L. Gasser, L. Fischer, B. Wellig, J. Worlitschek, «Improve flexibility for heat pumps in smart-grids by the integration of a thermal storage system». 10th International Renewable Energy Storage Conference (IRES), 2016, Düsseldorf, Germany.
- A. Abdon, M. von Atzigen, A. Stamatiou, J. Worlitschek, «Techno-Economic Evaluation of an electro-thermal Energy Storage Concept in the Electricity Trading Market». 10th International Renewable Energy Storage Conference (IRES), 2016, Düsseldorf, Germany.

Publications

Work Package «Heat – Thermal Energy Storage»

- L. Geissbühler, M. Kolman, G. Zanganeh, A. Haselbacher, A. Steinfeld, Analysis of industrial-scale high temperature combined sensible/latent thermal energy storage. *Applied Thermal Engineering* **101**, 657–668, 2016.
- S. Ströhle, A. Haselbacher, Z.R. Jovanovic, A. Steinfeld, «The Effect of the Gas-Solid Contacting Pattern in a High Temperature Thermochemical Energy Storage on the Performance of a Concentrated Solar Power Plant». *Energy & Environmental Science* **9,** 1375–1389, 2016.
- S.A. Zavattoni, L. Geissbühler, M.C. Barbato, G. Zanganeh, A. Haselbacher, A. Steinfeld, «High Temperature Thermocline TES Combining Sensible and Latent Heat – CFD Modeling and Experimental Validation». *SolarPACES*, 2016.
- E. Rezaei, S. Haussener, S. Gianella, A. Ortona, «Early-stage oxidation behavior at high temperatures of SiSiC cellular architectures in a porous burner». *Ceramics International* **42**, 16255–16261, 2016.

Work Package «Batteries – Advanced Batteries and Battery Materials»

- S.-L. Abram, J.-P. Brog, P.S. Brunetto, A. Crochet, J. Gagnon, N.H. Kwon, S. Maharajan, M. Priebe, K.M. Fromm, «Going Nano for batteries and drug delivery». *Chimia* **70**, 661, 2016.
- N.H. Kwon, H. Yin, T. Vavrova, J.H-W. Lim, U. Steiner, B. Grobéty, K.M. Fromm, «Nanoparticle shapes of $LiMnPO_4$, Li^+ diffusion orientation and diffusion coefficients for high volumetric energy Li^+ ion cathodes». *J. Power Sources*, accepted for publication.
- N.H. Kwon, S. Maharajan, K.M. Fromm, «Sn/C composite anode materials for high energy lithium/sodium ion batteries». *Acta Crystallographica Sec. A: Foundations and Advances* **72,** (a1):s286, 2016.
- L.O. Vogt, C. Villevieille, «Understanding the complex reaction mechanisms of $FeSn_2$ and $CoSn_2$ negative electrode for Na-ion batteries». *Journal of Materials Chemistry A*, 2016.
- C. Marino, T. Block, R. Pöttgen, C. Villevieille, «$CuSbS_2$ as negative electrode material for sodium ion batteries». *Journal of Power Sources*, 2016.
- L. Vogt, C. Villevieille, «$MnSn_2$ negative electrode for Na-ion batteries: a conversion-based reaction dissected». *Journal of Materials Chemistry A*, **4**, 19116, 2016.
- L. Vogt, C. Villevieille, $FeSn_2$ and $CoSn_2$ as promising electrode materials for Na-ion batteries. *Journal of Electrochemical Society*, 2016, 163, A1306.
- P. Kitschke, M. Walter, T. Rueffer, A. Seifert, F. Speck, T. Seyller, S. Spange, H. Lang, A.A. Auer, M. Kovalenko, M. Mehring, «Porous Ge@C materials via Twin polymerization of germanium(II) salicyl alcoholates for Li-ion batteries». *J. Mater. Chem. A*, **4**, 2705–2719, 2016.
- P. Kitschke, M. Walter, T. Rueffer, H. Lang, M. Kovalenko, M. Mehring, «From molecular germanates to microporous Ge@C via twin polymerization». *Dalton Trans.* **45**, 5741–5751, 2016.
- M. Walter, S. Doswald, M. Kovalenko, «Inexpensive Colloidal SnSb Nanoalloys as Efficient Anode Materials for Lithium- and Sodium-Ion Batteries». *J. Mater. Chem. A*, **4**, 7053–7059, 2016.

Work Package «Hydrogen – Production and Storage»

- P. Peljo, H. Vrubel, V. Amstutz, J. Pandard, J. Morgado, A. Santasalo-Aarnio, D. Lloyd, F. Gumy, C.R. Dennison, K.E. Toghill, H.H. Girault, «All-Vanadium dual circuit redox flow battery for renewable hydrogen generation and desulfurization». *Green Chem.* **18**, 1785–1797, 2016.
- M. Montandon-Clerc, A. Dalebrook, G. Laurenczy, «Quantitative aqueous phase formic acid dehydrogenation using iron(II) based catalysts». *J. Catal.* **343**, 62, 2016.
- C. Fink, S. Katsyuba, G. Laurenczy, «Calorimetric and spectroscopic studies on solvation energetics for H_2 storage in the CO_2/HCOOH system». *Phys. Chem. Chem. Phys.* **18**, 10764, 2016.
- C. Fink, G. Laurenczy, «CO_2 as a hydrogen vector – transition metal diamine catalysts for selective HCOOH dehydrogenation». *Dalton Trans.* **46**, 1670, 2017.

Publications

Work Package «Synthetic Fuels – Development of Advanced Catalysts»

- E. Oakton, G. Siddiqi, A. Fedorov, C. Christophe, «Tungsten oxide by non-hydrolytic sol-gel: Effect of molecular precursor on morphology, phase and photocatalytic performance». *New Journal of Chemistry* **1**, 40, 217—222, 2016.
- A. Comas-Vives, K. Furman, D. Gajan, C.M. Akatay, A. Lesage, F.H. Ribeiro, C. Copéret, «Predictive morphology, stoichiometry and structure of surface species in supported Ru nanoparticles under H_2 and CO atmospheres from combined experimental and DFT studies». *Physical Chemistry Chemical Physics* **3**, 18, 1969–1979, 2016.
- E. Oakton, J. Tillier, G. Siddiqi, Z. Mickovic, O. Sereda, A. Fedorov, C. Copéret, «Structural differences between Sb- and Nb-doped tin oxides and consequences for electrical conductivity». *New Journal of Chemistry* **3**, 40, 2655–2660, 2016.
- M.-C. Silaghi, A. Comas-Vives, C. Copéret, «CO_2 Activation on Ni/γ-Al_2O_3 Catalysts by First-Principles Calculations: From Ideal Surfaces to Supported Nanoparticles». *ACS Catalysis* **7** ,6, 4501–4505, 2016.
- D. Baudouin, T. Margossian, U. Rodemerck, P.B. Webb, L. Veyre, F. Krumeich, J.-P. Candy, C. Thieuleux, C. Copéret, «Origin of the Improved Performance in Lanthanum-doped Silica-supported Ni Catalysts». *Chemcatchem*, 2016.
- C. Copéret, D.P. Estes, K. Larmier, K. Searles, «Isolated Surface Hydrides: Formation, Structure, and Reactivity». *Chemical Reviews* **15**, 116, 8463–8505, 2016.
- K. Larmier, S. Tada, A. Comas-Vives, C. Copéret, «Surface Sites in Cu-Nanoparticles: Chemical Reactivity or Microscopy?». *Journal of Physical Chemistry, Letters* **7**, 16, 3259–3263,2016
- T. Margossian, S.P. Culver, K. Larmier, F. Zhu, R.L. Brutchey, C. Copéret, «Composition-dependent surface chemistry of colloidal Ba: $XSr_{1-x}TiO_3$ perovskite nanocrystals». *Chemical Communications: ChemComm* **95**, 52,13791–13794, 2016.
- L. Foppa, C. Copéret, A. Comas-Vives. «Increased Back-Bonding Explains Step-Edge Reactivity and Particle Size Effect for CO Activation on Ru Nanoparticles». *Journal of the American Chemical Society* **51**, 138, 16655–1666, 20168.
- A.V. Rudnev, U.E. Zhumaev, A. Kuzume, S. Vesztergom, J. Furrer, P. Broekmann, T. Wandlowski, «The promoting effect of water on the electroreduction of CO_2 in acetonitrile». *Electrochim. Acta* **189,** 38–44, 2016.
- A. Dutta, M. Rahaman, N.C. Luedi, M. Mohos, P. Broekmann, «Morphology Matters: Tuning the Product Distribution of CO_2 Electroreduction on Oxide-Derived Cu Foam Catalysts». *ACS Catal.* **6,** 3804–3814, 2016.
- S. Das, F.D. Bobbink, S. Bulut, M. Soudani, P.J. Dyson, «Thiazolium carbene catalysts for the fixation of CO_2 onto amines». *Chem. Commun.* **52**, 2497 (2016).
- M. Hulla, F.D. Bobbink, S. Das, P.J. Dyson, «Carbon Dioxide Based N-Formylation of Amines Catalyzed by Fluoride and Hydroxide Anions». *ChemCatChem.* **8**, 3338–3342, 2016.
- F.D. Bobbink, Z. Fei, R. Scopelliti, S. Das, P.J. Dyson, «Functionalized Ionic (Poly)Styrenes and their Application as Catalysts in the Cycloaddition of CO_2 to Epoxides». *Helv. Chim. Acta.* **99**, 821–829, 2016.
- F.D. Bobbink, A.P. Van Muyden, A. Gopakumar, Z. Fei, P.J. Dyson, «Design of ionic polymer catalysts for the synthesis of carbonates from CO_2 and Epoxides». *Chempluschem.* **81**, 1–9, 2016.
- F.D. Bobbink, W. Gruszka, M. Hulla, S. Das, P.J. Dyson, «Synthesis of cyclic carbonates from diols and CO_2 catalyzed by carbenes». *Chem. Commun.* **52**, 71, 10787–10790, 2016.
- G.P.S. Lau, M. Schreier, D. Vasilyev, R. Scopelliti, M. Grätzel, P.J. Dyson, «New Insights into the Role of Imidazolium-Based Promoters for the Electroreduction of CO_2 on a Silver Electrode». *J. Am. Chem. Soc.* **138,** 25, 7820–7823, 2016.
- F.L. Formal, N. Guijarro, W.S. Boureé, A. Gopakumar, M.S. Prévot, A. Daubry, L. Lombardo, C. Sornay, J. Voit, A. Magrez, P.J. Dyson, K. Sivula, «Formation of Efficient Water Oxidation Electrocatalyst on Gibeon Meteorite and Stainless Steel Electrodes». *Energy Environ. Sci.* **9**, 3448, 2016.
- J. Herranz, J. Durst, E. Fabbri, A. Pătru, X. Cheng, A. Permyakova, T.J. Schmidt, «Interfacial Effects on the Catalysis of the Hydrogen Evolution, Oxygen Evolution and CO_2-Reduction Reactions for (co-)Electrolyzer Development». *Nano Energy* **29**, 4–28,2016, doi: 10.1016/j.nanoen.2016.01.027.
- O. Nibel, T.J. Schmidt, L. Gubler, «Bi-Functional Ion-Conducting Polymer Electrolyte for the Vanadium Redox Flow Battery with High Selectivit». *J. Electrochem. Soc.* **163**, A2563–A2570, 2016, doi: 10.1169/2.0441613.jes.

Publications

- D.F. Abbott, D. Lebedev, K. Waltar, M. Povia, M. Nachtegaal, E. Fabbri, C. Coperet, T.J. Schmidt, «Iridium Oxide for the Oxygen Evolution Reaction: Correlation between Particle Size, Morphology and the Surface Hydroxo Layer from Operando XAS». *Chem. Mater.* **28**, 6591–6604, 2016, doi: 10.1021/acs.chemmater.6b02625.
- S.M. Taylor, A. Pătru, D. Streich, M. El Kazzi, E. Fabbri, T.J. Schmidt, «Vanadium (V) Reduction Reaction on Modified Glassy Carbon Electrodes – Role of Oxygen Functionalities and Microstructure». *Carbon* **109**, 472–478, 2016, doi: 10.1016/j.carbon.2016.08.044.
- J. Tillier, T. Binninger, M. Garganourakis, A. Pătru, E. Fabbri, T.J. Schmidt, O. Sereda, «Electrochemical Flow-Cell Setup for In Situ X-Ray Investigations. II. Cell for SAXS on a Multi-Purpose Laboratory Diffractometer». *J. Electrochem. Soc.* **163**, H913–H920, 2016, doi: 10.1149/2.0211610jes.
- T. Binninger, E. Fabbri, A. Pătru, M. Garganourakis, J. Han, D.F. Abbott, O. Sereda, R. Kötz, A. Menzel, M. Nachtegaal, T.J. Schmidt, «Electrochemical Flow-Cell Setup for In Situ X-Ray Investigations. I. Cell for SAXS and XAS at Synchroton Facilities». *J. Electrochem. Soc.* **163**, H906–H912, 2016, doi: 10.1149/2.0201610jes.
- M. Suermann, T.J. Schmidt, F. Buechi, «Cell Performance Determining Parameters in High-Pressure Water Electrolysis». *Electrochim. Acta* **211**, 989–997, 2016, doi: 10.1016/j.electacta.2016.06.120.
- A. Albert, T. Lochner, T.J. Schmidt, L. Gubler, «Stability and Degradation Mechanisms of Radiation-Grafted Polymer Electrolyte Membranes for Water Electrolysis». *ACS Appl. Mater. Interfaces* **8**, 15297–15306, 2016, doi: 10.1021/acsami.6b03050.
- J. Seweryn, J. Biesdorf, T.J. Schmidt, P. Boillat, «Neutron Radiography of the Water/Gas Distribution in the Porous Layers of an Operating Electrolyser». *J. Electrochem. Soc.* **163**, F3009–F3011, 2016, doi: 10.1149/2.0641607jes.
- E. Oakton, D. Lebedev, A. Fedorov, F. Krumeich, J. Tillier, O. Sereda, T.J. Schmidt, C. Coperet, «A Simple One-Pot Adams Method Route to Conductive High-Surface Area IrO_2-TiO_2 Materials». *New J. Chem.* **40**, 1834–1838, 2016, doi: 10.1039/C5NJ02400E.
- N. Biliskov, D. Vojta, L. Kotai, et al., «High Influence of Potassium Bromide on Thermal Decomposition of Ammonia Borane». *Journal of Physical Chemistry C*, **120**, 44, 25276–25288, 2016.
- E. Callini, K.-F. Aguey-Zinsou, R. Ahuja, et al., «Nanostructured materials for solid-state hydrogen storage: A review of the achievement of COST Action MP1103». *Int. J. Hydrogen Energy* **41**, 32, 14404–14428, 2016.
- S. Kato, S.K. Matam, P. Kerger, et al., «The Origin of the Catalytic Activity of a Metal Hydride in CO_2 Reduction». *Angewandte Chemie-International Edition* **55**, 20, 6028–6032, May 10, 2016.
- E. Callini, Z. Oezlem Kocabas Atakli, B.C. Hauback, et al., «Complex and liquid hydrides for energy storage». *Applied Physics A – Materials Scienence & Processing* **122**, 4, 353, April 2016.
- J. Huang, Y. Yan, A. Remhof, et al., «A novel method for the synthesis of solvent-free $Mg(B_3H_8)_2$». *Dalton Transactions* **45**, 9, 3687–3690, 2016.
- E. Callini, P.A. Szilagyi, M. Paskevicius, et al., «Stabilization of volatile $Ti(BH_4)_3$ by nano-confinement in a metal-organic framework». *Chemical Science* **7**, 1, 666–672, 2016.
- A. Fernandez, G.M. Arzac, U.F. Vogt, et al., «Investigation of a Pt containing washcoat on SiC foam for hydrogen combustion applications». *Applied Catalysis B-Environmental* **180**, 336–343, Jan. 2016.

Work Package «Assessment – Interactions of Storage Systems»

- B. Meier, F. Ruoss, M. Friedl, «Investigation of carbon flows in Switzerland under special consideration of carbon dioxide as a feedstock for sustainable energy carriers». *Energy Technology*. online: Nov. 23, 2016, http://onlinelibrary.wiley.com/doi/10.1002/ente.201600554/full.
- M. Friedl, B. Meier, F. Ruoss, L. Schmidlin, «Thermodynamik von Power-to-Gas». Report published on the website of IET-HSR, Oct. 20, 2016.
- X. Zhang, C. Bauer, C. Mutel, K. Volkart, «Life Cycle Assessment of Power-to-Gas: Approaches, system variations and their environmental implications». *Applied energy* **190**, 326–338, 2017, doi: http://dx.doi.org/10.1016/j.apenergy.2016.12.098.
- D. Parra, M.K. Patel, «Effect of tariffs on the performance and economic benefits of PV-coupled battery systems». *Applied energy* **164**, 175–187, 2016.

Publications

- D. Parra, M.K. Patel, «Techno-economic implications of the electrolyser technology and size for power-to-gas systems». *International Journal of Hydrogen Energy* **41** (6), 3748–3761, 2016.
- A. Abdon, X. Zhang, D. Parra, M.K. Patel, C. Bauer, J. Worlitschek, «Techno-economic and environmental assessment of energy storage technologies for different time scales». To be submitted to *Energy*.
- D. Parra, S. Zhang, C. Bauer, M.K. Patel, «An integrated techno-economic and environmental assessment of power-to-gas systems». Submitted to *Applied Energy*, 2016.
- D. Parra, M. Swierczynski, D.I. Stroe, S.A. Norman, T. O'Doherty, L.T. Rodrigues, S. Zhang, C. Bauer, A. Abdon, J. Worlitschek, M.K. Patel, «An interdisciplinary review of energy storage for communities: challenges and perspectives». Submitted to *Renewable & Sustainable Energy Reviews*, 2016.
- R. Segundo, D. Parra, N. Wyrsch, M.K. Patel, F. Kienzle, P. Korba (forthcoming), «Techno-economic analysis of battery storage and curtailment in a distribution grid with high PV penetration». Submitted to *IEEE Transactions on Sustainable Energy*, 2016.
- K. Volkart, C. Bauer, P. Burgherr, S. Hirschberg, W. Schenler, M. Spada, «Interdisciplinary assessment of renewable, nuclear and fossil power generation with and without carbon capture and storage in view of the new Swiss energy policy». *International Journal of Greenhouse Gas control* **54**, 1, 1–14, 2016.
- B. Steubing, G. Wernet, J. Reinhard, C. Bauer, E. Moreno-Ruiz, «The ecoinvent database version 3 (part II): analyzing LCA results and comparison to version 2». *The International Journal of LCA* **21**, 9, 1269–1281, September 2016,
- G. Wernet, C. Bauer, B. Steubing, J. Reinhard, E. Moreno-Ruiz, B. Weidema, «The ecoinvent database version 3 (part I): overview and methodology». *The International Journal of LCA* **21** (9), 1218–1230, 2016.
- A. Stamatiou, M. Obermeyer, P. Schütz, L. Fischer, J. Worlitschek, «Investigation of Unbranched, Saturated, Carboxylic Esters as Phase Change Materials». Submitted to *Renewable Energy*, 2016.

Organized Events

4th Annual Symposium, SCCER Heat and Electricity Storage, October 24, 2016

The 4th Annual Symposium «SCCER Heat & Electricity Storage» was held on October 24, 2016, at Hochschule Luzern – Technik und Architektur.

Organizers Thomas J. Schmidt, Jörg Roth, Ursula Ludgate, Jörg Worlitschek, Svetlana Vangesova

Speakers
Prof. Mark O'Malley, Energy Institute and Electricity Research Centre University College Dublin, Ireland
Dipl.-Wirt.-Ing. Julia Badeda, RWTH Aachen, D
Dr. David Hart, E4tech, Lausanne, CH
Prof. Dr. Brigit Scheppat, Hochschule Rhein Main, D
Prof. Dr. Sophia Haussener, EPFL, CH
Dr. Claire Villevieille, Paul Scherrer Institut, CH
Prof. Dr. Hubert Girault, EPFL, CH
Prof. Dr. Christophe Copéret, ETHZ, CH
Dr. Christian Bauer, Paul Scherrer Institut, CH
Prof. Martin Patel, University of Geneva, CH

Oral Presentations

- M. O'Malley, «The Value of Energy Storage: The Good, the Bad and the Ugly».
- J. Badeda, «Development of the PV homestorage market and the implications for local distribution grids».
- D. Hart, «Policies for energy storage? I wouldn't start from here...».
- B. Scheppat, «Energiepark Mainz: Operational and Economical Experiences of the worldwide largest Power-to-Gas plant with PEM electrolysis».
- S. Haussener, «High Temperature Heat Storage System Performance and Design».
- C. Villevieille, «Recent development in Na-ion batteries».
- H. Girault, «Grid to Mobility».
- C. Copéret, «Strategies and Current State of the Art in CO_2 Conversion processes within Hae».
- C. Bauer, M.K. Patel, «Integrated evaluation of energy storage technologies: economic and environmental aspects».

Posters

Battery and Materials

- J. Cabañero, C. Marino, C. Villevieille, «Almond Shell-Derived Carbonaceous Materials as Anodes for Sodium-Ion Batteries».
- C. Marino, S. Park, C. Villevieille, «Electrode formulation of a P2-layered oxide material for Na-ion batteries».
- C. Marino, S. Park, C. Villevieille, «P2–$Na_{0.67}(Mn_{0.6}Fe_{0.25}Co_{0.15-x}Al_x)O_2$ as cathode material for Na-ion batteries».
- B. Baichette, K.M. Fromm, «Heterometallic single precursor of oxides for Na-ion battery cathode materials».
- N. P. Stadie, S. Wang, K. Kravchyk, M.V. Kovalenko, «Ordered Microporous Carbons as the Cathode for High Energy and Power Density Aluminum Batteries».
- N.H. Kwon, Y. Sheima, K.M. Fromm, «Rechargeable Dual Electrolytes for Li-Air and Li-Water Batteries».
- S. Maharajan, N.H. Kwon, K.M. Fromm, «Sn/C composite anode materials for high energy batteries».
- H. Yao, K. M Fromm, «Ionic Liquids based on Crown Ethers as electrolytes for batteries».
- P. Sutton, M. Fischer, I. Gunkel, U. Steiner, «Solid polymer electrolytes for lithium batteries».
- E. Cuervo Reyes, E. Stilp, C.P. Scheller, M. Held, U. Sennhauser, «Footprint of Sub-diffusive Transport in the Impedance Spectrum of Lithium Ion Batteries».
- C. Brivio, V. Musolino, M. Merlo, P.-J. Alet, L.-E. Perret-Aebi, C. Ballif, «Battery modeling and performances evaluation».
- A. Fuerst, A. Haktanir, H. Roth, B. Löffel, M. Müller, «Pilot production line for battery cell manufacturing».

Organized Events

Thermal Energy Storage

- L. Geissbühler, V. Becattini, A. Haselbacher, A. Steinfeld, «Dynamic Modelling of the Thermal Storage and Cavern of an AA-CAES Pilot Plant».
- L. Geissbühler, A. Mularczyk, A. Haselbacher, A. Steinfeld, «Thermocline Control for Sensible Thermal Energy Storage».
- S. Zavattoni, M. Barbato, L. Geissbühler, A. Haselbacher, G. Zanganeh, A. Steinfeld, «CFD modeling of the Pollegio AA-CAES prototype TES system».
- M. Dudita, X. Daguenet-Frick, P. Gantenbein, «Increasing the heat and mass transfer by improving surface wetting of adsorbers in sorption storage systems».
- X. Daguenet-Frick, M. Dudita, P. Gantenbein, «Thermal absorption storage: experimental assessment and modelling results considerations for the falling film tube bundle heat and mass exchanger units».
- D. Perraudin, S.R. Binder, S. Haussener, «Degradation Characterization of Encapsulated Phase Change Material Systems for High Temperature Heat Storage».
- E. Rezaei, M. Barbato, S. Gianella, S. Haussener, A. Ortona, «High temperature tubular SiSiC structures for solar applications».
- A. Stamatiou, D. Leemann, J. Worlitschek, «High Power Thermal Energy Storage for Industrial Applications using Phase Change Material Slurry».
- S. Maranda, R. Waser, A. Stamatiou, L. Fischer, J. Worlitschek, «Modeling and experimental investigation on the solidification in a latent heat storage unit using a finned tube bundle heat exchanger».
- G. Seitz, R. Helmig , H. Class, «Numerical Model of a CaO/$Ca(OH)_2$-heat storage tank».

Hydrogen Generation and Storage

- F. Le Formal, N. Guijarro, W.S. Bourée, A. Gopakumar, M.S. Prévot, A. Magrez, P.J. Dyson, Kevin Sivula, «Efficient Electrocatalyst for Water Oxidation in Alkaline Electrolyte Derived from the Gibeon Meteorite».
- S. Kato, M. Spodaryk, A. Züttel, «Metal Hydride Catalyst for Energy Storage».
- C. Fink, G. Laurenczy, «Screening for Potential Catalysts for Selective Formic Acid Dehydrogenation of the type [Cp*Ir(N,N)Cl]».
- M. Montandon-Clerc, A.F. Dalebrook, G. Laurenczy, «Hydrogen Storage Using the Formic Acid/CO_2 Couple in Aqueous Solution Catalyzed by First Row Transition Metal Complexes».

Synthetic Fuels

- A.A. Permyakova, A. Pătru, J. Herranz, T.J. Schmidt, «Electrochemical reduction of CO_2 to renewable fuels – reaction study in liquid and gas phase».
- A. Dutta, M. Rahaman, A. Zanetti, N.C. Luedi, M. Mohos, P. Broekmann, «CO_2 to Value».
- A. Dutta, A. Kuzume, M. Rahaman, S. Vesztergom, P. Broekmann, «Monitoring the Chemical State of Catalysts for CO_2 Electroreduction: An in operando Raman Spectroscopic study».
- A. Dutta, A. Zanetti, M. Rahaman, P. Broekmann, «CO_2 electro-reduction on 2D and 3D Cu skeleton catalysts».
- M. Rahaman, A. Dutta, P. Broekmann, «Energy Efficient CO_2 Conversion to Formate at Very Low Overpotential on Size Selective Pd Nanoparticles».
- M. Rahaman, C. Morstein, A. Dutta, P. Broekmann, «Electrodeposited Ag Microcrystals for CO_2 Electroreduction».
- N. Kaeffer, H.-J. Liu, C. Coperet, «Surface-supported Cu-based catalysts towards CO_2 conversion».
- P. Wolf, K. Larmier, S. Tada, C. Copéret, «Cu-ZrO_2 Interface Enhances CO_2 Hydrogenation Activity and Selectivity to Methanol».
- D. Lebedev, D. Abbott, M. Povia, K. Waltar, E. Fabbri, A. Fedorov, T.J. Schmidt, C. Coperet, «Highly active and stable iridium oxide and pyrochlore materials for the oxygen evolution reaction».
- M. Spodaryk, S. Kato, A. Züttel, «Electrochemical CO_2 reduction with H_2 to synthetic fuels».

Organizers and speakers (from left to right):

Top
Søren Klein,
Sivarajakumar Maharajan,
Christophe Copéret,
Julia Badeda,
Claire Villeveille

Middle
Jörg Worlitschek,
Christian Bauer,
Birgit Scheppat,
Markus Friedl,
Hubert Girault

Bottom
Mark O'Malley,
Sophia Haussener,
Thomas J. Schmidt,
Jörg Roth,
David Hart

Organized Events

- N. Hérault, V. Kaliginedi, P. Broekmann, K.M. Fromm, «TiO_2 nanocontainers and nanospheres as photocatalysts for CO_2 reduction and photoelectrochemical water splitting: Structural modification».

Assessment of Storage Systems

- A. Abdon, X. Zhang, D. Parra, C. Bauer, C. Mutel, M.K. Patel, J. Worlitschek, «Combined assessment of electricity storage for stationary grid applications: economic and environmental aspects».
- D. Parra, M. K. Patel, «Assessment of energy storage technologies for further renewable energy penetration, and beyond».
- P. Schuetz, D. Gwerder, L. Gasser, B. Wellig, J. Worlitschek, «Thermal storage facilitates higher flexibility in smart grids for residential heating systems with heat pumps».

Contact

Swiss Competence Center for Energy Research
Heat and Electricity Storage (SCCER HaE-Storage)
c/o Paul Scherrer Institut
5232 Villigen PSI, Switzerland

Phone: +41 56 310 5396

E-mail: info@sccer-hae.ch
Internet: www.sccer-hae.ch

Thomas J. Schmidt, Head

Phone: +41 56 310 5765
E-mail: thomasjustus.schmidt@psi.ch

We thank the following industrial and cooperation partners:

In cooperation with the CTI

Energy funding programme
Swiss Competence Centers for Energy Research

Schweizerische Eidgenossenschaft
Confédération suisse
Confederazione Svizzera
Confederaziun svizra

Swiss Confederation

Commission for Technology and Innovation CTI